**Highly sensitive flow cytometry for the characterisation of extracellular vesicles**

*A study into analytical aspects, artefacts, and challenges that can influence the interpretation of results from clinical studies*

Botha, Jaco

*Publication date:*
2021

*Document Version*
Publisher's PDF, also known as Version of record

[Link to publication from Aalborg University](#)

# HIGHLY SENSITIVE FLOW CYTOMETRY FOR THE CHARACTERISATION OF EXTRACELLULAR VESICLES

## A STUDY INTO ANALYTICAL ASPECTS, ARTEFACTS, AND CHALLENGES THAT CAN INFLUENCE THE INTERPRETATION OF RESULTS FROM CLINICAL STUDIES

**BY**
**JACO BOTHA**

DISSERTATION SUBMITTED 2021

AALBORG UNIVERSITY
DENMARK

# HIGHLY SENSITIVE FLOW CYTOMETRY FOR THE CHARACTERISATION OF EXTRACELLULAR VESICLES

## A STUDY INTO ANALYTICAL ASPECTS, ARTEFACTS, AND CHALLENGES THAT CAN INFLUENCE THE INTERPRETATION OF RESULTS FROM CLINICAL STUDIES

by

Jaco Botha

**AALBORG UNIVERSITY**
DENMARK

Dissertation submitted October 2021

# CURRICULUM VITAE

**Jaco Botha, MSc**
Born: September 20th, 1989

Dorfgade 3A,
9330 Dronninglund

Email: **j.botha@rn.dk**

| Academic career | |
|---|---|
| 2016-2021 | **Clinical Assistant & PhD Student**, Laboratory for Metabolic Diseases, Department of Clinical Biochemistry, Aalborg University Hospital, North Denmark Region, Denmark |
| 2015-2016 | **Research Assistant**, Department of Clinical Biochemistry, Aalborg University Hospital, North Denmark Region, Denmark |
| 2015 | **Research Assistant**, Department of Clinical Medicine, Aalborg University, Denmark |
| 2014-2015 | **Research Assistant**, *Klinik Anæstesi*, Aalborg University Hospital, North Denmark Region, Denmark |

| Education | |
|---|---|
| 2011-2013 | **MSc** in Medicine with Industrial Specialization (Biomedicine), Aalborg University, Denmark |
| 2008-2012 | **BSc** in Medicine with Industrial Specialization, Aalborg University, Denmark |

| Teaching experience | |
|---|---|
| 2014 | Research project co-supervisor for 6th semester Medicine and Medicine with Industrial Specialization students |

| Reviewer experience | |
|---|---|
| 2015-2021 | *Ad hoc* reviewer for *Journal of Extracellular Vesicles*, *Theranostics*, *Journal of Diabetes Research*, *Scientific Reports* and several others. |

| Publications, presentations, and meetings/symposia | |
|---|---|
| 2014-2021 | See *Appendix E* for full list. |

# ENGLISH SUMMARY

Extracellular vesicles (EVs) are a heterogenous group of membrane-bound biological nanoparticles released by all cells into their surroundings. EVs carry cargo that often reflects that of their parent cells and can deliver their cargo to and elicit specific reactions in distant cells. As such, EVs have gained much attention as potential biomarkers and therapeutical targets. Flow cytometry is a method popularly used to characterise EVs due to its ability to determine multiple parameters on single particles in a high-throughput manner. However, due to their small size, the majority of EVs often present with dim signals that are either impossible to distinguish from noise or fall below the lower detection limit of all but the most sensitive dedicated flow cytometers. Furthermore, biological fluids such as blood are complex and contain numerous other sub-micron sized particles that can mimic EVs in various assays. Therefore, the four studies contained in this thesis aimed to address specific issues with flow cytometry characterisation of EVs that could confound on data interpretation from clinical studies and thereby reduce their reproducibility and robustness.

In study 1, we assessed the ability of three different flow cytometry platforms to resolve small particles in the EV size range from background, detect different EV phenotypes, and intra-day, inter-day, and global variabilities in quantifying different EV phenotypes in blood plasma. In study 2, we determined the extent to which fluorescent antibody and protein label aggregates can be detected by highly sensitive flow cytometry and compared the extent to which three different high-speed centrifugation and two filtration protocols of reagents prior to staining reduce fluorescent aggregates. In study 3, we optimised a labelling protocol for large lipoproteins including the very-low density lipoprotein and chylomicrons and investigated to which extent these nanoparticles confound on results from EV studies, where lipid-based methods are used to define EVs including labelling of membrane-bound phosphatidylserine or detergent lysis of samples to control for EV-specificity of marker positive events. In study 4, we present a systematic method for optimisation of analytical parameters such as laser power and PMT voltage, where the quantum efficiency and background noise of detectors are used to calculate the lower resolution limit in standardised units, and how this metric can be used to define which settings are optimal for measuring dim signals from sub-micron particles such as EVs.

The papers contained in this thesis contributes to a growing body of literature, whose focus is on defining and overcoming pitfalls in EV research and standardisation of methodology and reporting. Specifically, several important pre-analytical and analytical issues related to flow cytometry characterisation of EVs are addressed that can influence result interpretation including choice of analytical platform, treatment of reagents prior to use, methodological considerations when working with complex biological samples, and optimisation of analytical settings.

# DANSK RESUMÉ

Extracellulære vesikler (EV'er) er en heterogen gruppe af membranafgrænsede biologiske nanopartikler, som frigives af celler, og hvis indhold afspejler cellerne de stammer fra i frigivelsesøjeblikket. EV'er kan levere deres indhold til øvrige celler og igangsætte specifikke processer i disse. Derfor er EV'er interessante som potentielle biomarkører og behandlingsmål. Flowcytometri er en populær metode brugt til karakterisering af EV'er grundet muligheden for at analysere mange parametre samtidigt på enkelte partikler kombineret med hurtig analyse af mange partikler. Imidlertid er EV'er så små, at signalerne fra størstedelen enten ikke kan adskilles fra baggrundsstøj eller er under detektionsgrænsen for alle andre end de mest sensitive flowcytometre. Biologiske væsker såsom blod er komplekse og indeholder mange andre nanopartikler, som kan ligne EV'er i forskellige analyser. Derfor søgte vi med de fire studier præsenteret i denne afhandling at adressere specifikke problemstillinger vedrørende flowcytometrisk karakterisering af EV'er, som kan være problematiske for fortolkning af data fra kliniske studier og dermed reducere deres reproducerbarhed og robusthed.

I studie 1 undersøgte vi 3 flowcytometres resolutionsevne for partikler i EV-størrelsesordenen, deres detektion af forskellige EV-fænotyper og variabilitet i kvantificering af disse indenfor samme dag og mellem analysedage. I studie 2 undersøgte vi, hvorvidt aggregater af fluorescerende antistoffer og proteinmarkører kan detekteres ved høj-sensitiv flowcytometri og sammenlignede i hvilken grad 3 forskellige højhastighedscentrifugerings- og to forskellige filtreringsprotokoller implementeret før farvning kunne reducere disse aggregater. I studie 3 optimerede vi en farvningsprotokol til store lipoproteiner, inklusiv VLDL (very-low density lipoproteins) og kylomikroner. Vi undersøgte i hvilken grad disse nanopartikler interfererer med resultater fra EV-studier, hvor lipidbaserede metoder bruges til at definere EV'er, bl.a. gennem farvning af membranbunden fosfatidylserin eller detergenslysering af prøver for at kontrollere EV-specificiteten af de identificerede markørbærere. I studie 4 præsenteres en systematisk metode til optimering af analytiske parametre såsom laserstyrke og PMT-spænding, hvor kvanteeffektiviteten og baggrundsstøjen for detektorer bruges til at beregne den nedre resolutionsgrænse i standardiserede enheder, samt hvordan dette kan bruges til at definere optimale indstillinger til brug ved detektion af svage signaler fra nanopartikler som EV'er.

Artiklerne i denne afhandling bidrager til en voksende litteratur omhandlende definering af og løsninger til de faldgruber der er forbundet med EV-forskning og standardisering af metoder og rapportering. Specifikt adresseres flere vigtige preanalytiske og analytiske udfordringer vedrørende flowcytometrisk karakterisering af EV'er som kan have indflydelse på fortolkning af resultater, heriblandt valg af analytisk platform, behandling af reagenser, metodehensyn ved analyse af komplekse biologiske prøver og optimering af analytiske indstillinger.

# PREFACE

This project was conducted at the Cardiometabolic Laboratory (previously Laboratory for Metabolic Diseases), which is a part of the Department of Clinical Biochemistry at Aalborg University Hospital in Aalborg, Denmark. One of the focus points of this laboratory was to look into the potential of extracellular vesicles (EVs) as biomarkers for diagnosis and disease or treatment prognosis in relation to metabolic disorder with special interest towards obesity and obesity-related disorders. In the beginning of my employment, I was tasked with writing a manuscript about the role of monocyte-derived and CD36-bearing EVs in relation to type II diabetes mellitus, which was followed by another about the same EV-phenotypes as the previous one, but this time in relation to morbid obesity followed by gastric bypass surgery. In this period, we gradually became more interested in a specific set of obesity-related disorders, namely non-alcoholic fatty liver disease (NAFLD) and non-alcoholic steatohepatitis (NASH), disorders that are seemingly highly abundant among obese individuals, whose pathogenesis, comorbidities, and long-term side effects are relatively severe, and with both invasive and imprecise diagnosis procedures. Thus, the original draft of the plan for this PhD project was drafted, and I officially became a PhD student. Even though this project was originally conceived as a clinical one, whose focus was on finding markers to detect hepatocyte-derived extracellular vesicles and determine their potential as biomarkers for NAFLD and NASH using highly sensitive flow cytometry, it became clear quite early on that we did not quite have the necessary tools or understanding of the tools we had to achieve what we set out to do. As such, we had to make the necessary adjustments to the project to at least be moving in the right direction if we could not achieve all our initial goals. Little did we know at the time what this rabbit hole would bring, nor how deep and complex it would be.

First and foremost, I would like to extend my thanks to my main supervisor, Professor Aase Handberg, who never denied me any opportunity to pursue each project path, idea, conference symposium, meeting etc. that was necessary to keep the project moving in the right direction, advance my own career goals, or both – even if it could be to my own detriment. I would further like to extend my gratitude for being included in so many different and varied projects of yours in the years I worked at the Department of Clinical Biochemistry and for being able to contribute with my knowledge and experience in any way I could. Not only did this help to keep my racing mind stimulated, tamed and fed, it also made me feel useful and gave me purpose, which was especially important during the dry periods, where nothing seemed to work or go as planned (*i.e.*, constantly cracked crystals, the case of the invisible endothelial cell-derived EVs, the disappearing act magically pulled off by the monocyte-derived EVs, and many more). Finally, I would like to extend my deepest and most heartfelt thanks for putting up with my overly self-critical way of doing things, which, I know, you have felt frustrated over on way too many occasions, even though you did not always express it. Although I do feel that I have come a long

way in terms of doing tasks to slightly lower standards to decrease the time spent on them significantly, I still have some ways to go, and I am working on it. If anything, this is possibly the most important skill I was forced to cultivate during my employment as your Clinical Assistant and PhD student.

Second, I would like to extend my thanks to all who have helped me along the way with small tasks, discussions, favours or putting me in contact with the right person to advance one of my projects. Specifically, I would like to thank my colleague Mathilde Sanden, who spent many an evening in the lab trying to fix things that weren't supposed to be broken. I would further like to specifically thank my colleague Rikke W. Rasmussen for never refusing to lend a helping hand with any task – no matter how large or small. Moreover, I would like to thank Haley Pugsley and Owen Hughes at the Luminex corporation for making it possible for me to visit the Amnis production facility in Seattle, WA, to analyse samples on their imaging flow cytometry platforms for the first study in this thesis. I would additionally like to thank Jens B. Simonsen from the Technical University of Denmark for many rewarding discussions on intricacies and practicalities of high-resolution flow cytometry, and the physicochemical attributes of lipoproteins and EVs. Finally, I would like to thank the staff in the ambulatory at the Department of Clinical Biochemistry and at the Danish Blood Bank for providing all human blood samples used in this project.

Third, I would like to thank my colleagues at the Department of Clinical Biochemistry, with who I have shared an office, countless coffee and lunch breaks, and many enjoyable work-related and non-work-related social escapades. Without you I would not know which TV-series was the best in the world, feel nervous each time I see a semicolon, seen the full splendour of Mount Fuji, have a decent third place in an "official" limbo competition, or been witness to crazy dancing in the streets of Rotterdam after midnight.

Lastly, I would like to express my gratitude towards my friends and family for their support and understanding, and I would also like to express my apologies for way too many times being late for social events due to work getting in the way, and, especially, for long periods of time where I certainly should have been better at keeping in touch. I would especially like to acknowledge my partner, Christine, for her support during this whole process, and more importantly her understanding, patience, and kindness when the only thing I would do was push harder every time I hit a wall in my project without much thought for the cost of it all. If it was not for you or the way you care for me, I would not have succeeded in this endeavour, and the rabbit hole would have swallowed me whole. For that I am eternally grateful.

With my warmest regards,

*Jaco Botha*

# LIST OF PAPERS CONTAINED IN THIS THESIS

*Paper 1*

**Conventional, High-Resolution and Imaging Flow Cytometry: Benchmarking Performance in Characterisation of Extracellular Vesicles.**
<u>**Botha J**</u>, Pugsley HR, Handberg A. (2021). *Biomedicines* 9(2):124.

*Paper 2*

**Zoom in on Antibody Aggregates: A Potential Pitfall in the Search of Rare EV Populations.**
Rasmussen RW, <u>**Botha J**</u>, Prip F, Sanden M, Nielsen MH, Handberg A. (2021). *Biomedicines* 9(2):206.

*Paper 3*

**Lipid-based strategies used to identify extracellular vesicles in flow cytometry can be confounded by lipoproteins.**
<u>**Botha J**</u>, Handberg A, Simonsen JB. *Submitted to Journal of Extracellular Vesicles*.

*Paper 4*

**A systematic approach to optimise analysis protocols for flow cytometry characterisation of sub-micron particles.**
<u>**Botha J**</u>, Sanden M, Rasmussen RW, Nielsen MH, Mellergaard M, Handberg A. *Manuscript in preparation*.

# ABBREVIATIONS

| | |
|---|---|
| ADC | Analogue-to-digital converter |
| Anx5 | Annexin A5 |
| APC | Allophycocyanin |
| APD | Avalanche photodiode |
| ApoB100 | Apolipoprotein B100 |
| ApoB48 | Apolipoprotein B48 |
| ARRDC1 | Human arresting domain-containing protein 1 |
| ATP | Adenosine triphosphate |
| B | Background |
| BP | Band pass |
| $Ca^{2+}$ | Calcium ion |
| CCD | Charge-coupled device |
| CD | Cluster of differentiation |
| CFSE | Carboxyfluorescein succinimidyl ester |
| CV | Coefficient of variability |
| DNA | Deoxyribonucleic acid |
| DNR | Dynamic detection range |
| ELISA | Enzyme-linked immunosorbent assay |
| EpCAM | Epithelial calcium-dependent adhesion molecule |
| ERF | Equivalent of reference fluorophore |
| ESCRT | Endosomal Sorting Complex Required for Transport |

| EV | Extracellular vesicle |
|---|---|
| FITC | Fluorescein isothiocyanate |
| FSC | Forward scattered light or forward scatter |
| GTP | Guanosine triphosphate |
| HDL | High-density lipoprotein |
| IDL | Intermediate-density lipoprotein |
| ILV | Intraluminal vesicle |
| J | Measured signal per statistical photoelectron |
| K | Measured signal per standardised unit |
| LAF | Lipid-anchored fluorophore |
| LALS | Large-angle light scatter |
| LBPA | Lysobisphosphatidic acid |
| LDL | Low-density lipoprotein |
| LoD | Limit of detection |
| LoQ | Limit of quantification |
| LP | Long pass |
| MALS | Medium-angle light scatter |
| MESF | Molecular equivalent of soluble fluorophore |
| MHC-II | Major histocompatibility complex class II |
| miRNA | Micro RNA |
| mRNA | Messenger RNA |
| MVB | Multivesicular body |

| | |
|---|---|
| NAFLD | Non-alcoholic fatty liver disease |
| NASH | Non-alcoholic steatohepatitis |
| ND | Neutral density |
| NTA | Nanoparticle tracking analysis |
| PC | Phosphatidylcholine |
| PE | Phycoerythrin |
| PMT | Photon-electron multiplier tube |
| PPP | Platelet-poor plasma |
| PS | Phosphatidylserine |
| PWM | Pulse-width modulated |
| Q | Quantum efficiency |
| R | Theoretical lower resolution limit |
| RNA | Ribonucleic acid |
| SALS | Small-angle light scatter |
| sCD36 | Soluble CD36 |
| SD | Standard deviation |
| SDS | Sodium dodecyl sulphate |
| SDS-PAGE | Sodium dodecyl sulphate polyacrylamide gel electrophoreses |
| SEC | Size exclusion chromatography |
| SNARE | Soluble NSF-attachment protein receptor |
| SP | Short pass |
| SSC | Side scattered light or side scatter |

| | |
|---|---|
| TDI | Time-delay integration |
| TEM | Transmission electron microscopy |
| TRPS | Tuneable resistive pulse sensing |
| TTL | Transistor-transistor logic |
| VAMP | Vesicle-associated membrane proteins |
| VLDL | Very low-density lipoprotein |

# TABLE OF CONTENTS

# INTRODUCTION

Medical diagnosis is the process of determining a disease or condition based on symptoms and signs presented in the sufferer and has been a cornerstone in medicine since ancient times and has been described in papyruses from ancient Egypt as early as 2600 BC. Medical diagnosis requires information such as disease history and physical examinations. With the birth of modern medicine and several key discoveries and advancements in technology, the use of biological markers – "*biomarkers*" – for diagnosis has become very common, and many different types of biomarkers are abundantly in use in routine diagnosis of most diseases.

The Biomarker Definition Working Group released a framework for definitions of terms used to describe biological markers and clinical outcomes in order to improve communication on terms with overlapping meanings, and to remove ambiguity and uncertainty on the meanings of these terms [1]. According to the framework, a biomarker is defined as:

> "A characteristic that is objectively measured and evaluated as an indicator of normal biological processes, pathogenic processes, or pharmacologic responses to a therapeutic intervention." Biomarker Definition Working Group, 2001 [1].

Another term that has become increasingly popular in relation to biomarkers in recent years is "*liquid biopsy*". The term liquid biopsy was originally coined by Dr. Robert B. Sorrels describing the analysis of synovial fluid [2], after which its use fell out of fashion until 2010, where it was adopted to describe the use of circulating tumour cells for monitoring therapeutic outcomes of drug-resistant prostate cancer [3]. In recent years, focus has fallen on discovering less-invasive alternatives to tissue biopsies or exploratory surgery for a whole number of diseases. This has led to the proposed use of biomarkers that are detectable in body-fluids including blood, which can be obtained in reasonable quantities in a minimally invasive manner. This has led to the term liquid biopsy being widely adopted to describe minimally invasive body-fluid-based biomarker alternatives to invasive procedures for diagnosis, staging, prognosis, and therapeutic response. Among these alternatives are extracellular vesicles (EVs), which are small particles present in most biological fluids. While promising, measuring and characterising these small particles have proven difficult, and their use as clinical markers of disease has been somewhat limited so far.

# CHAPTER 1. BACKGROUND

## 1.1. EXTRACELLULAR VESICLES

### 1.1.1. HISTORICAL PERSPECTIVE

EVs constitute a species of biological particles that have garnered significant and ever-growing interest as potential biomarkers and conveyors of physiological and pathological processes. EVs were first structurally described by Palay and Palade in 1955 while studying the fine structure of neurons with electron microscopy [4]. In the decades to come, these particles were reportedly observed by multiple other researchers, but were considered to be nothing more than cellular "dust" or virus-like particles of unknown significance due to a lack of methods to properly isolate and characterise these newly discovered particles [5,6]. Some years later, when investigating the maturation of reticulocytes into mature red blood cells, it was demonstrated that some EVs are formed inside the cell in multivesicular bodies (MVBs) [7]. It was additionally demonstrated that vesicles inside MVBs and those released into the circulatory system contained different transmembrane proteins, and that the sorting process of transmembrane proteins into MVBs was highly selective in the sense that certain proteins such as transferrin, which are specific to the reticulocyte, were sorted into the "*exosomes*" that formed inside the MVBs, while others that were also abundantly present on the mature red blood cell such as the anion transporter were not sorted into MVBs. Furthermore, this process seemed to be conserved across multiple taxonomical classes (*i.e.* mammals and birds), although the sorting of specific proteins seemed to vary across species [8]. These observations thus demonstrated that cell-derived vesicles might indeed be more than just cellular dust, and that they could be sophisticated, functional machinery that serves essential functions as to be conserved across different taxonomical classes.

In the decades to come, research interest into EVs grew gradually, with several important discoveries being made regarding their biogenesis, contents, and potential functions. Although it had been known for some time that apoptotic cells package degraded cell contents into vesicles that are shed from the plasma membrane [9], it was only shown later that a heterogeneous group of vesicles could also be released from the plasma membrane upon cell activation or stimulation from non-apoptotic cells [10–15]. Furthermore, EVs were discovered to be present in most body fluids including blood products such as serum and plasma [16], urine [17], saliva [18], breast milk [19], nasal and bronchial discharge fluid [20], amniotic fluid [18,21], and seminal fluid [22]. Studies also started to demonstrate functional aspects of EVs beyond simply shedding proteins during differentiation, including their ability to initiate and partake in thrombosis and haemostasis [11,12], presentation of antigens

to elicit T-cell responses [23], conference of specific cell functions or processes [24], or dissemination of pathogens [25].

The discovery that EVs contained different ribonucleic acid (RNA) species including messenger RNA (mRNA) and micro RNA (miRNA) and could horizontally transfer their transcriptomic contents between cells further conveyed the importance of EVs as mediators of cell to cell communication [26,27]. During this period, research interest into the contents and functions of EVs and their potential as biomarkers and therapeutic agents started to grow exponentially [28,29], all of which culminated in the creation of the International Society for Extracellular Vesicle Research (ISEV) in 2011. The years following the creation of ISEV saw rapid advancements in methodological approaches to purify and characterise EVs, development of platforms with adequate sensitivity to study single EVs, and several attempts and revisions to standardise most aspects of EV research. This aided significantly in further characterisation of the contents and functions of EVs as well as improving the robustness of data and reporting in general.

## 1.1.2. ANATOMY, BIOGENESIS AND NOMENCLATURE OF EXTRACELLULAR VESICLES

EVs constitute a very heterogeneous species of particles that are abundantly present in most body fluids and released by most cell types. Regardless of the organism they stem from to some extent, their cellular origin, or the mechanisms leading to their release from cells, EVs are generally composed of the same components. Anatomically, at least when looking at a nanoscopic perspective, EVs can generally be described as consisting of a double-layered lipid membrane encapsuling proteins, deoxyribonucleic acid (DNA), RNA, transcription factors, metabolites, and lipids (reviewed in [30–35], figure 1A). EVs have generally been demonstrated to range in size from about 30 nm to well above 1000 nm with a left-skewed size distribution, where the relative abundance increases with decreasing size [36–38]. While EVs mostly present with a spherical morphology, various other morphological presentations have been described including ovular, tubular, filamentous (large tubule, which can fold due to its size), incomplete (larger membrane fragments), pleiomorphic (morphology not categorised by other morphological descriptions), or multiple vesicles nested inside a single vesicle [37].

Although EVs from different organisms have the similar broad features described above, there are distinct differences in biogenesis between eukaryotes and prokaryotes. For the sake of brevity, the following section will focus on EVs released from eukaryotic cells, and, more specifically, those released from mammalian cells.

**Biogenesis of extracellular vesicles**
In eukaryotic cells, EVs are generally classified into three distinct categories based on their biogenesis (figure 1B), namely: (1) exosomes, which form by inward budding

into early endosomes creating the aforementioned MVBs; (2) microvesicles, which are released directly from the cell membrane; and (3) apoptotic bodies, which are large vesicles in which degraded cellular components are packaged and shed from the plasma membrane upon apoptosis of the parent cell [31]. In the following review, the main focus will be on exosomes and microvesicles, as these subgroups of extracellular vesicles are characterised to a greater extent in terms of biogenesis, composition and function than apoptotic bodies, and are often referred to collectively in studies as "*extracellular vesicles*".

## *Exosomes*

As described above, exosomes are a group of EVs that originate from inward budding of the limiting membrane into endosomes throughout their maturation process. Endosomes containing multiple vesicles are often referred to as MVBs (*multivesicular bodies*) and the vesicles inside MVBs are often referred to as intraluminal vesicles (ILVs) [39]. The mechanisms resulting in the formation of exosomes have, perhaps, been studied more extensively than those that lead to the formation of microvesicles and apoptotic bodies due to the apparent ability of cells to selectively sort cargo into endosomes, which is, in turn, enriched in exosomes compared to the parent cell.

The best described machinery that leads to the formation of exosomes within endosomes is that belonging to the endosomal sorting complex required for transport (ESCRT) [40]. ESCRT machinery is comprised of five different protein complexes, which act in a concerted manner to sort cargo and generate ILVs (extensively reviewed in [41–43]). In brief, ESCRT-0 binds endosomal membrane sections containing ubiquinated cargo, which it keeps engaged until sequestration of ubiquitin and excision of the ILV. ESCRT-0 functions as a binding site for ESCRT-I, which additionally binds ESCRT-II, then creation invaginations in the exosomal membrane, which is enriched in ubiquinated cargo. ESCRT-II provides a site for assembly of ESCRT-III, which drives further budding of endosomal membrane into the endosome. Finally, ESCRT-III is disassembled and recycled by Vps4, which results in the excision of the vesicle into the lumen of the endosome.

Although ESCRT is well described, several studies have demonstrated that other mechanisms exist the can elicit the formation of ILVs and MVBs, and subsequent release of exosomes enriched for certain cellular components. While these mechanisms involve the accumulation of cholesterol [44] or lysobisphosphatidic acid (LBPA) [45] in the endosomal membrane and ILVs, presence of tetraspannins [45,46] and heat shock proteins [47], the precise mechanisms leading to the formation of ESCRT-independent exosomes are not yet understood. While it is uncertain whether ESCRT-dependent and independent mechanisms of ILV formation occur in the same MVB, evidence suggests that there is some heterogeneity in MVBs in a single cell [43].
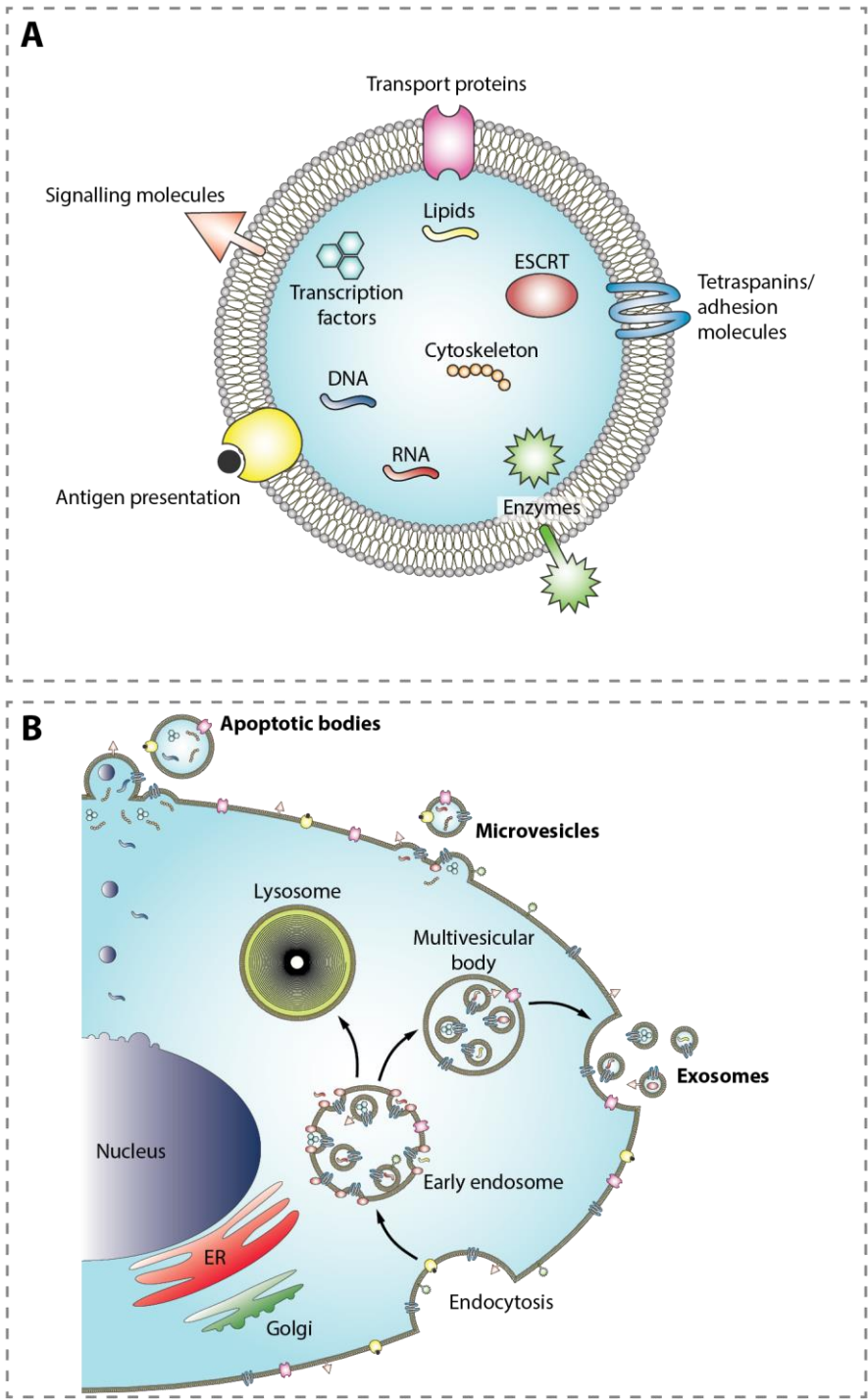
**Figure 1: Anatomy and biogenesis of extracellular vesicles. A)** Typical contents and cargo of extracellular vesicles **B)** Biogenesis and secretion of exosomes, microvesicles and apoptotic bodies.

After MVBs are created, they can either be sorted into lysosomes destined for destruction or towards the plasma membrane, where ILVs are released as exosomes from the cell [41,43,48]. Although the exact process and the stimuli or signals that determine which MVBs fuse with the plasma membrane of the cell and release their exosomal content remains to be understood, some evidence exists for the involvement of proteins belonging to the Rab family of small GTPase proteins [49,50]. Rab proteins are generally involved in vesicle trafficking and fate in the cell, vesicle budding, transport of vesicles or organelles between different compartments in the cell by interactions with the cytoskeleton, and docking of vesicles to their target compartment [51,52]. After docking, fusion of the MVBs to the plasma membrane and subsequent release of exosomes appears to be mediated by a series of different soluble NSF-attachment protein receptor (SNARE) proteins including vesicle-associated membrane proteins (VAMPs) [53–55] through mechanisms that are not yet fully understood.

*Microvesicles*
In contrast to exosomes, microvesicles are formed by direct budding and excision of the plasma membrane, where they are released into the extracellular space surrounding the cell. Although less studied than exosomes in terms of biogenesis, several different mechanisms have been described that could lead to the release of microvesicles from cells.

One of the mechanisms that has been proposed for the formation of microvesicles involves the sudden influx of calcium ions ($Ca^{2+}$) [56,57]. In non-pathological, non-stimulated and non-apoptotic conditions, phospholipids are distributed asymmetrically in the inner and outer leaflets of the plasma membrane, which encapsules the cell. This asymmetry is essential for normal cellular and physiological functions, and is maintained by a series of lipid-translocating enzymes that can be grouped into three different categories: flippases, which translocate certain phospholipids such as the negatively charged aminophospholipid phosphatidylserine (PS) to the inner leaflet of the membrane; floppases, which translocate cholesterol and the choline-containing phospholipid phosphatidylcholine (PC) to the outer leaflet; and scramblases, which randomly and, for the most part, non-specifically scrambles the positions of phospholipids between the inner and outer leaflets. Flippases and floppases both require energy in the form of adenosine triphosphate (ATP) in order to function, while scramblases are activated by intracellular $Ca^{2+}$ flux (reviewed in [58,59]). With the influx of $Ca^{2+}$, membrane asymmetry is lost, and PS is translocated to the outer leaflet of the cell. In addition, $Ca^{2+}$ elicits activation of calpain, which cleaves and initiates remodelling cytoskeletal proteins [60–62]. Together, these

effects result in localised outward budding of the plasma membrane and subsequent release of microvesicles (reviewed in [31,34]).

Some components of the ESCRT machinery have also been implicated in the formation and release of microvesicles. The human arrestin domain-containing protein 1 (ARRDC1) has been shown to recruit the TSG101 and Alix components of the ESCRT-I complex to the plasma membrane [63], which then causes outward budding of the plasma membrane in a similar fashion as in MVBs [63–65]. Similar to exosomes, this is followed by fusion and excision of the vesicle resulting in its subsequent release, and degradation and recycling of ESCRT machinery by Vps4. Interestingly, microvesicles formed in this fashion are also enriched in some tetraspannins that are usually associated with exosomes [64,65].

## Molecular contents of extracellular vesicles

As mentioned above, EVs can contain various molecular contents from the cells that they stem from including lipids, proteins, DNA, RNA, transcription factors and metabolites. The following section will focus on protein and lipid contents of EVs, and their potential as markers for detection, discrimination, and/or isolation of EVs.

### *Proteins*

The proteins and post-translation modifications of proteins contained in EVs have previously been demonstrated to reflect the cellular origin of the specific EV, the compartment and mechanisms that led to the formation and secretion of the EV from the cell, and, to some extent, the state of the parent cell [66–68]. Several other factors can also have an influence on the specific protein content of EVs. First, a single cell can secrete different EVs based on environmental factors such as oxygen tension or cellular topography [69]. Next, the stimulus leading to the release of EVs from a cell can also affect their contents [70–72]. Finally, as hinted to above, a single cell can contain MVBs with differential processing of cargo and formation of exosomes, which could also affect the contents of EVs in the different MVB compartments [43]. As such, finding a pan-EV marker of protein origin has proven difficult.

However, while there is no consensus on a pan-EV marker, several markers have consistently been identified in EVs from several different cell types and in several different body fluids. Among these, proteins belonging to the machinery that is responsible for the formation of EVs including the ESCRT-I sub-domain TSG101 and the ESCRT-III binding protein Alix have often been used to confirm the presence of EVs after purification [28,49,73–76]. In addition, the tetraspannins cluster of differentiation (CD) 9, CD63, and CD81 have also been shown to be preferentially sorted into exosomes [45], and are also commonly used to identify EVs in samples and preparations [20,28,49,73,75,77]. While many of these markers have originally been used to differentially define exosomes from microvesicles and apoptotic bodies, ESCRT machinery and tetraspannins including CD9, CD63 and CD81 have been shown to, partly, play a part in the formation of microvesicles and apoptotic bodies

[63–65,78]. Furthermore, CD9, CD63 and CD81 have also been shown to be present on the plasma membrane of certain cells [79] and multiple types of EVs [76,80], which further strengthens the hypothesis that these markers are not specific for a single type of EVs.

EVs have also been shown to contain cell phenotype specific markers on their surface, which has often been used in discriminating between EVs from different cell types in blood products. Among these are the two different sub-units of the integrin $\alpha_{IIb}\beta_3$ fibrinogen receptor, namely CD41 and CD61, which are both solely expressed on the surface of megakaryocytes and platelets [81], which has often been used to define EVs of platelet origin [82–85]. Likewise, the endothelial markers CD62E (E-selectin), CD144 and CD146 have been used to identify endothelial EVs [86–88]. Another marker, which has garnered some attention in terms of functioning as a potential disease biomarker when detected in circulating EVs, is the epithelial calcium-dependent adhesion molecule (EpCAM), which has been described to be expressed in multiple types of cancer [89] and, thus, used to identify circulating EVs of tumour origin [73,90,91].

A number of non-cell-specific functional proteins associated with certain functions, stimuli or stress have also been demonstrated to be present in EVs. Tissue factor, a protein involved in coagulation, has been demonstrated to not only be present on EVs, but also able to actively participate in haemostasis [92]. EVs with peptide-laden major histocompatibility complex class II (MHC-II) on their surface have been shown to travel into lymph nodes and attach to resident dendritic cells, where they elicit a lymphocyte response [23,93,94]. The scavenger receptors CD36 and CD163 have also been reported to be differentially expressed on EVs in certain diseases, and they have been shown to be functionally involved in physiological and pathophysiological processes [95,96].

### Lipids

Several different lipids have been implicated in being instrumental to the biogenesis and function of EVs. First, certain lipids have been demonstrated to be selectively enriched in EVs compared to their parent cells [97,98] and differentially expressed on the surface of EVs elicited by different physiological states [99]. As mentioned above, PS has been shown to be externalised to the outer leaflet of the plasma membrane preceding the formation of microvesicles, and, as such, it has often been used as a marker to define EVs in body fluids and preparations. This has often been accomplished by staining samples with annexin A5 (Anx5), which has an affinity towards PS in the presence of $Ca^{2+}$ [84,85,100]. Although PS was traditionally thought to be specifically located on microvesicles, PS has been shown to be present at a higher concentration in endosomes than on the plasma membrane [101], and on the surface of exosomes [102].

Cholesterol accumulates in the membrane endosomes giving rise to ILVs [33,97] and on the plasma membrane, from where microvesicles are released [103]. While the high cholesterol content in microvesicles seem to associated to lipid rafts [103], that of exosomes seems clearly distinct from lipid rafts, as the molar ratio between cholesterol, sphingomyelin and glycerophospholipids differ from those in lipid rafts [104]. Instead, endosomal cholesterol content seems to recruit LBPA to the endosomal membrane, where the concentration increases gradually through endosomal maturation [105], and functions as an anchor for ESCRT machinery [106]. LBPA has, however, only been reported to be present in very low amounts on the surface of exosomes, suggesting that it is conserved in the endosomal membrane after ILV formation [33,97,104].

## 1.1.3. CONFOUNDERS ON CHARACTERISING EXTRACELLULAR VESICLES

Biofluids that contain EVs are often complex and contain several different entities that can mimic EVs, which can complicate ascribing certain characteristics or functions to EVs. These entities include various classes of lipoproteins, cells and non-EV-derived cell debris, protein complexes, and many more [28,29,107]. Lipoproteins are a species of colloidal particles that transport hydrophobic lipids in various body fluids, including blood and lymph. The plasma lipoproteins family is constituted by high-density lipoprotein (HDL), low-density lipoprotein (LDL), intermediate-density lipoprotein (IDL), very low-density lipoprotein (VLDL), and chylomicrons. Regardless of sub-class, lipoproteins consist of a lipid core containing cholesterol, fatty acids, and triglycerides, which is covered with a layer of phospholipids with amphiphilic proteins embedded in into the membrane. These proteins are termed apolipoproteins, and the class and number of apolipoprotein embedded in the particle depends on the class of lipoprotein (reviewed in [108,109]). Lipoproteins are common confounders in EV preparations due to their similar physical properties to EVs (*i.e.,* size and density) [110], and their abundance, which is several orders of magnitudes greater than that of EVs in blood products [29]. Other particles that are often confound on EV characterisation are cells and cell debris, such as platelets [111–113] and erythrocyte ghosts [36,82,114], and proteins and protein complexes [115], all of which are also abundantly present in biofluids and commonly co-isolate with EVs.

To overcome issues with contaminants, several different strategies have been proposed to either selectively isolate EVs or reduce the number and extent of contamination. Of these, the most common primary isolation and concentration method is differential ultracentrifugation, in which samples are subjected to sequential cycles of high-speed centrifugation at different speeds (*i.e.* 300 x g for 10 minutes, 2.000 x g for 20 minutes, 10.000 x g for 40 minutes and 100.000 x g for 90 minutes), where pellets are collected after each centrifugation step and resuspended for further analysis [73,78,116,117].

Another method that is often used is the use of a density gradient or sucrose cushion ultracentrifugation. Gradients are constructed by stacking solutions of sucrose with differing specific gravities on top of or below a sample, after which particles in the sample are separated into the different specific gravity zones by ultracentrifugation. This allows for the separation of EVs from other components with differing specific gravities [78,118,119].

Size-exclusion chromatography (SEC) is another method that has gained popularity for EV isolation due to being less laboursome than ultracentrifugation and density gradient centrifugation while exertion of large forces on the purified EVs is avoided. In principle, samples are loaded onto a column, which contains a porous hydrogel, in which larger particles such as EVs are separated from the smaller proteins and lipoproteins, which are captured in the pores of the hydrogel [120–122].

Additional methods for isolation of EVs include sedimentation of EVs with synthetic polymers such as polyethylene glycol (PEG) [123], ultrafiltration with high-molecular wight cut-off membranes [124,125], affinity purification by using antibodies or labels with a specificity towards EV components [69,78] or contaminants such as lipoproteins [126], and several others.

While EV purification methods have aided in increasing our understanding of EV contents and functions, contaminating factors are often still present in preparations [78]. One of the main reasons for this is the fact that contaminants including lipoproteins and protein aggregates and complexes often have similar physical properties to EVs including overlapping size and densities [29,110,119], or they contain similar molecules on their surface such as PS in the case of lipoproteins [127], which could provide a surface for the binding of coagulation factors [84] (figure 2). In addition, purification methods can affect the EVs in the sample [28,128,129], different purification methods yield different EV populations [130,131], and the same method can confer some variability to the EV concentrations and purity [132].

## 1.1.4. CHARACTERISATION OF EXTRACELLULAR VESICLES

EV characterisation is typically performed by multiple, complementary methods that aim to quantify the number of EVs and determine their size distribution, determine whether EVs contain molecular contents typically associated with EVs, to which degree contaminants are present in the sample, characterise the abundance of specific functional cargo, and finally determine the physiological or therapeutical function of EVs [28]. In the following sections, the most commonly used characterisation methodology will be divided into (1) bulk characterisation methods and (2) single-particle characterisation methods.
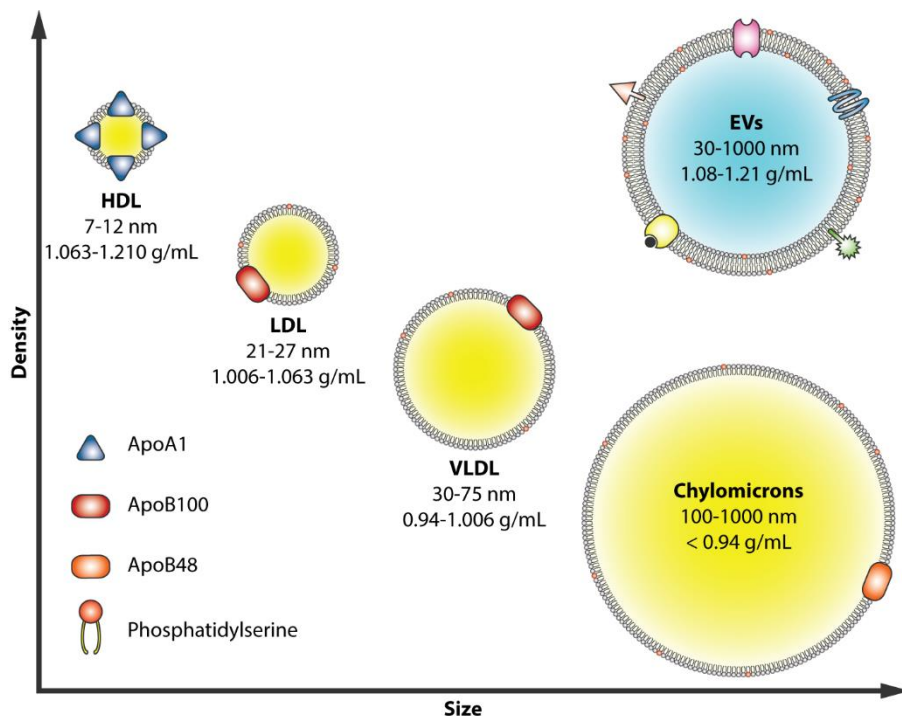
**Figure 2: Physicochemical properties of extracellular vesicles and common lipoprotein contaminants.**

## Bulk characterisation methods

Of bulk characterisation methods, sodium dodecyl sulphate polyacrylamide gel electrophoreses (SDS-PAGE) and western blot are some of the most common methods to verify whether EV markers such as tetraspannins or the degree of contaminants such as serum proteins are present in the EV preparation [28,78,116]. In terms of quantifying the number of a specific or a certain set of molecules, enzyme-linked immunosorbent assay (ELISA) has been used for capturing EVs based on their expression of a certain molecule and detecting and comparing the total expression of EV-specific molecules such as tetraspannins between samples [133–135]. Multiplex versions of this methodology are also in use including a microarray-based multiplex assay (EV Array) [136–138] and bead-based flow cytometry platforms [139,140].

Novel -omics-based technologies have driven much of the discovery of specific contents and cargo of EVs. These methods normally require a large input of material in order to adequately detect specific contents over contaminants and artefacts, and, therefore, are not able to characterise the content of single EVs [141]. This also holds true for functional studies, as single EVs would be unlikely to elicit measurable physiological functions in cells [142–144].

As such, it is important to contrast bulk characterisation to single particle characterisation, as bulk characterisation methods characterise specific features of all or a specific subset of EVs in a sample, regardless of how sensitive the technology is.

## Single-particle characterisation methods
### Transmission electron microscopy
The gold-standard method to determine the presence and lipidic membrane nature of EVs in preparations is electron microscopy including TEM [28]. This is partly due to the high sensitivity and resolution of TEM, which enables it to differentially detect details down to approximately 1 nm [38], and the ability to use colloidal gold-conjugated antibodies against specific markers (*i.e.* CD9, CD63 and CD81) to demonstrate the presence of specific markers on the surface of EVs [7,56,117]. Although TEM has been utilised since the early days of EV research, the preparation process involving dehydration and fixation has posed several problems in determining the size distribution of EVs, as EVs have been shown to shrink and present with non-natural morphologies in response to this. Furthermore, quality of images and results have been shown to be protocol and operator-dependant, thus limiting its use to quantify EVs [145]. Recently, cryo-TEM has been demonstrated for EV characterisation due to not requiring fixation and dehydration of samples. Although cryo-TEM and has allowed for more accurate size, morphology, and concentration determination of EVs [36], it is time consuming and not widely available, and not very widely used [145].

### Nanoparticle tracking analysis
Nanoparticle tracking analysis (NTA) is an optical method, which tracks the dark-field light scatter of particles illuminated by a laser beam in suspension and infers their size based on their Brownian motion in the solution [146]. Due to its sensitivity towards small particles ($\geq$ 70 nm EVs, [38]) and relatively high sample and particle throughput, NTA has become a popular method for determining EV concentrations and size distributions [28,116,147]. Furthermore, NTA has been demonstrated to provide reproducible concentration determinations of samples, albeit with an experienced operator, settings optimised for the sample being measured, and dependent on the platform used [148,149]. A significant drawback with light-scatter-based NTA is the fact that it cannot discriminate between different species of particles present in a sample, and sample contamination with lipoproteins have been shown to affect concentration determinations significantly [126,150]. Using fluorophore-conjugated antibodies and tracking particles based on their bound antibody-mediated fluorescence can be used to selectively characterise specific populations of particles [151], however the sensitivity of this approach in terms of minimum number of fluorophores has not been investigated, and its utility for EVs is not completely elucidated.

### Tuneable resistive pulse sensing
Another method that has gained some popularity as an alternative to NTA is tuneable

resistive pulse sensing (TRPS). TRPS is a non-optical method of determining particle size by measuring blockages in a membrane with a single pore as particles pass from one chamber into another. The passage of particles through the pore is measured as changes in the electrical resistance between two chambers separated by the pore, over which an electrical current flows [152]. TRPS has a similar lower size limit to NTA, however it requires the use of multiple membranes with different pore sizes in order to measure the entire EV size range [38]. Similar to light scatter-based NTA, TRPS cannot discriminate between different entities in a sample (*i.e.* EVs, lipoproteins, and protein aggregates/complexes), which could, therefore, impact concentration and size distribution determinations of EVs [150,152]. Finally, TRPS also has some more intra-sample variability than NTA, which possibly stems from changing and resetting the membrane [150,152], or the pore size gradually changing due to interactions between the membrane and the sample [153].

*Flow cytometry*

Since the early days of EV research, flow cytometry has been used to characterise EVs of different cellular origins in biological fluids such as blood [84,85,154]. This is due to its ability to measure multiple light scatter and fluorescence on the surface of single particles in a high throughput manner. Fluorophore-conjugated antibodies are often used to label single EVs based on surface markers, which can provide information on cellular origin, phenotype and activation status of EVs [155,156]. Despite its potentials, conventional flow cytometry lacks adequate sensitivity to detect the bulk of EVs [38,114], and it was only recently that technological advances have led to significant improvements in the sensitivity of dedicated, high-resolution flow cytometers to be able to measure smaller EVs [38]. Flow cytometry is discussed in more detail below.

## 1.2. FLOW CYTOMETRY

Flow cytometry has been a popular method in medical and biochemical sciences since the commercialisation of fluorescence flow cytometers and cell sorters by Beckton-Dickenson (BD) and Coulter (later Beckman Coulter) in the 1970s. This is greatly due to the ability of flow cytometers to measure multiple light scatter and fluorescence parameters off of single particles at a very fast rate ranging from tens of thousands to hundreds of thousands of events per minute in modern machines [157]. Traditionally, flow cytometry has popularly been utilised for characterisation and sorting of cells – specifically those in blood, and, more specifically even, those that have a function in the immune system [158]. In recent times, however, the use of flow cytometry has been appreciated in other fields due to its ability to provide an abundance of data on single particles in a high-throughput manner. One of these fields is the study of extracellular vesicles.

### 1.2.1. PRINCIPLES

As mentioned above, a flow cytometer is a type of apparatus designed for cells (hence "*cyto*") to be measured (and "*metry*"). By adding flow as a prefix, it implies that the cells are in suspension and flowing through the apparatus [158]. This is the rudimentary definition of what a flow cytometer is and does. Regardless of specific configurations, all flow cytometers consist of three basic elements that work together in order to accomplish measurement of single cells or particles: (1) illumination and optics; (2) fluidics; and (3) electronics. These components are discussed below into more detail and illustrated in figure 3.

### Illumination and optics
#### *Illumination*
Lasers are the preferred light source in flow cytometers due to polarised light with a stable energy output and a narrow wavelength range. Furthermore, light from lasers is collimated, making it simple to focus on a specific point without much or any need for correction of the beam. Laser beams are focussed into a tight ellipse across the stream of particles (sample core in figure 3A), and this point is termed the interrogation point. Flow cytometers are often equipped with several lasers with different wavelengths (*e.g.,* 405 nm violet, 488 nm cyan, and 638 nm red) focussed on different points along the sample core, which enables the flow cytometer to gather information on both light scatter and fluorescence from multiple fluorophores from the interrogated particles. The gathering of information on a given particle starts from the second the leading edge enters the first laser beam and ends when the trailing edge leaves the final laser beam, where data collection from each laser is time dispersed to account for the speed at which particles travel between the lasers [157–159].
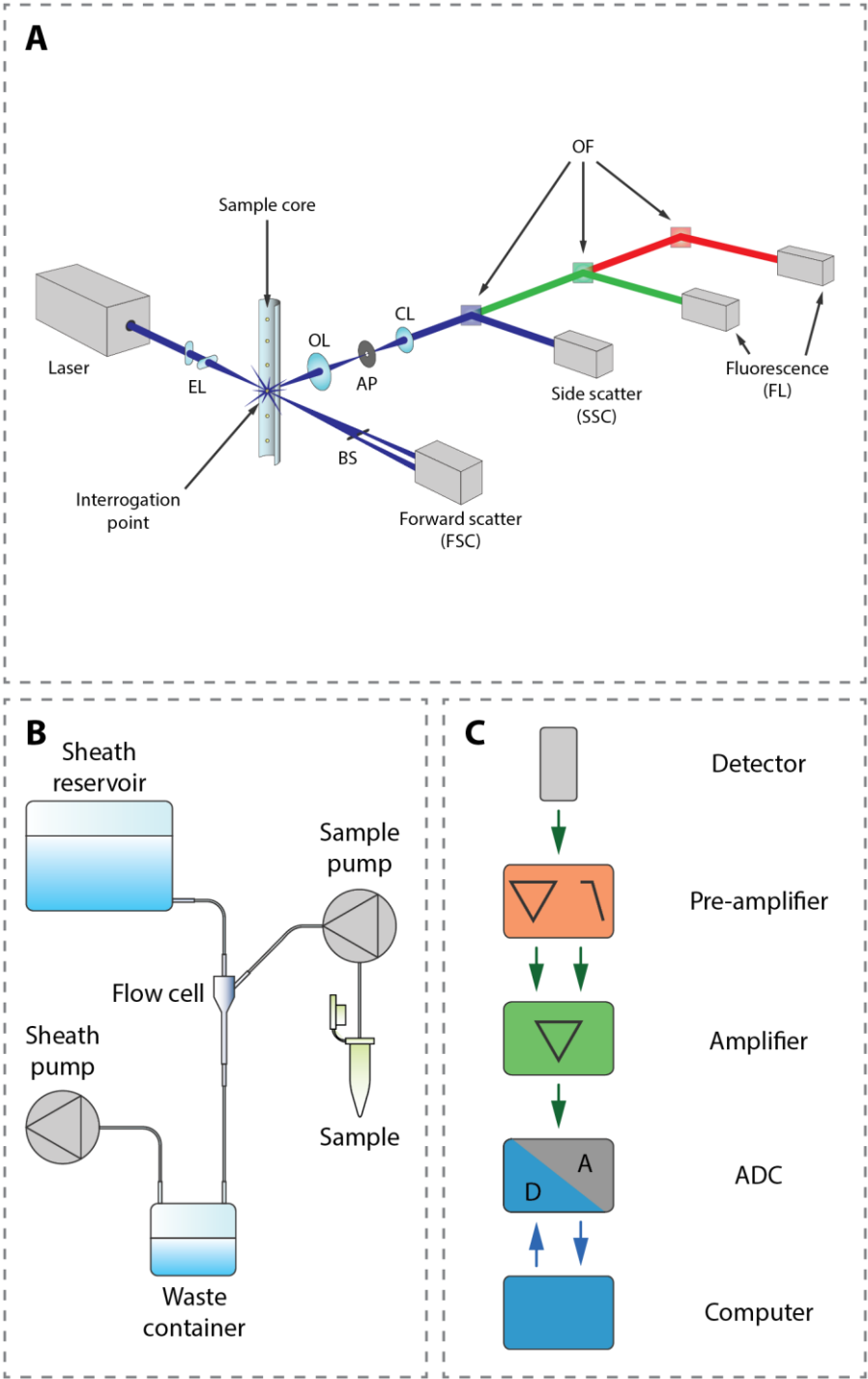
**Figure 3: Basic elements of a flow cytometer. A)** Illumination and optical components. **B)** Fluidic components. **C)** Electronic components. Abbreviations: ADC: Analogue-to-digital converter; AP: Aperture; BS: Beam stopper; CL: Collimating lens; EL: Non-spherical cylindrical lenses; OF: Optical filters; OL: Objective lens.

## *Optics*

The optics in a flow cytometer are responsible for collection light from the particles passing through the sample core. In most conventional flow cytometer set-ups, light is collected at two angles: (1) forward scattered light (FSC) proportionate to the scatter area of particles is collected directly in front of the laser, which has traditionally been used to determine the relative size of cells; and (2) side scattered light (SSC) and fluorescence are collected at an angle perpendicular to the laser [157–159]. Other configurations do, however, exist, where all signals are collected by a single set of optics and then divided into small-angle light scatter (1° to 15°; SALS), medium-angle light scatter (15° to 60°; MALS), large-angle light scatter (60° to 140°; LALS) and fluorescence from all of these angles [160].

The optical components of a flow cytometer are comprised of a set of lenses, dichroic mirrors, filters, apertures and beam stops that direct scattered and fluorescence light to appropriate channels where the light signals are interrogated. In most systems, there are three different sets of lenses. First, on the illumination side of the sample core, a set of cylindrical lenses (EL in figure 3A) shapes the laser beam into an elliptical shape as described above. This is to ensure that minor deviations in the sample core would not result in a lack of illumination. Next, on the collection side of the sample core, signals are collected by a convex objective lens (OL in figure 3A), which focusses scattered or fluorescence light from the particle stream into either an aspherical collimation lens (CL in figure 3A) or an optical fibre that transports it to the collection electronics, where it is passed through a collimator lens. The function of the collimator lens is to ensure that all light travels in a parallel fashion through the system to the collection electronics [157,159].

Another integral component of modern flow cytometers is the use an aperture (AP in figure 3A) on the collection side of the sample core. The aperture (or "*pinhole*") is a small opening in the plane after the collimator lens that ensures that all of the light from the sample core, which is in focussed by the collection lens passes through to the collection electronics, while light that is not in focus stemming from other components (*i.e.,* the flow cell or sheath fluid) is mostly blocked, thus increasing the signal-to-noise ratio significantly [161,162]. In addition, a beam stopper (BS in figure 3A) or blocker bar is often used in the forward direction to block light coming directly from the laser. When particles scatter light, the angle of light changes, and, in most systems, an angle of one degree or more is sufficient for light to pass by the blocker bar [157,160].

Finally, the collected light passes through a series of dichroic mirrors and optical filters (OF in figure 3A), which separates light based on wavelength. This allows for light scatter signals to be separated from fluorescence signals, and also for fluorescence signals from different fluorophores to be separated from each other [159]. Filters and dichroic mirrors are usually classified according to their properties into four main categories. First, long pass filters (LP) blocks light that have a wavelength shorter than the value specified for the filter, while light with a wavelength longer than the value is permitted to pass. Short pass (SP) filers do the opposite of LP filters and permit light with wavelengths shorter than the specified value to pass, while light with wavelengths longer than the value is blocked. Bandpass (BP) filters allow wavelengths within a specific range (bandwidth) to pass through while blocking all other wavelengths. Neutral density (ND) filters attenuate the intensity of light passing through the filter without having any preference towards wavelength. These filters are usually used to limit the amount of FSC in systems with high laser powers [157].

## Fluidics

A key requirement for flow cytometry to measure singe particles is that particles are flowing in single file past the interrogation point at a constant speed with ample separation between particles. This process is accomplished by the fluidics (figure 3B).

The flow in a flow cytometer starts in a reservoir containing the sheath fluid, which is the driving force for particles to flow past the laser at the interrogation point. Sheath fluid is usually driven by a pump, which either exerts positive air pressure on the reservoir and pushes the sheath fluid through the system [159], or exerts negative air pressure on an internal waste container and draws the sheath fluid through the flow cell in that manner. Sheath fluid typically consists of either de-ionised water or buffer, which has been filtered by a series of in-line particle filters before it arrives at the interrogation point in order to prevent unnecessary background signals and noise.

Apart from sheath fluid, the sample, which typically consists of particles suspended in a liquid, must be driven to the point of interrogation. This can either be accomplished by pressurising the sample with the same pump that drives the sheath fluid – albeit with a significant reduction in pressure in order to allow sheath fluid to be the driving force in the system), or with a separate pump that can move the sample independently. The ability to precisely control the pressure of the sample in relation to that of the sheath fluid is critical of optimal focussing of particles in the flow cell, thus making this set-up specifically attractive for applications that require stable measurement of signals [158,159].

The flow cell is the component at the interface between the illumination, optic, and fluidic systems in the flow cytometer, where the particles from the sample pass the lasers, and light signals from this passage is collected. As stated above, it is integral for particles to pass the laser in single file at a constant speed with ample separation in order to gather information on single particles. The flow cell achieves this by

injecting the sample into the centre of the sheath stream in the flow cell, after which the chamber edges of the chamber taper inward and constricts the fluid. As the sheath stream was already moving at a higher velocity into the flow cell than the sample, the sheath fluid determines the speed at which particles are drawn past the interrogation point. Furthermore, gradual constriction of the chamber causes laminar flow of the sheath fluid, which focuses the sample core further, thus resulting in a stable stream of particles passing the laser. If the sample flow rate is low enough and both lasers and collection lenses focussed precisely on the sample core, single particle measurement can be achieved [157].

## Electronics

After light signals have been collected from particles passing the interrogation point, photons must be converted to electrons, which in turn have to be amplified and turned into digital signals, that are finally read and interpreted by a computer (figure 3C).

### *Detectors*

Detectors are the component that detects the photons and converts them into electrons. This is a challenging process, as light signals can often be very dim, their dynamic range (the ratio between the smallest and largest signal) very high, and the rate at which particles are interrogated high.

Traditionally, photon-electron multiplier tubes (PMTs) have been used in flow cytometers, as they satisfy all these criteria. In essence, a PMT is a vacuum tube with a photocathode at the end, where the photons enter the tube, several dynodes stacked through the length of the tube, and an anode at the opposite end of the tube to the cathode. A high voltage potential is placed over the PMT, where each consecutive dynode from the cathode to the anode is held at a higher potential electrical potential. This forces electrons to travel in a very controlled and specific direction through the PMT, thus yielding stable and comparable electrical signals. When a photon strikes the photocathode, electrons are released and fly to the first dynode. This, in turn, ejects a controlled number of multiple electrons from the dynode, which then fly to the next dynode, where each electron here releases a similar number of electrons to the first dynode. This results in an exponential increase in number of electrons as electrons pass from one dynode to the next, which, finally, causes a sharp spike in current to be released from the PMT, when the electrons hit the anode at the end of the PMT. By controlling the voltage potential over the PMT, the dynamic range can also be adjusted [157,163].

In recent years, avalanche photodiodes (APDs) have become increasingly common in flow cytometers. Similar to PMTs, APDs have an electrical potential placed over them. When a photon hits the photosensitive material of the APD, it elicits the release of electrons, after which a cascade effect inside causes the break-down of built up electrons, which then flow out of the avalanche photodiode and cause a spike in current, that can be measured. Although APDs have a lower dynamic range than

PMTs, they have a much higher quantum efficiency and lower intrinsic noise, making them especially good at detecting signals of very low intensity [158,163].

Another detector technology, which deserves an introduction is charged-coupled device (CCD) sensors. These consist of pixels represented by photosensitive semiconductor capacitors coupled to one another in arrays. When a photon elicits the release of electrons from a pixel, it causes the initiation of a controlled shifting of electrons from one pixel to its neighbour, which then shifts the contents further down the chain in so-called shift registers. In this way, the charges can be read one pixel line array at a time and either transformed into a one-dimensional array or a two-dimensional image. CCDs are widely used in microscopy due to their high quantum efficiency and low noise [163], and, recently, they have also seen use in imaging flow cytometers.

Regardless of type or implementation in a flow cytometer, the overall detection characteristics of a detector or parameter can be explained by two main characteristics. The first is quantum efficiency also termed $Q$, which describes how large a signal in terms of photoelectrons a detector yields per unit of light that reaches the detector. The second characteristic is the level of background also termed $B$, which describes the level of background noise stemming from the detector due to either electronic or optical noise [157,158,164–166]. Together, these properties can be used to determine the lower and upper limits of detection on a parameter as well as the smallest signal to noise ratio required to fully discriminate a signal from background noise [158,167,168]. $Q$ and $B$ was originally determined for detectors in flow cytometers by using dim light flashes from light emitting diodes (LEDs) to determine photoelectron noise, and bright beads were used as surrogates for ideal light sources, after which $Q$ and $B$ could be extrapolated by the levels and distribution of beads and the dim light signals [164,166]. More recently, a method using only a set of beads with known coefficients of variability (CV), standard deviations (SD, and intensities in standardized units was proposed for fluorescence [165] and light scatter sensitivity determinations [169]. This made determination of $Q$ and $B$ more accessible, as it does not require operators to install LEDs on their detectors and also no proprietary software to determine photoelectron noise based on LED flashes.

*Amplifiers and signal processing*
After an electrical signal is generated in the detector, it needs to be processed through several steps to be interpretable by a computer. This is accomplished by amplifiers and signal converters.

Pre-amplifiers are located immediately after the detector hardware and amplifies the voltage signal (PMTs) or converts current to voltage (APD & CCD), while it simultaneously pre-shapes the signal and filters out some noise by limiting the bandwidth of signals that are allowed to pass through to the amplifier. Next, the main

amplifier shifts the now pre-shaped and cleaned signal to a level, that the analogue-to-digital converter (ADC) can handle [157].

As signals from detectors are often analogue signals – meaning one-dimensional voltages – they have to be converted to digital pulse-width modulated (PWM) transistor-transistor logic (TTL) signals in order for at computer to be able to interpret them. TTL signals are sent from the ADC to the computer at a specified, high frequency (10-250 kHz), where the width of each pulse is modulated based on the voltage received from the amplifier circuit. This further prevents noise from affecting data interpretation, as all signals with frequencies other than that of the ADC can be filtered out. Furthermore, the functional resolution of a modern flow cytometer is also determined by that of the ADC, meaning that a 10-bit ADC used in a conventional flow cytometer would only allow for a maximum of 4 decades for signal interpretation (by only having 1024 steps of differing pulse widths, which is termed the dynamic detection range or DNR), while modern flow cytometers with 16 or 22-bit ADCs have a DNR of more than 6 decades [157,158].

Another concept warranting an introduction is that of the triggering threshold. Since signals coming from the detectors through the processing electronic circuits and components can consist of a near-infinite number of single pulses when deconstructed (*i.e.,* random electronic or optical noise, signals from unwanted entities in the samples *etc.*), some pre-processing is needed to make the signal processable by subsequent electronic circuits or the computer. The way this is done is by implementing a minimum threshold on a specific channel or multiple channels using logic combinations and electrical components called comparators, where the signal amplitude must be above the specified threshold level before it can be further processed. All signals that have maximum amplitudes below this threshold are rejected, while all signals with thresholds above this threshold are sent for further processing by the computer [157].

When the TTL signal reaches the computer from the ADC, further interpretation is performed. Here, TTL signals are reconstituted into pulses measured by the PMT, which are representative of cells passing the interrogation point. These pulses are then converted into metrics that are more useful for describing the measure particles, such as maximum signal amplitude (height), full-width half-max (width) or integration of the whole signal (area) [157,158]. These values are then saved for each particle in each measured channel to a standardised .FCS file format accompanied by metadata describing instrument settings and experimental parameters [170].

## 1.2.2. CHARACTERISATION OF EXTRACELLULAR VESICLES BY FLOW CYTOMETRY

As mentioned above, flow cytometry has been a popular method used for the characterisation of EVs. Many early EV characterisation studies were of a clinical

nature, in which different EV populations from the different blood cells were differentially quantified between clinical cohort groups based on their expression of surface markers [84,85,171–175]. As newer single-particle characterisation technologies such as NTA and TRPS became more abundantly used for quantification and size distribution quantification, it became evident that the concentration of EVs measured by flow cytometry was up to several orders of magnitude below that of the other methods [29,38]. While some of this could stem from NTA and TRPS failing to discriminate between EVs and the far more abundant lipoproteins in biofluids [29], TEM data still suggested that the lower detection limit of flow cytometers were between 300 and 500 nm, which is above the bulk of EVs [82]. Furthermore, several conventional flow cytometers were also unable synthetic polystyrene nanospheres smaller than 500 nm with a refractive index far above that of EVs, thus scattering light similar to 800 nm to 1000 nm EVs [176,177]. As such, there has been some doubt to whether flow cytometry is a practical method to measure EVs, which often have a diameter well below that of the wavelength of source of illumination, making their detection by triggering on light scatter somewhat problematic. Several approaches were developed to work around the issue of flow cytometry lacking the sufficient sensitivity to characterise EVs, and these are described below.

*Bead-based multiplex phenotype characterisation*
Large, antibody-coated synthetic beads are used to capture EVs, which are then stained by a second set of antibodies against CD9, CD63 and CD81 [139,140,178]. The large beads are easily detectable by conventional flow cytometers and using multiple beads with differing intrinsic fluorescence characteristics and different capturing antibodies, multiple EV phenotypes can be quantified based on the fluorescence signal from the detection antibodies. This approach assumes similar expression of the markers detected by the detection antibodies, and it does not discriminate between single EVs.

*Fluorescence triggering*
Much of the issues with detecting EVs on conventional flow cytometers stemmed from the low amounts of light scattered from EVs. As particle size decreases below a certain diameter, the scattered light from particles drop off rapidly [38]. In contrast, assuming that the expression of surface antigens and the affinity of labels are constant, changes in particle diameter would result in a constant reduction of surface area and, thereby, fluorescence that is equal to the square of the reduction in radius. The use of fluorescence triggering has, therefore, commonly been used in the detection and characterisation of virus particles [179,180]. Furthermore, fluorescence triggering has also been shown to yield better results on synthetic fluorescent beads regarding particle concentration and fluorescence and light scatter brightness [168], and EV could also be detected sufficiently using this strategy [161]. It was further demonstrated that using a fluorescence triggering threshold could detect 15 and 75-fold more fluorescently labelled EVs [114], which corresponded to a lower detection limit between 100 and 150 nm for EVs as suggested by TEM [82].

*Imaging flow cytometry*

Imaging flow cytometry has also shown remarkable sensitivity towards measuring small particles including EVs [181–184]. Unlike traditional flow cytometry, where light scatter and fluorescence signals are all measured as one-dimensional numbers, imaging flow cytometry records an image of particles as they pass the interrogation point, which can later be adjusted and analysed Imaging flow cytometry uses CCDs for the detection of particles, which has a higher quantum efficiency than PMTs and lower noise ratio. With time-delay integration (TDI) of signals, signal intensities for the whole period each particle transitions through the interrogation point are summed and reconstructed into a single image that depicts the morphology and different signal intensities in the particle.

This strategy is particularly good for detecting signals of very low intensities, thus making it a good option for detecting EVs. Due to these features, imaging flow cytometry could detect fluorescent synthetic beads down a 20 nm in diameter based on their fluorescence signal [181] and, additionally, small EVs based on the isolation methods used to purify EVs [183]. Imaging flow cytometry was also shown to outperform conventional flow cytometers in detecting label-positive EVs, regardless of whether a light scatter or fluorescence triggering threshold was being used [182]. Apart from an increased sensitivity to particles with low signals, imaging flow cytometry was also demonstrated to be able to overcome coincident detection of particles by using intelligent image analysis to distinguish particles in different areas from each other, thus enabling the exclusion of some erroneous data [184,185].

*High-resolution flow cytometers*

Apart from the abovementioned strategies for detecting EVs, high-resolution flow cytometers dedicated to measuring small particles that are able to detect light scatter signals from virus particles have been available for some time [186]. Interestingly, these have not seen much use in the field of EV research, and it was only relatively recently that high-resolution flow cytometers began to see their use for EV characterisation. Most high-resolution flow cytometers are based on the same technology and principles as conventional flow cytometers with a few significant differences. These differences revolve mainly around improvements in illumination and detection, whose focus is to either increase the light scatter and fluorescence signals emitted from particles or reduce the amount of background signals and noise.

First, higher laser powers are common in high resolution flow cytometers and have been shown to improve separation of particles on both fluorescence and light scatter [169,187]. This is due to the intensities of both light scatter and fluorescence being directly proportionate to the intensity of the light that illuminates the particle. Next, longer passage time of particles through the interrogation point by reducing the sheath pressure or flow rate has also been demonstrated to improve signal intensities significantly [188], which likely yields better reading of signals and discrimination between true signals and noise. Third, detection of light scatter signals can be

improved by the use of a violet laser [189], as the refractive index of particles increases with decreasing illumination wavelength, thus resulting in more light scatter from the particle when illuminated with lower wavelengths [190]. Fourth, improvements to optical component configurations including obscuration bar or beam stopper sizes and geometries and aperture sizes and placement have been shown to decrease background signals significantly and, thus, increase signal-to-noise ratios [191,192]. Improvement of these parameters have even given rise to flow cytometers that can measure and discriminate light scatter signals that are smaller than fluorescence from a single fluorophore from background [193], thus enabling these cytometers to measure even the smallest EVs and yield a size distribution similar to that for TEM [194].

## 1.2.3. CONTROLS AND PITFALLS IN EXTRACELLULAR VESICLE FLOW CYTOMETRY

A common misconception about EV characterisation with flow cytometry is that EVs have to be purified from the sample in order to avoid pitfalls. While it is true that flow cytometers cannot intrinsically distinguish between light or fluorescence signals from EVs or other entities in a sample, using labels or antibodies against EV-specific proteins, lipids, or components can preferentially identify EVs over other entities. That said, several different factors can confound on interpretation of results. While some of these factors stem from the sample, others can stem from treatment of the sample or from the flow cytometry platform itself. In order be able to interpret EV flow cytometry data correctly, multiple different controls must be prepared to account for specificity of the labels used to identify subsets of EVs, presence and abundance of contaminating entities that can mimic EVs, how protocols and procedures affect the data acquired, and standardisation of signals acquired in order to ensure reproducibility and enable inter-study comparisons.

*Controls for specificity of labels*
Similar to flow cytometry analysis of cells, monoclonal fluorophore-conjugated antibodies are often used to stain specific markers on the surface of EVs in order to determine (1) their presence on the surface of EVs, (2) the number or proportion of EVs that present the marker, and (3) to what extent the marker is expressed on single EVs. Similar to experiments with cells, antibodies can react in a non-specific manner with EVs giving rise to events that are falsely being classified as being positive for a marker [184,195]. In order to account for the extent of this, samples are often stained with non-specific antibodies matched on concentration, clonality, organism, heavy and light chains, fluorophore, and fluorophore to protein ration, where the number of positive events for both the specifically labelled and isotype control labelled are reported [196].

As mentioned above, fluorophore-conjugated Anx5 has often been used for the detection of externalised PS on the surface of EVs. Anx5 requires $Ca^{2+}$ in order to

have an adequate affinity for PS, and, thus, including a control where Anx5 staining is performed without $Ca^{2+}$ has often been used to control for the specificity of Anx5 in defining PS-positive events [82]. In contrast to Anx5, specificity controls are not always as simple for other non-antibody-based labels, and direct controls for EV-specificity are often not available. Although not very common, markers for which there were no direct specificity control have been validated by staining non-EV fractions from purification (*e.g.*, supernatant after high-speed centrifugation [114], or non-EV fractions in density gradient centrifugation [197] or SEC [198]).

## *Events mimicking EVs and procedural controls*

As mentioned above, samples can contain several entities that can mimic EVs when characterised by flow cytometry. One of the main confounders from the sample is the presence of large amounts of lipoproteins. Large lipoproteins such as VLDL and chylomicrons can have similar sizes to small or even medium-sized EVs [110,199–201] and have generally been reported to have higher refractive indices than EVs [202,203]. As such, large lipoproteins generally scatter more light than similarly sized EVs, and are detectable on flow cytometers in samples, where these lipoproteins are present [203,204]. Furthermore, several different generic, non-antibody markers that have commonly been used to label EVs including calcein (intra-vesicular), carboxyfluorescein succinimidyl ester (CFSE; intra-vesicular), di-8-ANEPPS (membrane), Anx5 (membrane), and lactadherin (membrane) have been shown to label lipoproteins in addition to EVs, or, in the case of calcein and di-8-ANEPPS, preferentially label lipoproteins [197,198]. Similar to lipoproteins, protein components in samples have also been shown to be capable of eliciting false-positive events when using generic markers [198]. One method to verify whether measured particles are EVs is to subject stained samples to treatment with detergents, such as Triton X-100, sodium dodecyl sulphate (SDS), or Tween 20. The rationale behind this is control is that lysis of the membrane with detergents would result in the destruction of EVs due to their lack of an internal skeleton, thus leading to a significant decrease in the number of detected positive events, while other, non-EV entities would be unaffected [114,167,196].

False-positive events can also stem from reagents used in preparing EV samples for analysis or the labels used to fluorescently label EVs. Antibodies and other fluorescent proteins used to label EVs contain varying amounts of protein aggregates that can be measured on flow cytometers [205,206]. Even though high-speed centrifugation [114,184,197,204–206] or filtration [206] of antibodies are commonly used to reduce the number of fluorescent aggregates in reagents, there are still aggregates present in the reagents that can be interpreted as marker-positive events and complicate data analysis. In addition to antibody aggregates, lipid anchored fluorophore (LAF) dyes such as PKH26 or di-8-ANEPPS have been shown to create dye aggregates with comparable sizes to EVs making them impossible to discriminate from EVs [207,208]. LAFs can additionally associate with other components complex samples such as blood plasma or serum-containing cell culture medium including lipoproteins

and proteins, thus making these particles impossible to discriminate from EVs on a flow cytometer [209]. To control for the extents of these phenomena, procedural controls such as dilution buffer stained with equivalent concentrations of reagents are often used to quantify the amount of antibody aggregates or LAF particles [114,167,196,205,206].

Another phenomenon that can occur when measuring EVs in samples is coincident or "*swarm*" detection, where multiple EVs are detected as a single event due to their simultaneous passage past the interrogation point [168,177]. This phenomenon has a higher likelihood of occurring if samples are too concentrated, which does not leave ample separation between particles in the sample core. In addition, when two particles transition the interrogation point simultaneously, their light scatter and fluorescence signals are merged and counted as a single event, which can give rise to non-physiological and erroneous phenotypes being detected (*i.e.,* platelet EVs positive for erythrocyte markers). A common way to ensure that single events are being detected is by performing serial dilutions of stained samples, in which concentrations should be chosen where the event-rate of specific phenotypes decreases linearly with a rate corresponding to that of the dilution factor, while the fluorescence levels of marker positive events remain constant [114,167,196,210].

*System controls and standardisation*

Flow cytometry experiments often involve the use of multiple antibodies against different markers on the surface of EVs, each conjugated to different fluorophores including fluorescein isothiocyanate (FITC), phycoerythrin (PE), and allophycocyanin (APC). Fluorophores often have broad emission spectra, which means that there is often some overlap between different fluorophores, which cannot be excluded by using specific filters. For example, particles that have FITC-conjugated (emission peak: 519-525 nm) antibodies bound to their surface would have measurable fluorescence signals corresponding to approximately 20 % of the height of the FITC signal in the channel dedicated to detecting PE (BP 575/30). This phenomenon is known as spectral overlap, or, more commonly in flow cytometry, spill-over. Spectral overlap is normally compensated for by analysing single-stained samples and determining the degree of overlap into all other channels and subsequently subtracting the spill-over from other channels as a linear function [211–214]. In addition, it is also common to present compensated single-stained controls to demonstrate the resulting compensated fluorescence parameters.

When defining which events are positive for a specific marker, it is implied that events that are negative for the marker are defined as well. As such, if either positive or negative events can be identified, the opposite population can also be defined. In EV flow cytometry, it is common to use unstained samples to do just this [114,196]. As there are no fluorescent probes in these samples, they give a good depiction of the level of background fluorescence level of non-fluorescent particles, which corresponds to intrinsic electronic and optical noise in the system.

Other controls that are recommended for ensuring reproducibility of data and interpretability between different studies and platforms include (1) volumetric calibration with counting beads [215], (2) standardisation of fluorescence signals to molecular equivalent of soluble fluorophore (MESF) or equivalent of reference fluorophore (ERF) units [82,114,196,210,216], and (3) refractive index-specific calibration of light scatter signals to scatter surface area in nm$^2$, spherical or hydrodynamic diameter in nm, or particle volume in nm$^3$ [202,210].

# CHAPTER 2. PROJECT AIMS

Prior to the initiation of this project, the main focus of the Laboratory for Metabolic Diseases (Department of Clinical Biochemistry, Aalborg University Hospital, North Denmark Region, Aalborg, Denmark) was to characterise the role and potential of circulating CD36 and EVs as biomarkers in relation to metabolic diseases and disorders, including obesity, the metabolic syndrome, atherosclerosis and familial hypercholesterolaemia.

A central feature linking most of the abovementioned metabolic disorders is the unhealthy accumulation of fat in the abdominal lumen and internal organs [217], and the common pathophysiological mechanisms involved in the pathogenesis and progression of these diseases include inflammation and intracellular oxidative stress [218,219]. CD36 is a class B scavenger receptor that has been demonstrated to be differentially expressed in a variety of cells in individuals with metabolic disorders [220–222], where its functions range from transporting fatty acids into the cell [220,223] to eliciting inflammatory responses via the PPAR$_\gamma$ pathway in response to binding to oxidated LDL [224,225]. Furthermore, circulating CD36 is elevated in several metabolic disorders including abdominal fat accumulation [226], insulin resistance [227], atherosclerosis [155] and non-alcoholic fatty liver disease (NAFLD) and non-alcoholic steatohepatitis (NASH) [228]. Moreover, circulating CD36 is associated with EVs to some degree [229]. In line with the abovementioned observations, we have demonstrated that CD36-bearing EVs are increased in various metabolic disorders, including atherosclerosis [230], obesity [231], familial hypercholesterolaemia [155], lipoprotein-associated oxidative stress [232], and correlated with components of the metabolic syndrome [233]. However, most of our studies and those published by others investigating levels of specific EVs in relation to different metabolic disorders focussed on EVs stemming from different cells directly in contact with blood, including platelets, erythrocytes, monocytes and endothelium. While somewhat informative regarding inflammation and, to some degree, systematic oxidative stress, these blood cell-derived EVs do not provide much information on the state of the affected organs and tissues.

Around the onset of this project, several studies started to report that hepatocyte-specific proteins and transcriptomic products are present in EV purified from blood plasma or serum, and that their expression is altered and often increased in liver disease [234–237]. As such, the original aims of this project were to define and validate antibody panels to identify circulating liver-derived EVs, comparatively analyse their levels and phenotypes in patients with NAFLD and healthy obese and normal weight controls, and to characterize the effect of clinical intervention improving NAFLD on liver-derived EV levels and phenotypes. Quite early on, however, we discovered that several methodological aspects needed to fall into place to be able to conduct robust studies to answer these questions.

## 2.1. STUDY 1: COMPARISON OF DIFFERENT CYTOMETRY PLATFORMS

Although high-resolution and imaging flow cytometers had been available for some time at the onset of this project, their use for comparatively analysing EVs from clinical cohorts had not been significantly compared. Furthermore, few attempts had been made to benchmark the performance of high-resolution and imaging flow cytometers compared to conventional flow cytometers, and most of these either only attempted to demonstrate the smallest detectable synthetic nanospheres [181,238], non-complex samples including purified EVs from cell cultures [161,188], or only single samples, in which the variability of the platform was not assessed [38]. Moreover, the different platforms had not been compared with each other with regards sensitivity and reproducibility, and no standardised methodology to do so had been proposed. This made it hard to gauge how sensitive each method was in detecting and quantifying small particles such as EVs. Furthermore, and more importantly, we and others have previously demonstrated that intra-group variability in patient cohorts were often larger than inter-group differences, which often complicated comparisons of different groups and interpretation of results [155,227,230,233].

Since variability from different sources (*i.e.,* samples, pre-analytical and analytical factors) stacks, it would be imperative to choose a method with low variability to reduce the overall variability in sample EV concentrations. However, since the only attempts to characterise variability had been made on conventional flow cytometers [156,239], it was unknown how well high-resolution and imaging flow cytometers would perform with regards to reproducibility in EV concentration determinations.

Therefore, the specific aims of this study were to [240]:

1) Assess the ability of each platform to detect, resolve and quantify particles within the EV size range;
2) Evaluate the ability of each platform to detect different EV phenotypes directly in a complex biological fluid using blood plasma as a surrogate;
3) Determine intra-day, inter-day, and global variability in detecting and quantifying different EV concentrations directly in blood plasma.

## 2.2. STUDY 2: INVESTIGATION OF METHODS TO REDUCE FLUORESCENT LABEL AGGREGATES

As mentioned above, fluorescent aggregates in labels and antibodies can mimic EVs when samples stained with these reagents are measured by flow cytometry [205,206]. When attempting to detect rare EV populations such as monocyte-derived EVs or organ or tissue-specific EVs in blood plasma, these aggregates can complicate their detection and quantification by conferring additional variability to the quantification of these rare events, or by obscuring them completely. Previously, high-speed

centrifugation was suggested as an effective method of reducing the number of aggregated labels in reagents [205], and this is also widely used [114,184,197,204–206]. In addition, filtration through porous membrane filters has also been suggested as a possible means to remove label aggregates from reagents, and filtration also seemed more effective than centrifugation [206].

Even though high-speed centrifugation is the preferred method of reducing label aggregates, multiple different protocols are being employed with little rationale or evidence provided for choice of protocol. Furthermore, although both centrifugation and filtration have been demonstrated to be able to reduce the number of aggregates in reagents, the variability of these methods in aggregate reduction have not been determined.

As such, the specific aims of this study were to [241]:

1) Investigate the extent of aggregates in labels and antibodies commonly used for EV analysis;
2) Determine efficacy and variability of different centrifugation protocols and filtration to reduce the amount of aggregates in reagents;
3) Demonstrate that labels are still functional after treatment with the preferred aggregate reduction method.

## 2.3. STUDY 3: EVALUATION OF LIPID-BASED METHODS TO IDENTIFY EVS

Although no pan-EV marker has been identified, the lipidic nature of the EV membrane is commonly exploited in defining EVs in flow cytometry experiments. One of the previously most common methods for defining EVs in flow cytometry was using labels against PS, as EVs are thought to expose PS on their surface to some degree [82,84,85,114,156]. Common labels for detecting PS include Anx5 [82,114] and lactadherin [156]. Furthermore, another method that is often used to confirm the specificity of labels towards EVs is the use of a detergent lysis control of positively stained samples [114,167,196]. Due to the lack of an internal skeleton, disruption of the EV membrane results in the complete destruction of EVs, which translates to the near complete abolition of marker-positive events [242]. While both membrane labelling PS and detergent lysis are widely used, lipoproteins could still potentially confound on result interpretation. Similar to EVs, lipoproteins are also covered in a layer of outward-facing phospholipids, of which some proportion is constituted by PS [127,243–246]. Furthermore, lipoproteins have been demonstrated to mimic EVs when treated with detergents such as triton X-100 [204]. As such, lipoproteins such as VLDL and chylomicrons, which are detectable by flow cytometry, resemble EVs on the surface, and whether common labels and detergent lysis strategies can distinguish between EVs and lipoproteins remains somewhat unanswered. Finally, the concentration of PS-containing events has previously been demonstrated to (1) be

increased in postprandial samples compared to fasting samples or after spiking in either VLDL or LDL lipoproteins into fasting samples [247], and (2) correlate significantly with plasma triglyceride levels in cohorts of subjects with various metabolic disorders [230,231,233].

Thus, the aims of this study were to [248]:

1) Optimise and validate labelling of VLDL and chylomicrons with fluorescent polyclonal antibodies against the apolipoproteins B100 (ApoB100; LDL, IDL and VLDL) and B48 (ApoB48; chylomicrons), collectively termed as ApoB48/100 from here on;
2) Evaluate to which degree the common PS labels Anx5 and lactadherin co-stain with ApoB48/100 in blood plasma;
3) Determine whether treatment with triton X-100 affects lipoproteins and especially those positive for the expression of PS markers.

## 2.4. STUDY 4: OPTIMISATION OF ANALYTICAL PARAMETERS FOR CHARACTERISATION OF EVS

Due to their small size, sub-micron particles such as EVs generally present with dim light scatter and fluorescence signals with a large proportion of those falling below the lower detection threshold of most flow cytometers [38]. The lower detection threshold can differ from one flow cytometer to another [38,238] or on the same flow cytometer when different settings are used [169,187,191], which could lead to differences in numbers and phenotypes of EV populations detected [196,240]. Since the concentration of EVs increase exponentially with decreasing size, even small changes in the lower resolution limit of a flow cytometer could result in large differences in detected EV concentrations or phenotypes [38]. Moreover, improper choice of analytical parameters such as laser power and PMT voltage can adversely impact the lower resolution limit of a flow cytometer, which could either lead to excessive background noise or improper separation of dim signals from background [187]. These factors could confer additional variability to results from clinical studies and thus further complicate their interpretation.

Currently, it is becoming common practice to report the lower and upper detection limits of flow cytometers in standardised units to enable reproducibility and comparison across platforms and studies [196]. Although standardised units for fluorescence signals such as MESF and ERF are common [165,216,249] and for light scatter signals such as scatter cross section area becoming increasingly common [169,202,210], these are rarely – if ever – used for determining optimal analytical parameters. Moreover, reporting limits of detection for only one combination of analytical settings does not provide any information on whether the limit is governed by low quantum efficiency ($Q$) or high background noise ($B$) [165], nor whether the reported combination of settings are optimal for the flow cytometer being used.

Therefore, the aims of this study were to [250]:

1) Systematically vary analytical parameters that affect detection of dim signals including laser power and PMT voltage while measuring synthetic nanospheres, whose signals are either well-defined or calculated in terms of standardised units.

2) Calculate and illustrate quantum efficiency $Q$, background noise $B$, and the theoretical lower resolution limit $R$ based on $Q$ and $B$ in standardised units for each combination of analytical settings in order to define optimal settings for measuring dim fluorescence and light scatter signals.

# CHAPTER 3. CONVENTIONAL, HIGH-RESOLUTION AND IMAGING FLOW CYTOMETRY: BENCHMARKING PERFORMANCE IN CHARACTERISATION OF EXTRACELLULAR VESICLES

## 3.1. METHODS

### 3.1.1. FLOW CYTOMETRY PLATFORMS

Three different flow cytometry platforms were included for benchmarking in this study:

- BD FACS Aria[TM] III high-speed cell sorter (BD Biosciences, San Jose, CA, USA) was included to represent conventional flow cytometers, as this was the platform we had used previously in multiple clinical cohorts [156,231,233].
- Apogee A60 Micro-PLUS high-resolution flow cytometer (Apogee Flow Systems, Hemel Hempstead, UK) was included in the comparison, as this platform had previously been demonstrated to provide significant improvements to the detection of small particles when compared to conventional flow cytometers, including synthetic nanospheres [238] and EVs [38].
- Amnis® ImageStream® X Mk II (Luminex Corporation, Seattle, WA, USA) was included due to its ability to detect synthetic nanospheres down to 20 nm in size based on fluorescence [181] and its supposed ability to measure small EVs [182].

### 3.1.2. LIMITS OF DETECTION AND QUANTIFICATION

To assess the limits of detection (LoD) and quantification (LoQ), a mixture of non-fluorescent silica (sizes: 180 nm, 240 nm, 300 nm, 590 nm, 880 nm, 1300 nm; RI = 1.47 @ $\lambda$ = 405 nm) and fluorescent polystyrene (sizes: 110 nm, 280 nm and 500 nm; RI = 1.63 @ $\lambda$ = 405 nm) nanospheres were measured five times on each platform, and gates were placed on each population. In addition, as high-resolution and imaging

flow cytometry were able to detect the dimmest light scattering nanospheres (180 nm silica), in-house, dimly fluorescent 100 nm silica nanospheres (RI = 1.47 @ $\lambda$ = 405 nm) were analysed separately to investigate whether these can be detected on the two platforms. LoD was defined as the smallest nanosphere population that could be defined on a given platform. LoQ was defined as the smallest nanosphere population, which could be quantified with a coefficient of variability below 20 %. Finally, the concentrations of each nanosphere population detected were compared between the different cytometry platforms to assess the ability of each platform to detect nanospheres of different sizes.

### 3.1.3. DETECTION OF EVS IN COMPLEX BIOLOGICAL FLUIDS

To test the ability of the different cytometry platforms to detect EVs in complex biological fluids, we decided to stain EVs directly in platelet-poor blood plasma (PPP). PPP was purified from waste whole blood collected from healthy blood donors at the Danish Blood Bank (Department of Clinical Immunology, Aalborg University Hospital, North Denmark Region, Aalborg, Denmark). PPP was collected from whole blood by a two-step centrifugation protocol as described previously [111] consisting of sequential centrifugations of (1) whole blood and (2) supernatant from the first centrifugation step at 2500 x $g$ for 15 minutes, where the supernatant from the last cycle is collected and used for analysis. PPP from the different donors was pooled and aliquoted to have comparable samples to analyse on all platforms.

PPP was stained with FITC-conjugated lactadherin to label PS on the surface of EVs, PE-conjugated antibody against CD36, and APC-conjugated antibody against CD41. PS was used as a "universal" EV marker and used for triggering on the FACS Aria III and Apogee A60 Micro-PLUS. Based on these labels, we defined four populations of interest whose concentrations were comparatively analysed between platforms. These were (1) PS+, (2) PS+|CD41+, (3) PS+|CD36+, and (4) PS+|CD41+|CD36+.

### 3.1.4. REPRODUCIBILITY OF MEASUREMENTS

Four different measures of variability were determined for each EV phenotype described above. First, intra-day variability was assessed by labelling 20 PPP aliquots and measuring them on each platform during a single analysis day. Next, inter-day variability was assessed by labelling 5 aliquots for five consecutive analysis days, where daily means were compared. Finally, global variability was assessed by measuring the variability across all samples from intra and inter-day samples to assess the variability expected to be present when analysing an entire cohort of samples across multiple analysis days.

## 3.2. KEY RESULTS

### 3.2.1. DETECTION OF SYNTHETIC NANOSPHERES

The Apogee A60 Micro-PLUS and the ImageStream X Mk II hade the lowest LoDs
by being able to detect both the fluorescent 110 nm polystyrene nanospheres and the
dimly fluorescent 100 nm silica nanospheres. Although the FACS Aria III had a
significantly higher LoD than the Apogee A60 Micro-PLUS and the ImageStream X
Mk II based on non-fluorescent silica nanospheres (LoD = 300 nm), it was able to
detect fluorescent 110 nm polystyrene nanospheres when triggering on fluorescence,
thus confirming that the functional LoD for this platform is increased when using
fluorescence triggering instead of light scatter triggering (figure 2 in [240]).

The Apogee A60 Micro-PLUS had the lowest LoQ of the three platforms tested, being
able to reproducibly quantify all nanosphere populations. The ImageStream X Mk II
had a higher LoD than the Apogee A60 Micro-PLUS for non-fluorescent silica
nanospheres, only being able to detect silica nanospheres larger than 240 nm with
sufficient reproducibility. Interestingly, the LoQ for fluorescent polystyrene
nanospheres was lower on the ImageStream X Mk II than that of silica nanospheres,
which was likely to be due to these nanospheres being clearly distinguishable from
background. The FACS Aria III could not quantify any of the nanospheres with an
acceptable reproducibility, regardless of having used BD TruCount[TM] counting beads
to volumetrically standardise sample flow rate (figure 3 in [240]).

In line with observations of LoD and LoQ, the Apogee A60 Micro-PLUS detected
larger concentrations of small nanospheres than the two other platforms and was
followed by the ImageStream X Mk II. All three platforms detected similar
concentrations of the larger nanospheres (silica: 590-1300 nm; polystyrene: 280 &
500 nm) (figure 2H in [240]).

### 3.2.2. DETECTION OF EVS

The ImageStream X Mk II could detect significantly higher concentrations of all EV
phenotypes than the two other platforms with the exception of the triple-stained
PS+|CD41+|CD36+ population, which was similar for the Apogee A60 Micro-PLUS.
Finally, the Apogee A60 Micro-PLUS could detect significantly higher
concentrations of all phenotypes than the FACS Aria III (figure 4A-D in [240]).

### 3.2.3. REPRODUCIBILITY OF EV MEASUREMENTS

The Apogee A60 Micro-PLUS (CV = 5.5 – 7.5 %) and FACS Aria III (CV = 6.2 –
9.2 %) both had low intra-day variabilities in quantifying all of the EV phenotypes,
while the ImageStream X Mk II had significantly higher intra-day variabilities (CV =
13.9 – 19-2 %) (figure 4E-H in [240]). Conversely, the ImageStream X Mk II had the

lowest inter-day variabilities (CV = 4.4 – 13.1 %), while the Apogee A60 Micro-PLUS had similar or slightly higher inter-day variabilities (CV = 6.3 – 12.7 %), and the FACS Aria III had markedly increased inter-day variabilities (CV = 10.9 – 15.0 %) (figure 4I-L in [240]). Finally, the global variabilities for all platforms were higher than both the intra and inter-day variabilities. The Apogee A60 Micro-PLUS had the lowest global variabilities (CV = 9.3 – 12.5 %) followed by the FACS Aria III (CV = 13.5 – 16.9 %) and, finally, the ImageStream X Mk II (CV = 13.0 – 20.5 %) (figure 4 M-P in [240]).

## 3.3. DISCUSSION

As stated above, sensitivity to detect small particles with dim light scatter and fluorescence signals, and the ability to quantify different EV phenotypes reproducibly are both important for the clinical applicability of EV flow cytometry. In this study, we assessed both parameters.

### 3.3.1. LIMITS OF DETECTION

By using a set of synthetic nanospheres with varying bead sizes, refractive indices, and fluorescence properties, we determined the LoD and LoQ of the three platforms. This approach yielded similar LoDs for the high-resolution and the imaging flow cytometers, whereas the conventional flow cytometer had a significantly higher LoD than the two other platforms. There are three main issues with this strategy.

First, the LoD of both the high-resolution and imaging flow cytometer were equal to the smallest bead measured, by which it cannot be excluded that the true LoD is below what is reported in this study. While there is no data regarding this matter for the Apogee A60 Micro-PLUS, the ImageStream X Mk II has been demonstrated to measure fluorescent polystyrene nanospheres down to approximately 20 nm based on their fluorescence, although they were not discriminable from 100 nm fluorescent nanospheres in the SSC channel [181].

Second, the use of synthetic nanospheres top determine functional LoDs is hard to translate to the biological equivalent due to differing refractive indices between the nanospheres and biological EVs. Polystyrene nanospheres have a refractive index around 1.59 – 1.63 [251,252] and silica 1.45 [251–253] at wavelengths commonly used for light scatter illumination in flow cytometers. On the other hand, the refractive index for biological EVs has been determined to be below 1.40 on average [254]. As such, depending on the optical and illumination setup of the flow cytometry platform, polystyrene and silica nanospheres could scatter between 40 and 300 or 5 and 50-fold more light than biological EVs of similar sizes [176,202,252]. Recently, however, several different methods have been proposed to standardise light scatter signals into scatter area based on Mie light scatter theory, which can then be converted into either diameter, surface area or volume [192,202,210]. These signals can then be used to

infer the relative diameter of an EV particle based on the light scattered from the synthetic nanospheres, thus yielding a value that is more interpretable in relation to practical LoD when measuring EVs.

Third, connected to the second issue, this study did not investigate the fluorescence LoDs for the three platforms, which could have been more informative to their actual sensitivities, as (1) triggering on fluorescence markers has been shown to improve sensitivity of conventional flow cytometers towards detecting small particles significantly [82], and (2) being able to distinguish different EV phenotypes from each other based on their staining with fluorescent labels is more important than determining the size profiles of EVs, if specific EV phenotypes are to be used as biomarkers for disease. In order to have a standardisable measure of fluorescence LoD units such as MESF or ERF would have to be used [249]. One considerable hurdle in doing this is that most nanospheres whose fluorescence values are calculated in standardised units are well above the median levels of epitopes on the surface of EVs and, additionally, well above what high-resolution or imaging flow cytometers can detect in terms of fluorescence [167,184,198,210], thus making them unsuitable for determining LoD as done in this study. Alternatively, these calibration nanospheres can be used to determine the quantum efficiency of the system to detect fluorescence light (Q) and the background levels of light and noise (B) [165], which can then be used to calculate the fluorescence resolution or LoD [164,167]. Additionally, this methodology can also be applied to light scatter signals, where beads with known sizes and refractive indices are used to calculate Q and B in terms of scatter area and subsequently used to calculate the functional LoD in light scatter channels [169]. This is presented in more depth and expanded upon in study 4 of this thesis [250].

## 3.3.2. VARIABILITY AND REPRODUCIBILITY

Although the LoD of measuring particles in this study might only be of limited use, the LoQs and efficiency of each platform to detect the different nanosphere populations are certainly interesting when interpreting EV variability measures for each platform.

First, the Apogee A60 Micro-PLUS demonstrated the lowest overall variabilities in quantifying EVs and all nanosphere populations, and it also detected consistently more of the smaller nanospheres than the other platforms. This suggests that the flow of sheath fluid is extremely stable with a narrow and stable sample core, thus resulting in stable and consistent detection of all nanosphere populations including those exhibiting low light signals regardless of when the sample is analysed.

Second, while the ImageStream X Mk II presented with the lowest inter-day variability, it had the overall highest intra-day and global variabilities compared to the other platforms. When looking at the data on the different nanosphere populations, the ImageStream X Mk II detected generally fewer of the smaller nanospheres or those

with low fluorescence signals, and the variability of these populations were also higher than the cut-off value of 20 %. Three of the main factors that could influence this are (1) a large sample core, which would cause particles to be out of focus and disproportionately affect smaller particles or those with dim fluorescence signals; (2) unstable sample stream, as trade-offs had to be made between sensitivity and stability for the system to optimally detect EVs; and (3) interpretation of results by proprietary software, where object detection and masking protocols are mainly optimised for detection of cells. Considering that the number of EVs increases exponentially with decreasing size – and thereby also surface area and available epitopes for labels to bind to – it could be speculated that the variability in concentrations of different EV populations is mainly due to smaller EVs or those with lower fluorescence signals. It follows that the variability would especially be exacerbated by the fact that the ImageStream X Mk II generally detected larger concentrations of all of the investigated phenotypes than the other platforms, which is largely owed to an increase in sensitivity to dim signals and, therefore, smaller EVs [240].

Third, although the FACS Aria III had similar intra-day variabilities to the Apogee A60 Micro-PLUS, it presented with the highest inter-day variabilities and moderately high global variabilities for concentration determinations. Interestingly, all the measured nanosphere populations had variabilities higher than the cut-off value of 20 %. Several factors could contribute to these results. Due to the system being optimised for cells regarding flow rates, the sample core is generally larger, meaning that smaller particles could pass the interrogation point in different areas, thus resulting in inconsistent illumination and signal readouts [215]. Moreover, minute differences in daily start-up calibration by BD CS&T beads could also influence the flow of particles and the placement of the sample core. This could result in the sample core moving slightly between different focal planes of the lasers and optics between analysis days, thus causing signals from particles to be out of focus, which could affect their detection.

# CHAPTER 4. ZOOM IN ON ANTIBODY AGGREGATES: A POTENTIAL PITFALL IN THE SEARCH OF RARE EV POPULATIONS

## 4.1. METHODS

### 4.1.1. TREATMENT OF FLUORESCENT LABELS

Five different treatments of fluorescent labels were investigated to reduce fluorescent aggregates. First, three centrifugation protocols were used, where labels were centrifuged at 17.000 x *g* for either 5 minutes, 10 minutes, or 30 minutes, after which supernatant was used for staining samples. Next, filtration of labels was investigated, where labels were subjected to gravity filtration through hydrophilic centrifugal filters with 0.45 µm pore sizes. In addition, it was tested whether pre-wetting of filters by pre-filtration of buffer improved the efficacy of this treatment. Finally, untreated labels were used as comparators.

### 4.1.2. SET-UP

The extent of label aggregates being present in fluorescent labels was assessed by comparing unstained buffer with buffer stained with untreated labels.

To test the efficacy of treatments to reduce fluorescent label aggregates, buffer was stained with untreated or treated fluorescent labels. A total of 8 different labels were included, and 5 aliquots of buffer were stained with panels of antibodies and labels (described in table 1 of [241]), and this was repeated for 5 consecutive days. Thus, a total of 70 data points were produced for each label treatment method, and mean reductions in fluorescent event was calculated compared to untreated labels, as was the coefficient of variability for reductions in aggregates.

Finally, PPP from healthy individuals (collection described above) was stained with labels subjected to filtration in to test their functionality after treatment.

## 4.2. KEY RESULTS

### 4.2.1. PRESENCE OF FLUORESCENT AGGREGATES

First, we demonstrated that fluorescent aggregates were present in all fluorescent labels tested in this study. Furthermore, different labels also presented with different amounts of aggregates regardless of fluorophore, and the same label could present with different amounts of aggregates in different antibody panels. For the same fluorescent label, concentrations could vary between 6 and 648-fold compared to unstained PBS depending on the panel (table 3, figure 2, and supplementary figures S3 and S4 in [241]). Moreover, some proportion of label aggregates also seemed to be functional and capable of binding to EVs (figure 4 in [241]).

### 4.2.2. EFFICACY OF TREATMENT TO REMOVE FLUORESCENT AGGREGATES

Filtration and pre-wetted filtration significantly reduced the number of fluorescent aggregates in labels compared to untreated labels. Furthermore, of the centrifugation protocols, only centrifugation for 30 minutes significantly reduced the number of aggregates in labels, albeit only moderately (figure 3 and table 4 in [241]). Apart from having the highest reductions in aggregates, filtration and pre-wetted filtration also had the lowest variabilities in reducing label aggregates (table 4 in [241]).

### 4.2.3. FUNCTION OF LABELS AFTER FILTRATION

After filtration, different markers on EVs could still be successfully stained in PPP. This also revealed that filtration preferentially removes larger label aggregates that scatter more light and are more fluorescent (*i.e.*, more proteins or fluorophores aggregated together), while, for certain labels, the reduction in aggregates is only mild (figure 4 in [241]).

## 4.3. DISCUSSION

Although the observation that label aggregates are present in commercial fluorescent labels has been described previously [167,205,206], the extent and intricacies of this issue has not to our knowledge. The most striking of our observations were those that there generally were much variability in the number of aggregates between different labels, and that the same label could appear to have differing amounts of aggregates depending on the panel it was present in. One explanation for this could be the presence of soluble denatured oligomers called aggregation nuclei in certain labels, which could initiate further aggregation with multiple other labels when additional labels are added [255]. This process could be somewhat variable depending on external factors including temperature, pressure, shaking and shearing, solvent properties and protein concentration [256], all of which could confer the variability in

the number of aggregates observed in this study. Furthermore, we additionally demonstrated that some label aggregates are still functional and capable of binding to their specified antigens, and that these aggregates are likely able to bind multiple EVs, which could give rise to populations with erroneous or nonsensical expression of surface markers, thus complicating data interpretation.

Next, contrary to previous reports [167,205,206], we did not see a consistent effect in reduction of label aggregates by high-speed centrifugation apart from the 30 minute centrifugation protocol, which only resulted in a moderate and somewhat variable reduction in aggregates. One of the main issues with this protocol is that it is highly sensitive to disturbances, which could result in resuspension of aggregated proteins. Another element of variability in high-speed centrifugation protocols is the fact that sedimentation is both dependant on particle size and density relative to that of the displaced medium [257], where sizes of aggregates can vary much depending on the factors that have led to their formation [256], and protein density is inversely related to size to a certain extent [258]. Taking into account that aggregates are often a heterogeneous population, it follows that all aggregates are not sedimented equally by high-speed centrifugation, and that the number of aggregates present in labels are, furthermore, dependent on the length of the tube, centrifugation time, and the volume of labels used for staining. As such, it is not surprising that 30-minute centrifugation of labels was the only centrifugation protocol to reduce the number of aggregates significantly, nor that the variability in reduction of aggregates was variable with this protocol.

On the other hand, it has also been demonstrated previously that filtration of labels is more effective than centrifugation in removing fluorescent aggregates, and that labels were still viable after removal of aggregates [206]. In this study, we additionally demonstrated that the method could be marginally improved by pre-wetting the filtration membrane. The rationale behind this step was to (1) clear the membrane of possible impurities from the manufacturing process, and (2) to slightly decrease the loss of viable label due to retention in the filter membrane. Although the reduction in aggregates was significantly different between pre-wetting and non-pre-wetting of the filtration membrane, there was little practical significance in the concentration of fluorescent aggregates present in the treated labels. Another interesting observation regarding filtration was that it preferentially removed fluorescent aggregates with higher light scatter and fluorescence signals, while those with lower signal intensities in some labels were largely unaffected. This could imply that only larger aggregates were removed with the 0.45 µm filter, and that the use of a filter with smaller pore diameters could offer some advantages in removing smaller aggregates. This was, however, not the case in a previous study by Inglis *et al.*, where no differences were observed between filters with 0.65, 0.45 and 0.22 µm pore sizes [206]. This could, however, be explained to some extent by different sensitivities to measuring small particles with weak signals, by the specific labels used, or by different instrument settings. Thus, a further investigation would be needed to answer this question fully.

# CHAPTER 5. LIPID-BASED STRATEGIES USED TO IDENTIFY EXTRACELLULAR VESICLES IN FLOW CYTOMETRY CAN BE CONFOUNDED BY LIPOPROTEINS

## 5.1. METHODS

### 5.1.1. LIPOPROTEIN LABELLING STRATEGY

Commercial VLDL (Lee BioSolutions, Maryland Heights, MO, USA) and chylomicrons (Lee BioSolutions) were used to validate the specificity of PE-conjugated goat polyclonal IgG anti-ApoB48/100 antibody (GeneTex, Irvine, Ca, USA).

First, the anti-ApoB48/100:ApoB concentration in commercial lipoprotein samples was optimised by staining serial dilutions of lipoprotein samples as described previously [204]. This was additionally done for PPP due to the abundance of ApoB-containing lipoproteins in blood, which could hamper the detection of lipoproteins if too few are present compared to the abundance of antigens in the sample.

Next, staining with specific antibody was compared to staining with a matched isotype control antibody, unstained sample, and buffer with reagent control in both lipoprotein samples and PPP.

Finally, the light scatter signals of the populations were correlated to silica nanospheres (RI = 1.47 @ $\lambda$ = 405 nm), which have similar refractive indices to lipoproteins and thus scatter light similarly [202,203].

### 5.1.2. LIPID-BASED STRATEGIES TO DETECT EVS

Frozen PPP and fresh PPP from three healthy, fasting subjects were collected as described above. PPP was labelled with anti-ApoB48/100, anti-CD41, and either lactadherin or Anx5, both PS markers, to investigate to which extent PS markers stain lipoproteins. CD41 was used as a comparator, as it is a trans-membrane part of the integrin $\alpha_{IIb}\beta_3$ fibrinogen receptor on platelets and megakaryocytes [81] and would, therefore, not be located on lipoproteins.

Next, samples stained with specific antibody were treated with triton X-100 at a final concentration of 1 % (vol/vol) for at least 30 minutes at room temperature to assess whether lipoproteins – and especially those that co-stain with EV markers – are lysed in addition to EVs when using this control.

## 5.2. KEY RESULTS

### 5.2.1. VALIDATION OF ANTIBODY LABELLING OF LIPOPROTEINS

First, we demonstrated that dilution of commercial VLDL and chylomicrons was necessary to label ApoB to a degree, where it could be detected on the flow cytometer. In addition, we demonstrated that the polyclonal anti-ApoB48/100 antibody detected populations at the adequate sample dilutions that were not present in isotype controls, unstained controls or buffer with reagent controls, thus suggesting that the anti-ApoB48/100 was specific towards ApoB-containing lipoproteins, and that we were detecting single ApoB events (figure 1A, B, D and supplementary figure 4A & B in [248]). Next, we demonstrated that a single population was detected in the VLDL sample with light scatter comparable to silica nanospheres between 100 and 180 nm. Chylomicrons, on the other hand, had two distinct populations: one with light scatter signals comparable to VLDL, and another with light scatter signals similar to 180 to 300 nm silica nanospheres (figure 1E in [248]). Finally, we demonstrated that ApoB-containing particles could also be detected in blood plasma after dilution of the sample (figure 1C and supplementary figure 4C in [248]).

### 5.2.2. CO-STAINING OF LIPOPROTEINS WITH PS LABELS

In frozen PPP, both Anx5 and lactadherin co-stained with anti-ApoB48/100, albeit to varying degrees (43 % vs. 7.6 %), while very little co-staining of CD41 and ApoB was observed (3.4 %), where most of this could be accounted for by non-specific interactions between the sample and the two antibodies (figure 2A in [248]). To investigate the possibility of this being an artefact that arises during freezing and thawing, we collected PPP from three fasting, healthy individuals and stained it similarly to frozen PPP. Again, both lactadherin and Anx5 co-stained with ApoB, and Anx5 to a higher degree than lactadherin ($19.6\pm5.0$ % vs. $5.3\pm1.7$ %), while CD41 did not co-stain significantly with ApoB ($2.3\pm0.2$ %; figure 2B in [248]). The fresh samples did, however, reveal that freezing and thawing affect EV populations, as more events with higher scatter and fluorescence values could be observed in these samples compared to those that were frozen and thawed (figure 2A vs. B in [248]).

### 5.2.3. DETERGENT LYSIS OF EVS AND LIPOPROTEINS

After treatment with triton X-100, the concentration of events positive for any of the markers included in the panels decreased. The concentration of Anx5 single-positive events were only mildly reduced by detergent lysis (38.1 %), while the concentration

of Anx5 and ApoB double-positive events were reduced significantly (73.5 %). Lactadherin-positive events were nearly completely abolished by detergent lysis (95.1 % reduction), as was lactadherin and ApoB double-positive events (88.1 %). Lysis of CD41 positive events was less pronounced than with lactadherin (72.2 %), however this could be due to the presence of a significant amount of anti-CD41 antibody aggregates (27.5 % of total CD41 population), and the CD41 and ApoB double positive population was only mildly affected, further strengthening the notion of these events being artefactual (figure 3 in [248]).

## 5.3. DISCUSSION

### 5.3.1. LABELLING OF LIPOPROTEINS

The use of polyclonal antibodies is not common in EV research due to batch-to-batch variability in affinity, specificity, and off-target effects. However, since ApoB-containing lipoproteins only contain one copy of the ApoB protein [259], the use of monoclonal antibodies was not a viable strategy due to their specificity towards a single epitope. Thus, to be able to detect VLDL and chylomicrons, we used polyclonal antibodies, which should, in theory, be able to label multiple epitopes on ApoB.

While there is ground for concern when using polyclonal antibodies, the staining of ApoB in our case was likely specific, as (1) a significant population of PE fluorescence-positive events could be seen appearing with gradually decreasing sample concentrations, which (2) was not present in isotype controls, (3) unstained controls, or (4) buffer with reagent controls. Furthermore, with a linearly decreasing concentration with post-stain sample dilutions and a stable median fluorescence intensity, it was unlikely for these events to arise from coincident detection.

Based on the dilution of PPP [29] and the staining concentration, we estimated that the antibody:ApoB ratio would be around 10-15. However, the median ERF value for ApoB was 104, which is significantly higher than our estimate. This could either be due to incomplete detection of all ApoB particles, stoichiometry of ApoB on larger lipoproteins such as VLDL and chylomicrons enabling binding of more antibodies on the surface of these lipoproteins than on smaller ApoB-containing lipoproteins, or both.

VLDL has traditionally been shown to have sizes between 30 and 80 nm [110]. Here, however, we estimated that the VLDL particles in our samples are between 100 and 180 nm in size based on light scatter of silica nanospheres with similar refractive indices to lipoproteins. On explanation could be that our estimation of size based on solid nanospheres could be too simplistic to account for the complex interplay between layers of differing refractive indices as on lipoproteins and EVs [252]. On the other hand, VLDL particles with sizes larger than 80 nm have been described, and these account for approximately 3 % of the total VLDL population [199–201].

## 5.3.2. LIPID-BASED EV METHODS AND LIPOPROTEINS

We demonstrated that both Anx5 and lactadherin can bind to ApoB-containing lipoproteins in PPP, which implies that these labels are able to stain PS on the surface of these particles in addition to that of cells and EVs. The presence of PS on lipoproteins has been somewhat contested with some studies failing to identify PS [260], whereas others have shown it to be present to varying degrees on the different ApoB-containing lipoprotein fractions [127,243–246]. As such, our results support the notion that PS is present on ApoB-containing lipoproteins. Furthermore, our results also suggest that the increase in PS-positive events in postprandial samples as reported previously [247] or the correlation of different EV phenotypes with triglycerides [230,231,233] could, in part, be due to direct labelling and detection of lipoproteins bearing PS on their surface.

Our results further imply that Anx5 and lactadherin have different affinities towards lipoprotein associated PS. This could, in part, be explained by the different binding preferences of these two labels. Although lactadherin has a higher affinity towards particles with a larger curvature, its affinity towards PS is nearly abolished when presented with a monolayer membrane such as on lipoproteins [261]. On the other hand, Anx5 has been shown to be capable of binding to monolayer membranes in the presence of $Ca^{2+}$ [262,263].

We further demonstrate that ApoB-containing lipoproteins are affected by detergent lysis, and this is especially true for the fractions of ApoB-containing lipoproteins that are also positive for the expression of PS. Our results are in line with what has been shown previously [204], however, to our knowledge, we are the first to demonstrate this for ApoB-containing lipoproteins positive for the expression of PS.

## 5.3.3. LIPOPROTEIN CORONA ON EVS

Previously, based on *in vitro* experiments, it has been proposed that one method in which LDL can mimic EVs and confound on results is by attaching itself to the surface of EVs [204]. Furthermore, LDL can interact with cells via specific membrane proteins including scavenger receptors such as CD36 [264–266], which are abundantly present on most cells [225] and EVs of various cellular origins [155,230–233]. We could, however, not find evidence of this in our analysis, as only a very small proportion of CD41-positive events were associated with ApoB-positive events, and most of these were likely due to non-specific interactions between the sample and antibodies.

# CHAPTER 6. A SYSTEMATIC APPROACH TO OPTIMISE ANALYSIS PROTOCOLS FOR FLOW CYTOMETRY CHARACTERISATION OF SUB-MICRON PARTICLES

## 6.1. METHODS

### 6.1.1. SYNTHETIC NANOSPHERES

For determination of lower detection limits in standardised units, two sets of nanospheres were used. For fluorescence signals, 6-peak fluorescent Ultra Rainbow Calibration Particles with known ERF values for each individual nanosphere population on APC, FITC and PE parameters were used. For light scatter, Apogee Calibration Bead Mix consisting of non-fluorescent silica (RI: 1.470 @ $\lambda = 405$ nm; Sizes: 180±21.6 nm; 240±28.8 nm; 300±30 nm; 590±59 nm; 880±88 nm; 1300±65 nm) and fluorescent polystyrene (RI: 1.63 @ $\lambda = 405$ nm; Sizes: 110±11 nm; 500±25 nm) was used. Light scatter cross section area for each bead population was integrated for all angles ($4\pi$ radians) using open-source software (MiePlot v. 4620 by Phillip Laven [267]) taking into account average bead diameter and refractive index, incident illumination wavelength, and sheath fluid refractive index (water: RI 1.345 @ $\lambda = 405$ nm) – all factors that influence the light scatter efficiency of single particles.

### 6.1.2. DETERMINATION OF QUANTUM EFFICIENCY, BACKGROUND, AND RESOLUTION LIMIT

Sensitivity of measurement parameters on flow cytometers can be interpreted by knowing the quantum detection efficiency $Q$, which describes the number of statistical photoelectrons generated in the detector per unit of fluorescence or light scatter, and the number of background photoelectrons $B$, which are resultant from light scatter and fluorescence signals from other components than the sample and electronic noise on the detectors and their associated electronics. In this study, $Q$ and $B$ were defined based on the nanosphere mixtures described in *Section 6.1.1* as described previously for fluorescence [165,166,186] and light scatter [169]. The lower resolution limit $R$, which describes the smallest signal that can be discriminated from background with at least 2 standard deviations of the background signal, was calculated using $Q$ and $B$ as described previously [167].

### 6.1.3. SET-UP

Flow cytometry was performed on an Apogee A60 Micro-PLUS high-resolution flow cytometer (Apogee Flow Systems). The flow cytometer was configured as described in study 1 of this thesis [240]. Based on this configuration, we experimented with varying laser powers and PMT voltages to determine optimal settings for detection of particles with dim light scatter (large-angle light scatter; LALS) and fluorescence signals (APC, FITC and FITC). Laser power was varied in 25 mW increments from 50 mW to 300 mW (LALS), 180 mW (APC), and 200 mW (FITC and PE). PMT voltages were varied in 50 V increments from 250 V to 550 V for all parameters. $Q$, $B$ and $R$ were determined for each setting using the nanosphere mixtures described above.

## 6.2. KEY RESULTS

### 6.2.1. VALIDATION OF METHODOLOGY

Standardisation of fluorescence parameters into ERF units was done by linear regression of 6-peak fluorescent Ultra Rainbow Calibration Particles fluorescence signals in APC, FITC and PE parameters versus the known ERF values for each nanosphere population ($R^2 > 0.99$, figure 2 in [250]). For standardisation of light scatter signals, regression of light scatter signals and the light scatter cross section area integrated over all angles ($4\pi$ radians) for all bead populations yielded different slopes for silica nanospheres and polystyrene nanospheres (figure 2D in [250]). As such, for the sake of including as many nanosphere populations as possible for regression and determination of $Q$, $B$, and $R$ without overly complicating standardisation of light scatter signals, we elected to only use silica nanospheres for light scatter sensitivity determination.

For $Q$, $B$ and $R$ to be determined from beads with known absolute fluorescence or light scatter cross section values, photoelectron noise should be derived and contribute observably to the overall variability of bead populations. With increasing signal intensity, the number of photoelectrons generated by particles increases proportionally, and intrinsic (bead-related) and illumination (laser power fluctuations, luminescence of optical components *etc.*) variabilities contribute proportionally more to the overall variability of the signal than photoelectron noise [165,169]. As such, variability due photoelectron noise could be derived by geometric subtraction of the background-corrected coefficient of variation of beads with a bright signal (*i.e.*, those with the largest ERF value or 1300 nm silica nanospheres), where photoelectron noise would contribute very little to the overall variability, from background-corrected variabilities of each population. Photoelectron noise contributed observably to all conditions with the exception of those, where laser power was set to 200 mW for PE and PMT voltage was set to 250 V for LALS, where regression coefficients ($R^2$) were less than 0.8 when deriving $J$ and $K$, which are intermediate factors necessary for

calculating $Q$ and $B$ (see data analysis section, figure 3B & 3C, and supplementary figure S1 in [250] for further information). In addition, the contribution of photoelectron noise to overall variability could not be assessed from PMT voltage set to 250 V on the FITC parameter, as only one nanosphere population could be detected, and, thus, this condition was excluded.

## 6.2.2. *Q*, *B* AND *R* AND THEIR RELATIONSHIP TO LASER POWER AND PMT VOLTAGE

In this study, we found differing dependencies of the quantum detection efficiency $Q$ to laser power for the parameters analysed. For APC and FITC fluorescence, $Q$ tended to be stable with increasing laser power, while $Q$ increased along with increasing laser power for PE fluorescence. For LALS, however, $Q$ increased along with laser power until 200 mW, after which $Q$ did not change any further (supplementary figure S3A in [250]). $Q$ had a positive linear relationship with PMT voltage for all fluorescence channels, while it was unaffected by PMT voltage for LALS (supplementary figure S3B in [250]). $B$, on the other hand, correlated negatively with laser power and PMT voltage for all fluorescence channels. For LALS, however, no trend could be observed between $B$ and laser power, while a $B$ decreased for PMT voltages up to 350 V, after which no consistent changes in $B$ could be observed (supplementary figure S3C and D in [250]).

For all parameters, a reciprocal relationship was observed between $R$ and laser power, where $R$ initially decreased until a specific laser power was reached, after which no further improvements in $R$ could be achieved by increasing laser power beyond this point (figure 4A in [250]). Similar results were observed for $R$ and PMT voltage for fluorescence parameters, with marked decreases in $R$ until an optimal PMT voltage was reached, after which further increases in PMT voltage did not result in further decreases in $R$. For LALS, however, no significant changes in $R$ could be observed for the tested PMT voltages (figure 4B in [250]). We further demonstrated that the obtained $R$ values were reproducible by comparing conditions with the same settings between the laser power and PMT voltage experiments for FITC (variability = 2.0 %), PE (variability = 3.7 %) and LALS (variability = 9.0 %), whereas significant deviations were observed for APC (variability = 58.6 %) between the two experiments. The source of this deviation is yet to be determined.

## 6.3. DISCUSSION

### 6.3.1. CONVERTING ARBITRARY LIGHT SCATTER SIGNALS TO STANDARDIZED UNITS

The different slopes yielded by silica and polystyrene nanospheres when correlating their light scatter cross section areas with the measured signals was non-surprising, as light scattered from polystyrene and silica nanospheres in the size range used in this

study falls predominantly in the Mie light scattering regime, and, therefore, these particles do not scatter light in an isotropic fashion (isotropic light scatter: equal proportions of incident light scattered in all directions) [190]. Thus, due to the having different refractive indices, it is to be expected that the total amount of light scattered in proportion to size can differ between polystyrene and silica. Furthermore, measurement of light scatter on flow cytometers is limited to a fixed, integrated range of angles (*i.e.*, 60 to 140 ° for LALS on the Apogee A60 Micro-PLUS), which could account for differing proportions of the total amount of scattered light from single particles [202], thereby yielding different slopes when plotted against the measured signals. This could be corrected to some extent by calculating the solid-collection angle-weighted light scatter cross section area by either weighting the light scatter cross section manually if solid collection angles and presence of any polarising filters are known [268] or estimated using open source [210] or commercially available software [196]. These approaches are, however, somewhat labour intensive and present with their own pitfalls including yielding different light scatter cross sections for the same particles on different flow cytometers, thus complicating cross-platform comparisons [169,268].

## 6.3.2. USING *Q, B* AND *R* TO DETERMINE OPTIMAL ANALYSIS SETTINGS

Although there was a general tendency for *Q* to increase and *B* to decrease with increasing laser power, there were some differences between the different fluorescence and light scatter parameters analysed. This result was somewhat surprising. With a larger number of photons being present in the interrogation point, it could be expected that fluorophores are excited to a greater extent, which would result in a proportionally higher emission of fluorescence light. However, several studies have previously demonstrated that fluorophores and fluorescence molecules can be saturated with high levels of illumination, which would result in a progressively lower proportional quantum yield with increasing illumination power beyond a certain point and under certain circumstances (*i.e.*, temperature) [269–271]. Thus, it is conceivable that the differences between the investigated fluorophores could be due to differences in saturation requirements. For light scatter, *Q* increased with increasing laser power until about 200 mW of laser power, after which no further improvements could be observed. Similar results were also described by de Rond *et al.*, who observed that returns in terms of *Q* were diminishing with increasing laser power [169]. Furthermore, no visible trend could be observed between laser power and *B* for light scatter. A probable explanation for these results is increasingly excessive contributions of luminescence and light scatter from optical components and sheath fluid to the overall signals.

Since *R* is both dependent on both *Q* and *B*, discrepancies in the way one or the other were affected by laser power or PMT voltage on single parameters did not affect the proportionality of *R* to either of these settings. As such, with *Q* either increasing, *B*

decreasing or both as a result of increasing laser power or PMT voltage, $R$ would invariably decrease (see equation 7 in [250]). Furthermore, in line with this, the decreasing improvements in $Q$ observed for increasing laser power and $B$ for PMT voltage both translated into gradual stabilisation of $R$ for increases in these settings. Therefore, the deflection point on curves of laser power/PMT voltage versus $R$ could be used to determine the best combination of settings that yields the best possible resolution for detection of dim signals.

Although it is becoming more common to report the lower and upper detection thresholds in standardised units in EV studies [196], these can hardly be used to determine the ability of a flow cytometer to detect and discriminate dim signals from background. Thresholds can be set either below or above the upper limit of background, which can thus result in either inclusion of background or exclusion of dim signals, respectively. Knowledge of both $Q$ and $B$ can, however, be used to define a lower detection threshold above background noise, while the limit of detection can be defined in standardised units, thereby also defining the level of the dimmest signals discriminable from background [165]. This can, however, be simplified to a single value by calculating the statistical lower resolution limit $R$, which accounts for both $Q$ and $B$ [206,250]. Thus, $R$ is a more useful metric to use than the lower detection limit defined by the triggering threshold or gate, as it takes both the level of background and quantum efficiency of the detector into consideration. Finally, $R$ can also be useful when optimising analytical settings on a flow cytometer, as it directly yields the lowest limit for discrimination of signals from background for a given set of settings, thus making optimisation more straightforward.

# CHAPTER 7. CONCLUSIONS

The overall purpose of this project was to investigate and address several important methodological aspects of flow cytometry, which could be detrimental to interpretation of data from characterisation and quantification of specific EV phenotypes in clinical studies.

In study 1, we demonstrated that different platforms could confer different amounts of variability to quantification of EVs. Although all platforms had global variabilities at or below 20 %, it could still be important to use a method with lower variability in biomarker discovery or validation studies, where either rare EV-populations are measured yielding few events in total, or differences between groups are much smaller than differences within groups. In addition to variability, this study also demonstrates that limit of detection is not a reliable measure on its own, as the proportion of particles detected in especially the smaller size ranges can be somewhat lower than that of larger particles due to various technical features of the flow cytometry platform utilised. As such, a disproportionate and unbalanced sample of EVs are detected and characterised, which could complicate interpretation of results, especially if the variable detection of dim signals is associated with some variability.

In study 2, we demonstrated that fluorescent label aggregates can complicate data interpretation by not only obscuring EV populations of interest, but also by potentially conferring variability to quantification of EV populations or binding of multiple EVs to larger aggregate complexes. This would be especially problematic for rare EV populations, where the number of aggregates could easily outnumber that of specific EV phenotypes. Finally, we demonstrated the importance of choosing a suitable method to reduce the number of fluorescent aggregates in commercial labels, as different methods have different efficacies and can also potentially confer variability to quantification of EVs.

In study 3, we demonstrated that single ApoB-containing lipoproteins can be detected on a sensitive flow cytometry platform by using polyclonal anti-ApoB48/100 antibodies. Furthermore, we demonstrated that Anx5 and lactadherin both label PS on ApoB-containing lipoproteins, however, Anx5 does so to a greater extent. We additionally demonstrate that lipoproteins are sensitive towards detergent lysis, which thus urges caution when interpreting this control with regards to EV-specificity of specific markers. Finally, our results do not support the notion of EVs bearing a lipoprotein corona, but rather that the use of trans-membrane proteins (*i.e.,* cell lineage specific proteins such as CD41 or the tetraspannins CD9, CD63 and CD81) might be a possible solution for distinguishing between EVs and lipoproteins in complex biological samples such as PPP.

In study 4, we demonstrated that $Q$, $B$ and $R$ can be used to determine optimal analysis settings for flow cytometry characterisation of sub-micron particles, where both laser power and PMT voltages can be optimised to yield the lowest possible lower resolution limit while preserving the dynamic range of parameters to detect signals with intensities varying over several orders of magnitude. We further demonstrated that determination of $R$ can be reproduced using the same settings on the flow cytometer. Finally, by using MESF or ERF-standardised beads for fluorescence and calculating light scatter cross section area for nanospheres with varying sizes, $Q$, $B$, and, importantly, $R$ can be determined in standardised units, thereby enabling better cross-platform and cross-study comparison of results.

In conclusion, the studies contained in this thesis address several important pre-analytical and analytical aspects that can influence interpretation of results from flow cytometry characterisation of EVs. As such, they contribute to an ever-expanding body of literature, whose sole aim is to identify and overcome pitfalls in EV research and improve robustness and reproducibility of studies by means of standardised methodology and reporting, thus bringing the field a few steps closer to using flow cytometry as a tool for EV-based biomarker discovery and clinical diagnosis.

# LITERATURE LIST

1.      Biomarkers Definitions Working Group. Biomarkers and surrogate endpoints: preferred definitions and conceptual framework. Clin Pharmacol Ther [Internet]. 2001 Mar;69(3):89–95. Available from: http://www.ncbi.nlm.nih.gov/pubmed/11240971

2.      Sorrells RB. Synovioanalysis ("liquid biopsy"). J Ark Med Soc [Internet]. 1974 Jun;71(1):59–62. Available from: http://www.ncbi.nlm.nih.gov/pubmed/4275449

3.      Lianidou ES, Mavroudis D, Sotiropoulou G, Agelaki S, Pantel K. What's new on circulating tumor cells? A meeting report. Breast Cancer Res [Internet]. 2010;12(4):307. Available from: http://www.ncbi.nlm.nih.gov/pubmed/20727231

4.      PALAY SL, PALADE GE. The fine structure of neurons. J Biophys Biochem Cytol [Internet]. 1955 Jan 19;1(1):69–88. Available from: http://www.ncbi.nlm.nih.gov/pubmed/19443737

5.      Dalton  a J. Microvesicles and vesicles of multivesicular bodies versus "virus-like" particles. J Natl Cancer Inst [Internet]. 1975 May;54(5):1137–48. Available from: http://www.ncbi.nlm.nih.gov/pubmed/165305

6.      Wolf P. The nature and significance of platelet products in human plasma. Br J Haematol [Internet]. 1967 May;13(3):269–88. Available from: http://www.ncbi.nlm.nih.gov/pubmed/6025241

7.      Pan BT, Teng K, Wu C, Adam M, Johnstone RM. Electron microscopic evidence for externalization of the transferrin receptor in vesicular form in sheep reticulocytes. J Cell Biol [Internet]. 1985 Sep;101(3):942–8. Available from:
http://jcb.rupress.org.libproxy1.nus.edu.sg/content/jcb/101/3/942.full.pdf

8.      Johnstone RM. The Jeanne Manery-Fisher Memorial Lecture 1991. Maturation of reticulocytes: formation of exosomes as a mechanism for shedding membrane proteins. Biochem Cell Biol [Internet]. 1992;70(3–4):179–90. Available from: http://www.ncbi.nlm.nih.gov/pubmed/1515120

9.      Kerr JF, Wyllie AH, Currie AR. Apoptosis: a basic biological phenomenon with wide-ranging implications in tissue kinetics. Br J Cancer [Internet]. 1972 Aug;26(4):239–57. Available from: http://www.ncbi.nlm.nih.gov/pubmed/4561027

10.     Sandberg H, Andersson LO, Höglund S. Isolation and characterization of lipid-protein particles containing platelet factor 3 released from human platelets. Biochem J [Internet]. 1982 Apr 1;203(1):303–11. Available from: http://www.ncbi.nlm.nih.gov/pubmed/7103943

11.     Bode AP, Sandberg H, Dombrose FA, Lentz BR. Association of factor V activity with membranous vesicles released from human platelets: requirement for platelet stimulation. Thromb Res [Internet]. 1985 Jul 1;39(1):49–61. Available from: http://www.ncbi.nlm.nih.gov/pubmed/3839943

12.     Sandberg H, Bode AP, Dombrose FA, Hoechli M, Lentz BR. Expression of coagulant activity in human platelets: release of membranous vesicles providing platelet factor 1 and platelet factor 3. Thromb Res [Internet]. 1985 Jul 1;39(1):63–79. Available from: http://www.ncbi.nlm.nih.gov/pubmed/3839944

13.     Hamilton KK, Hattori R, Esmon CT, Sims PJ. Complement proteins C5b-9 induce vesiculation of the endothelial plasma membrane and expose catalytic surface for assembly of the prothrombinase enzyme complex. J Biol Chem [Internet]. 1990 Mar 5;265(7):3809–14. Available from: http://dx.doi.org/10.1016/S0021-9258(19)39666-8

14.     Zucker-Franklin D, Karpatkin S. Red-cell and platelet fragmentation in idiopathic autoimmune thrombocytopenic purpura. N Engl J Med [Internet]. 1977 Sep 8;297(10):517–23. Available from: http://www.ncbi.nlm.nih.gov/pubmed/560627

15.     Heijnen HF, Schiel AE, Fijnheer R, Geuze HJ, Sixma JJ. Activated platelets release two types of membrane vesicles: microvesicles by surface shedding and exosomes derived from exocytosis of multivesicular bodies and alpha-granules. Blood [Internet]. 1999 Dec 1;94(11):3791–9. Available from: http://www.ncbi.nlm.nih.gov/pubmed/10572093

16.     Abrams CS, Ellison N, Budzynski AZ, Shattil SJ. Direct detection of activated platelets and platelet-derived microparticles in humans. Blood [Internet]. 1990 Jan 1 [cited 2014 Oct 22];75(1):128–38. Available from: http://bloodjournal.hematologylibrary.org/content/75/1/128.short

17.     Pisitkun T, Shen R-F, Knepper MA. Identification and proteomic profiling of exosomes in human urine. Proc Natl Acad Sci U S A [Internet]. 2004 Sep 7;101(36):13368–73. Available from: http://www.ncbi.nlm.nih.gov/pubmed/15326289

18.     Keller S, Ridinger J, Rupp A-K, Janssen JWG, Altevogt P. Body fluid derived exosomes as a novel template for clinical diagnostics. J Transl Med [Internet]. 2011 Jun 8;9:86. Available from: http://www.ncbi.nlm.nih.gov/pubmed/21651777

19.     Admyre C, Johansson SM, Qazi KR, Filén J-J, Lahesmaa R, Norman M, et al. Exosomes with immune modulatory features are present in human breast milk. J Immunol [Internet]. 2007 Aug 1;179(3):1969–78. Available from: http://www.ncbi.nlm.nih.gov/pubmed/17641064

20.     Lässer C, O'Neil SE, Ekerljung L, Ekström K, Sjöstrand M, Lötvall J. RNA-containing exosomes in human nasal secretions. Am J Rhinol Allergy [Internet]. 2011;25(2):89–93. Available from: http://www.ncbi.nlm.nih.gov/pubmed/21172122

21.     Asea A, Jean-Pierre C, Kaur P, Rao P, Linhares IM, Skupski D, et al. Heat shock protein-containing exosomes in mid-trimester amniotic fluids. J Reprod Immunol [Internet]. 2008 Oct;79(1):12–7. Available from: http://www.ncbi.nlm.nih.gov/pubmed/18715652

22.     Brody I, Ronquist G, Gottfries A. Ultrastructural localization of the prostasome - an organelle in human seminal plasma. Ups J Med Sci [Internet]. 1983;88(2):63–80. Available from: http://www.ncbi.nlm.nih.gov/pubmed/6649193

23.     Raposo G, Nijman HW, Stoorvogel W, Liejendekker R, Harding C V, Melief CJ, et al. B lymphocytes secrete antigen-presenting vesicles. J Exp Med [Internet]. 1996 Mar 1;183(3):1161–72. Available from: http://www.ncbi.nlm.nih.gov/pubmed/8642258

24.     Hristov M, Erl W, Linder S, Weber PC. Apoptotic bodies from endothelial cells enhance the number and initiate the differentiation of human endothelial progenitor cells in vitro. Blood [Internet]. 2004 Nov 1;104(9):2761–6. Available from: http://dx.doi.org/10.1182/blood-2003-10-3614

25.     Simák J, Holada K, D'Agnillo F, Janota J, Vostal JG. Cellular prion protein is expressed on endothelial cells and is released during apoptosis on membrane microparticles found in human plasma. Transfusion [Internet]. 2002 Mar;42(3):334–42. Available from: http://www.ncbi.nlm.nih.gov/pubmed/11961239

26.     Ratajczak J, Miekus K, Kucia M, Zhang J, Reca R, Dvorak P, et al. Embryonic stem cell-derived microvesicles reprogram hematopoietic progenitors: evidence for horizontal transfer of mRNA and protein delivery. Leukemia

[Internet]. 2006 May;20(5):847–56. Available from: http://www.ncbi.nlm.nih.gov/pubmed/16453000

27. Valadi H, Ekström K, Bossios A, Sjöstrand M, Lee JJ, Lötvall JO. Exosome-mediated transfer of mRNAs and microRNAs is a novel mechanism of genetic exchange between cells. Nat Cell Biol [Internet]. 2007 Jun;9(6):654–9. Available from: http://www.ncbi.nlm.nih.gov/pubmed/17486113

28. Théry C, Witwer KW, Aikawa E, Alcaraz MJ, Anderson JD, Andriantsitohaina R, et al. Minimal information for studies of extracellular vesicles 2018 (MISEV2018): a position statement of the International Society for Extracellular Vesicles and update of the MISEV2014 guidelines. J Extracell vesicles [Internet]. 2018;7(1):1535750. Available from: http://www.ncbi.nlm.nih.gov/pubmed/30637094

29. Johnsen KB, Gudbergsson JM, Andresen TL, Simonsen JB. What is the blood concentration of extracellular vesicles? Implications for the use of extracellular vesicles as blood-borne biomarkers of cancer. Biochim Biophys acta Rev cancer [Internet]. 2019;1871(1):109–16. Available from: https://doi.org/10.1016/j.bbcan.2018.11.006

30. Yáñez-Mó M, Siljander PR-M, Andreu Z, Zavec AB, Borràs FE, Buzas EI, et al. Biological properties of extracellular vesicles and their physiological functions. J Extracell Vesicles [Internet]. 2015;4:1–60. Available from: http://www.journalofextracellularvesicles.net/index.php/jev/article/view/270 66/xml_13

31. Colombo M, Raposo G, Théry C. Biogenesis, secretion, and intercellular interactions of exosomes and other extracellular vesicles. Annu Rev Cell Dev Biol [Internet]. 2014;30:255–89. Available from: http://www.ncbi.nlm.nih.gov/pubmed/25288114

32. van der Pol E, Böing AN, Harrison P, Sturk A, Nieuwland R. Classification, functions, and clinical relevance of extracellular vesicles. Pharmacol Rev [Internet]. 2012 Jul;64(3):676–705. Available from: http://www.ncbi.nlm.nih.gov/pubmed/22722893

33. Record M, Silvente-Poirot S, Poirot M, Wakelam MJO. Extracellular vesicles: lipids as key components of their biogenesis and functions. J Lipid Res [Internet]. 2018 Aug;59(8):1316–24. Available from: http://www.jlr.org/lookup/doi/10.1194/jlr.E086173

34. Raposo G, Stoorvogel W. Extracellular vesicles: exosomes, microvesicles, and friends. J Cell Biol [Internet]. 2013 Feb 18;200(4):373–83. Available

from: http://www.ncbi.nlm.nih.gov/pubmed/23420871

35. Herring JM, McMichael MA, Smith SA. Microparticles in health and disease. J Vet Intern Med [Internet]. 2013 Sep;27(5):1020–33. Available from: http://doi.wiley.com/10.1111/jvim.12128

36. Arraud N, Linares R, Tan S, Gounou C, Pasquet J-M, Mornet S, et al. Extracellular vesicles from blood plasma: determination of their morphology, size, phenotype and concentration. J Thromb Haemost [Internet]. 2014 May;12(5):614–27. Available from: http://www.ncbi.nlm.nih.gov/pubmed/24618123

37. Zabeo D, Cvjetkovic A, Lässer C, Schorb M, Lötvall J, Höög JL. Exosomes purified from a single cell type have diverse morphology. J Extracell vesicles [Internet]. 2017;6(1):1329476. Available from: http://www.ncbi.nlm.nih.gov/pubmed/28717422

38. van der Pol E, Coumans FAW, Grootemaat a. E, Gardiner C, Sargent IL, Harrison P, et al. Particle size distribution of exosomes and microvesicles determined by transmission electron microscopy, flow cytometry, nanoparticle tracking analysis, and resistive pulse sensing. J Thromb Haemost [Internet]. 2014 Jul [cited 2014 Jul 25];12(7):1182–92. Available from: http://www.ncbi.nlm.nih.gov/pubmed/24818656

39. Klumperman J, Raposo G. The complex ultrastructure of the endolysosomal system. Cold Spring Harb Perspect Biol [Internet]. 2014 May 22;6(10):a016857. Available from: http://www.ncbi.nlm.nih.gov/pubmed/24851870

40. Colombo M, Moita C, van Niel G, Kowal J, Vigneron J, Benaroch P, et al. Analysis of ESCRT functions in exosome biogenesis, composition and secretion highlights the heterogeneity of extracellular vesicles. J Cell Sci [Internet]. 2013;126(Pt 24):5553–65. Available from: http://www.ncbi.nlm.nih.gov/pubmed/24105262

41. McCullough J, Colf LA, Sundquist WI. Membrane fission reactions of the mammalian ESCRT pathway. Annu Rev Biochem [Internet]. 2013;82(1):663–92. Available from: http://www.annualreviews.org/doi/10.1146/annurev-biochem-072909-101058

42. Henne WM, Buchkovich NJ, Emr SD. The ESCRT pathway. Dev Cell [Internet]. 2011 Jul 19;21(1):77–91. Available from: http://dx.doi.org/10.1016/j.devcel.2011.05.015

43.     Kowal J, Tkach M, Théry C. Biogenesis and secretion of exosomes. Curr Opin Cell Biol. 2014;29(1):116–25.

44.     Strauss K, Goebel C, Runz H, Möbius W, Weiss S, Feussner I, et al. Exosome secretion ameliorates lysosomal storage of cholesterol in Niemann-Pick type C disease. J Biol Chem [Internet]. 2010 Aug 20;285(34):26279–88. Available from: http://dx.doi.org/10.1074/jbc.M110.134775

45.     Larios J, Mercier V, Roux A, Gruenberg J. ALIX- and ESCRT-III-dependent sorting of tetraspanins to exosomes. J Cell Biol [Internet]. 2020;219(3). Available from: http://www.ncbi.nlm.nih.gov/pubmed/32049272

46.     van Niel G, Charrin S, Simoes S, Romao M, Rochin L, Saftig P, et al. The tetraspanin CD63 regulates ESCRT-independent and -dependent endosomal sorting during melanogenesis. Dev Cell [Internet]. 2011 Oct 18;21(4):708–21. Available from: http://www.ncbi.nlm.nih.gov/pubmed/21962903

47.     Géminard C, De Gassart A, Blanc L, Vidal M. Degradation of AP2 during reticulocyte maturation enhances binding of hsc70 and Alix to a common site on TFR for sorting into exosomes. Traffic [Internet]. 2004 Mar;5(3):181–93. Available from: http://www.ncbi.nlm.nih.gov/pubmed/15086793

48.     Bobrie A, Colombo M, Raposo G, Théry C. Exosome secretion: molecular mechanisms and roles in immune responses. Traffic [Internet]. 2011 Dec;12(12):1659–68. Available from: http://www.ncbi.nlm.nih.gov/pubmed/21645191

49.     Ostrowski M, Carmo NB, Krumeich S, Fanget I, Raposo G, Savina A, et al. Rab27a and Rab27b control different steps of the exosome secretion pathway. Nat Cell Biol [Internet]. 2010 Jan;12(1):19–30; sup pp 1-13. Available from: http://dx.doi.org/10.1038/ncb2000

50.     Hsu C, Morohashi Y, Yoshimura S-I, Manrique-Hoyos N, Jung S, Lauterbach MA, et al. Regulation of exosome secretion by Rab35 and its GTPase-activating proteins TBC1D10A-C. J Cell Biol [Internet]. 2010 Apr 19;189(2):223–32. Available from: http://www.ncbi.nlm.nih.gov/pubmed/20404108

51.     Stenmark H. Rab GTPases as coordinators of vesicle traffic. Nat Rev Mol Cell Biol [Internet]. 2009 Aug;10(8):513–25. Available from: http://www.ncbi.nlm.nih.gov/pubmed/19603039

52.     Homma Y, Hiragi S, Fukuda M. Rab family of small GTPases: an updated view on their regulation and functions. FEBS J [Internet]. 2021

Jan;288(1):36–55. Available from: http://www.ncbi.nlm.nih.gov/pubmed/32542850

53. Yang L, Peng X, Li Y, Zhang X, Ma Y, Wu C, et al. Long non-coding RNA HOTAIR promotes exosome secretion by regulating RAB35 and SNAP23 in hepatocellular carcinoma. Mol Cancer [Internet]. 2019;18(1):78. Available from: http://www.ncbi.nlm.nih.gov/pubmed/30943982

54. Kumar R, Tang Q, Müller SA, Gao P, Mahlstedt D, Zampagni S, et al. Fibroblast Growth Factor 2-Mediated Regulation of Neuronal Exosome Release Depends on VAMP3/Cellubrevin in Hippocampal Neurons. Adv Sci (Weinheim, Baden-Wurttemberg, Ger [Internet]. 2020 Mar;7(6):1902372. Available from: http://www.ncbi.nlm.nih.gov/pubmed/32195080

55. Sun C, Wang P, Dong W, Liu H, Sun J, Zhao L. LncRNA PVT1 promotes exosome secretion through YKT6, RAB7, and VAMP3 in pancreatic cancer. Aging (Albany NY) [Internet]. 2020;12(11):10427–40. Available from: http://www.ncbi.nlm.nih.gov/pubmed/32499447

56. Raposo G, Tenza D, Mecheri S, Peronet R, Bonnerot C, Desaymard C. Accumulation of major histocompatibility complex class II molecules in mast cell secretory granules and their release upon degranulation. Mol Biol Cell [Internet]. 1997 Dec;8(12):2631–45. Available from: http://www.ncbi.nlm.nih.gov/pubmed/9398681

57. Savina A, Fader CM, Damiani MT, Colombo MI. Rab11 promotes docking and fusion of multivesicular bodies in a calcium-dependent manner. Traffic [Internet]. 2005 Feb;6(2):131–43. Available from: http://www.ncbi.nlm.nih.gov/pubmed/15634213

58. Daleke DL. Regulation of transbilayer plasma membrane phospholipid asymmetry. J Lipid Res [Internet]. 2003 Feb;44(2):233–42. Available from: http://dx.doi.org/10.1194/jlr.R200019-JLR200

59. Bevers EM, Comfurius P, Dekkers DWC, Zwaal RFA. Lipid translocation across the plasma membrane of mammalian cells. Biochim Biophys Acta [Internet]. 1999 Aug 18;1439(3):317–30. Available from: http://www.ncbi.nlm.nih.gov/pubmed/10446420

60. Pasquet JM, Dachary-Prigent J, Nurden AT. Calcium influx is a determining factor of calpain activation and microparticle formation in platelets. Eur J Biochem [Internet]. 1996 Aug 1;239(3):647–54. Available from: http://www.ncbi.nlm.nih.gov/pubmed/8774708

61. Di Vizio D, Kim J, Hager MH, Morello M, Yang W, Lafargue CJ, et al. Oncosome formation in prostate cancer: association with a region of frequent chromosomal deletion in metastatic disease. Cancer Res [Internet]. 2009 Jul 1;69(13):5601–9. Available from: http://www.ncbi.nlm.nih.gov/pubmed/19549916

62. Muralidharan-Chari V, Clancy J, Plou C, Romao M, Chavrier P, Raposo G, et al. ARF6-regulated shedding of tumor cell-derived plasma membrane microvesicles. Curr Biol [Internet]. 2009 Dec 1;19(22):1875–85. Available from: http://dx.doi.org/10.1016/j.cub.2009.09.059

63. Nabhan JF, Hu R, Oh RS, Cohen SN, Lu Q. Formation and release of arrestin domain-containing protein 1-mediated microvesicles (ARMMs) at plasma membrane by recruitment of TSG101 protein. Proc Natl Acad Sci U S A [Internet]. 2012 Mar 13;109(11):4146–51. Available from: http://www.ncbi.nlm.nih.gov/pubmed/22315426

64. Choudhuri K, Llodrá J, Roth EW, Tsai J, Gordo S, Wucherpfennig KW, et al. Polarized release of T-cell-receptor-enriched microvesicles at the immunological synapse. Nature [Internet]. 2014 Mar 6;507(7490):118–23. Available from: http://www.ncbi.nlm.nih.gov/pubmed/24487619

65. Booth AM, Fang Y, Fallon JK, Yang J-M, Hildreth JEK, Gould SJ. Exosomes and HIV Gag bud from endosome-like domains of the T cell plasma membrane. J Cell Biol [Internet]. 2006 Mar 13;172(6):923–35. Available from: http://www.ncbi.nlm.nih.gov/pubmed/16533950

66. Jeppesen DK, Nawrocki A, Jensen SG, Thorsen K, Whitehead B, Howard KA, et al. Quantitative proteomics of fractionated membrane and lumen exosome proteins from isogenic metastatic and nonmetastatic bladder cancer cells reveal differential expression of EMT factors. Proteomics [Internet]. 2014 Mar;14(6):699–712. Available from: http://www.ncbi.nlm.nih.gov/pubmed/24376083

67. Gonzales PA, Pisitkun T, Hoffert JD, Tchapyjnikov D, Star RA, Kleta R, et al. Large-scale proteomics and phosphoproteomics of urinary exosomes. J Am Soc Nephrol [Internet]. 2009 Feb;20(2):363–79. Available from: http://www.ncbi.nlm.nih.gov/pubmed/19056867

68. Escrevente C, Keller S, Altevogt P, Costa J. Interaction and uptake of exosomes by ovarian cancer cells. BMC Cancer [Internet]. 2011 Mar 27;11(1):108. Available from: http://www.ncbi.nlm.nih.gov/pubmed/32933846

69.    Tauro BJ, Greening DW, Mathias RA, Mathivanan S, Ji H, Simpson RJ. Two distinct populations of exosomes are released from LIM1863 colon carcinoma cell-derived organoids. Mol Cell Proteomics [Internet]. 2013 Mar;12(3):587–98. Available from: http://www.mcponline.org/cgi/doi/10.1074/mcp.M112.021303

70.    Pallet N, Sirois I, Bell C, Hanafi L-A, Hamelin K, Dieudé M, et al. A comprehensive characterization of membrane vesicles released by autophagic human endothelial cells. Proteomics [Internet]. 2013 Apr;13(7):1108–20. Available from: http://www.ncbi.nlm.nih.gov/pubmed/23436686

71.    Fel A, Lewandowska AE, Petrides PE, Wiśniewski JR. Comparison of Proteome Composition of Serum Enriched in Extracellular Vesicles Isolated from Polycythemia Vera Patients and Healthy Controls. Proteomes [Internet]. 2019 May 6;7(2):1–17. Available from: http://www.ncbi.nlm.nih.gov/pubmed/31064135

72.    Østergaard O, Nielsen CT, Tanassi JT, Iversen L V., Jacobsen S, Heegaard NHH. Distinct proteome pathology of circulating microparticles in systemic lupus erythematosus. Clin Proteomics [Internet]. 2017;14(1):23. Available from: http://www.ncbi.nlm.nih.gov/pubmed/28649187

73.    Ostenfeld MS, Jensen SG, Jeppesen DK, Christensen L, Thorsen SB, Stenvang J, et al. miRNA profiling of circulating EpCAM + extracellular vesicles: promising biomarkers of colorectal cancer. J Extracell Vesicles [Internet]. 2016 Aug 29;5:31488. Available from: http://www.ncbi.nlm.nih.gov/pubmed/27576678

74.    Witwer KW, Buzás EI, Bemis LT, Bora A, Lässer C, Lötvall J, et al. Standardization of sample collection, isolation and analysis methods in extracellular vesicle research. J Extracell vesicles [Internet]. 2013 Jan;2:1–25. Available from: http://www.pubmedcentral.nih.gov/articlerender.fcgi?artid=3760646&tool=pmcentrez&rendertype=abstract

75.    Lötvall J, Hill AF, Hochberg F, Buzás EI, Di Vizio D, Gardiner C, et al. Minimal experimental requirements for definition of extracellular vesicles and their functions: a position statement from the International Society for Extracellular Vesicles. J Extracell vesicles [Internet]. 2014;3:26913. Available from: http://www.pubmedcentral.nih.gov/articlerender.fcgi?artid=4275645&tool=pmcentrez&rendertype=abstract

76.    Hurwitz SN, Rider MA, Bundy JL, Liu X, Singh RK, Meckes DG. Proteomic

profiling of NCI-60 extracellular vesicles uncovers common protein cargo and cancer type-specific biomarkers. Oncotarget [Internet]. 2016 Dec 27;7(52):86999–7015. Available from: http://www.ncbi.nlm.nih.gov/pubmed/27894104

77.    Kagawa H, Nomura S, Miyake T, Miyazaki Y, Kido H, Suzuki M, et al. Expression of prothrombinase activity and CD9 antigen on the surface of small vesicles from stimulated human endothelial cells. Thromb Res [Internet]. 1995 Dec 15;80(6):451–60. Available from: http://www.ncbi.nlm.nih.gov/pubmed/8610273

78.    Kowal J, Arras G, Colombo M, Jouve M, Morath JP, Primdal-Bengtson B, et al. Proteomic comparison defines novel markers to characterize heterogeneous populations of extracellular vesicle subtypes. Proc Natl Acad Sci U S A [Internet]. 2016 Feb 23;113(8):E968-77. Available from: http://www.ncbi.nlm.nih.gov/pubmed/26858453%5Cnhttp://www.pubmedcentral.nih.gov/articlerender.fcgi?artid=PMC4776515

79.    Lewandrowski U, Wortelkamp S, Lohrig K, Zahedi RP, Wolters DA, Walter U, et al. Platelet membrane proteomics: a novel repository for functional research. Blood [Internet]. 2009 Jul 2;114(1):e10-9. Available from: http://www.ncbi.nlm.nih.gov/pubmed/19436052

80.    Dean WL, Lee MJ, Cummins TD, Schultz DJ, Powell DW. Proteomic and functional characterisation of platelet microparticle size classes. Thromb Haemost [Internet]. 2009 Oct;102(4):711–8. Available from: http://www.ncbi.nlm.nih.gov/pubmed/19806257

81.    Phillips DR, Charo IF, Parise L V, Fitzgerald LA. The platelet membrane glycoprotein IIb-IIIa complex. Blood [Internet]. 1988 Apr;71(4):831–43. Available from: http://www.ncbi.nlm.nih.gov/pubmed/2833328

82.    Arraud N, Gounou C, Linares R, Brisson AR. A simple flow cytometry method improves the detection of phosphatidylserine-exposing extracellular vesicles. J Thromb Haemost [Internet]. 2015 Feb;13(2):237–47. Available from: http://doi.wiley.com/10.1111/jth.12767

83.    Agouni A, Ducluzeau P-H, Benameur T, Faure S, Sladkova M, Duluc L, et al. Microparticles from patients with metabolic syndrome induce vascular hypo-reactivity via Fas/Fas-ligand pathway in mice. Reitsma PH, editor. PLoS One [Internet]. 2011 Nov 15;6(11):e27809. Available from: http://www.pubmedcentral.nih.gov/articlerender.fcgi?artid=3217000&tool=pmcentrez&rendertype=abstract

84. Nieuwland R, Berckmans RJ, Rotteveel-Eijkman RC, Maquelin KN, Roozendaal KJ, Jansen PG, et al. Cell-derived microparticles generated in patients during cardiopulmonary bypass are highly procoagulant. Circulation [Internet]. 1997 Nov 18;96(10):3534–41. Available from: http://www.ncbi.nlm.nih.gov/pubmed/9396452

85. Berckmans RJ, Nieuwland R, Böing AN, Romijn FP, Hack CE, Sturk A. Cell-derived microparticles circulate in healthy humans and support low grade thrombin generation. Thromb Haemost [Internet]. 2001 Apr;85(4):639–46. Available from: http://www.ncbi.nlm.nih.gov/pubmed/11341498

86. Amabile N, Heiss C, Chang V, Angeli FS, Damon L, Rame EJ, et al. Increased CD62e(+) endothelial microparticle levels predict poor outcome in pulmonary hypertension patients. J Heart Lung Transplant [Internet]. 2009 Oct [cited 2014 Oct 29];28(10):1081–6. Available from: http://www.ncbi.nlm.nih.gov/pubmed/19782291

87. Matijevic N, Wang YW, Holcomb JB, Kozar R, Cardenas JC, Wade CE. Microvesicle phenotypes are associated with transfusion requirements and mortality in subjects with severe injuries. J Extracell vesicles [Internet]. 2015;4:29338. Available from: http://www.ncbi.nlm.nih.gov/pubmed/26689982%5Cnhttp://www.pubmedce ntral.nih.gov/articlerender.fcgi?artid=PMC4685295

88. Takahashi T, Kobayashi S, Fujino N, Suzuki T, Ota C, Tando Y, et al. Differences in the released endothelial microparticle subtypes between human pulmonary microvascular endothelial cells and aortic endothelial cells in vitro. Exp Lung Res [Internet]. 2013 [cited 2014 Sep 29];39(4–5):155–61. Available from: http://www.ncbi.nlm.nih.gov/pubmed/23550836

89. Armstrong A, Eck SL. EpCAM: A new therapeutic target for an old cancer antigen. Cancer Biol Ther [Internet]. 2003;2(4):320–6. Available from: http://www.ncbi.nlm.nih.gov/pubmed/14508099

90. Rupp A-K, Rupp C, Keller S, Brase JC, Ehehalt R, Fogel M, et al. Loss of EpCAM expression in breast cancer derived serum exosomes: role of proteolytic cleavage. Gynecol Oncol. 2011 Aug;122(2):437–46.

91. Julich-Haertel H, Urban SK, Krawczyk M, Willms A, Jankowski K, Patkowski W, et al. Cancer-associated circulating large extracellular vesicles in cholangiocarcinoma and hepatocellular carcinoma. J Hepatol. 2017 Mar;

92. Basavaraj MG, Olsen JO, Østerud B, Hansen J-B. Differential ability of tissue factor antibody clones on detection of tissue factor in blood cells and

microparticles. Thromb Res [Internet]. 2012 Sep;130(3):538–46. Available from: http://dx.doi.org/10.1016/j.thromres.2012.06.001

93.    Denzer K, van Eijk M, Kleijmeer MJ, Jakobson E, de Groot C, Geuze HJ. Follicular dendritic cells carry MHC class II-expressing microvesicles at their surface. J Immunol [Internet]. 2000 Aug 1;165(3):1259–65. Available from: http://www.ncbi.nlm.nih.gov/pubmed/10903724

94.    Tkach M, Kowal J, Zucchetti AE, Enserink L, Jouve M, Lankar D, et al. Qualitative differences in T-cell activation by dendritic cell-derived extracellular vesicle subtypes. EMBO J [Internet]. 2017;36(20):3012–28. Available from: http://www.ncbi.nlm.nih.gov/pubmed/28923825

95.    Hrdinova T, Toman O, Dresler J, Klimentova J, Salovska B, Pajer P, et al. Exosomes released by imatinib-resistant K562 cells contain specific membrane markers, IFITM3, CD146 and CD36 and increase the survival of imatinib-sensitive cells in the presence of imatinib. Int J Oncol [Internet]. 2021;58(2):238–50.              Available              from: http://www.ncbi.nlm.nih.gov/pubmed/33491750

96.    Kvorning SL, Nielsen MC, Andersen NF, Hokland M, Andersen MN, Møller HJ. Circulating extracellular vesicle-associated CD163 and CD206 in multiple myeloma. Eur J Haematol [Internet]. 2020 May;104(5):409–19. Available from: http://www.ncbi.nlm.nih.gov/pubmed/31855290

97.    Subra C, Laulagnier K, Perret B, Record M. Exosome lipidomics unravels lipid sorting at the level of multivesicular bodies. Biochimie [Internet]. 2007 Feb;89(2):205–12.              Available              from: http://www.ncbi.nlm.nih.gov/pubmed/17157973

98.    Losito I, Conte E, Cataldi TRI, Cioffi N, Megli FM, Palmisano F. The phospholipidomic signatures of human blood microparticles, platelets and platelet-derived microparticles: a comparative HILIC-ESI-MS investigation. Lipids     [Internet].     2015     Jan;50(1):71–84.     Available     from: http://www.ncbi.nlm.nih.gov/pubmed/25502953

99.    Tushuizen ME, Diamant M, Peypers EG, Hoek FJ, Heine RJ, Sturk A, et al. Postprandial changes in the phospholipid composition of circulating microparticles are not associated with coagulation activation. Thromb Res [Internet].     2012     Jul;130(1):115–21.     Available     from: http://dx.doi.org/10.1016/j.thromres.2011.09.003

100.   Abid Hussein MN, Meesters EW, Osmanovic N, Romijn FPHTM, Nieuwland R, Sturk   a. Antigenic characterization of endothelial cell-derived

microparticles and their detection ex vivo. J Thromb Haemost [Internet]. 2003 Nov;1(11):2434–43. Available from: http://www.ncbi.nlm.nih.gov/pubmed/14629480

101.    Urade R, Hayashi Y, Kito M. Endosomes differ from plasma membranes in the phospholipid molecular species composition. Biochim Biophys Acta [Internet]. 1988 Dec 8;946(1):151–63. Available from: http://www.ncbi.nlm.nih.gov/pubmed/3264726

102.    Matsumura S, Minamisawa T, Suga K, Kishita H, Akagi T, Ichiki T, et al. Subtypes of tumour cell-derived small extracellular vesicles having differently externalized phosphatidylserine. J Extracell vesicles [Internet]. 2019;8(1):1579541. Available from: https://doi.org/10.1080/20013078.2019.1579541

103.    Del Conde I, Shrimpton CN, Thiagarajan P, López JA. Tissue-factor-bearing microvesicles arise from lipid rafts and fuse with activated platelets to initiate coagulation. Blood [Internet]. 2005 Sep 1;106(5):1604–11. Available from: http://www.ncbi.nlm.nih.gov/pubmed/15741221

104.    Laulagnier K, Motta C, Hamdi S, Roy S, Fauvelle F, Pageaux J-F, et al. Mast cell- and dendritic cell-derived exosomes display a specific lipid composition and an unusual membrane organization. Biochem J [Internet]. 2004 May 15;380(Pt 1):161–71. Available from: http://biochemj.org/lookup/doi/10.1042/bj20031594

105.    Kobayashi T, Beuchat MH, Lindsay M, Frias S, Palmiter RD, Sakuraba H, et al. Late endosomal membranes rich in lysobisphosphatidic acid regulate cholesterol transport. Nat Cell Biol [Internet]. 1999 Jun;1(2):113–8. Available from: http://www.ncbi.nlm.nih.gov/pubmed/10559883

106.    Record M, Carayon K, Poirot M, Silvente-Poirot S. Exosomes as new vesicular lipid transporters involved in cell-cell communication and various pathophysiologies. Biochim Biophys Acta [Internet]. 2014 Jan;1841(1):108–20. Available from: http://dx.doi.org/10.1016/j.bbalip.2013.10.004

107.    Mateescu B, Kowal EJK, van Balkom BWM, Bartel S, Bhattacharyya SN, Buzás EI, et al. Obstacles and opportunities in the functional analysis of extracellular vesicle RNA - an ISEV position paper. J Extracell vesicles [Internet]. 2017;6(1):1286095. Available from: https://www.tandfonline.com/doi/full/10.1080/20013078.2017.1286095

108.    German JB, Smilowitz JT, Zivkovic AM. Lipoproteins: When size really matters. Curr Opin Colloid Interface Sci [Internet]. 2006 Jun;11(2–3):171–

83. Available from: https://linkinghub.elsevier.com/retrieve/pii/S1359029405001238

109. Thaxton CS, Rink JS, Naha PC, Cormode DP. Lipoproteins and lipoprotein mimetics for imaging and drug delivery. Adv Drug Deliv Rev [Internet]. 2016;106(Pt A):116–31. Available from: http://dx.doi.org/10.1016/j.addr.2016.04.020

110. Simonsen JB. What Are We Looking At? Extracellular Vesicles, Lipoproteins, or Both? Circ Res [Internet]. 2017 Sep 29;121(8):920–2. Available from: https://www.ahajournals.org/doi/10.1161/CIRCRESAHA.117.311767

111. Lacroix R, Judicone C, Mooberry M, Boucekine M, Key NS, Dignat-George F, et al. Standardization of pre-analytical variables in plasma microparticle determination: results of the International Society on Thrombosis and Haemostasis SSC Collaborative workshop. J Thromb Haemost [Internet]. 2013 Apr 2;11(6):1190–3. Available from: http://www.ncbi.nlm.nih.gov/pubmed/23551930

112. Berckmans RJ, Lacroix R, Hau CM, Sturk A, Nieuwland R. Extracellular vesicles and coagulation in blood from healthy humans revisited. J Extracell vesicles [Internet]. 2019;8(1):1688936. Available from: https://doi.org/10.1080/20013078.2019.1688936

113. Rikkert LG, Coumans FAW, Hau CM, Terstappen LWMM, Nieuwland R. Platelet removal by single-step centrifugation. Platelets [Internet]. 2020 Jun 17;00(00):1–4. Available from: https://doi.org/10.1080/09537104.2020.1779924

114. Arraud N, Gounou C, Turpin D, Brisson AR. Fluorescence triggering: A general strategy for enumerating and phenotyping extracellular vesicles by flow cytometry. Cytometry A [Internet]. 2016 Feb;89(2):184–95. Available from: http://www.ncbi.nlm.nih.gov/pubmed/25857288

115. Østergaard O, Nielsen CT, Iversen L V., Jacobsen S, Tanassi JT, Heegaard NHH. Quantitative proteome profiling of normal human circulating microparticles. J Proteome Res [Internet]. 2012 Apr 6;11(4):2154–63. Available from: http://www.ncbi.nlm.nih.gov/pubmed/22329422

116. Gardiner C, Di Vizio D, Sahoo S, Théry C, Witwer KW, Wauben M, et al. Techniques used for the isolation and characterization of extracellular vesicles: results of a worldwide survey. J Extracell vesicles [Internet]. 2016;5(1):32945. Available from:

http://www.ncbi.nlm.nih.gov/pubmed/27802845

117. Bobrie A, Colombo M, Krumeich S, Raposo G, Théry C. Diverse subpopulations of vesicles secreted by different intracellular mechanisms are present in exosome preparations obtained by differential ultracentrifugation. J Electroanal Chem [Internet]. 2012;1. Available from: http://www.sciencedirect.com/science/article/pii/002207289302975N

118. Lobb RJ, Becker M, Wen SW, Wong CSF, Wiegmans AP, Leimgruber A, et al. Optimized exosome isolation protocol for cell culture supernatant and human plasma. J Extracell vesicles [Internet]. 2015;4(27031). Available from: http://www.journalofextracellularvesicles.net/index.php/jev/article/view/270 31

119. Yuana Y, Levels J, Grootemaat A, Sturk A, Nieuwland R. Co-isolation of extracellular vesicles and high-density lipoproteins using density gradient ultracentrifugation. J Extracell vesicles [Internet]. 2014;3:1–5. Available from: http://www.pubmedcentral.nih.gov/articlerender.fcgi?artid=4090368&tool= pmcentrez&rendertype=abstract

120. Böing AN, van der Pol E, Grootemaat AE, Coumans FAW, Sturk A, Nieuwland R. Single-step isolation of extracellular vesicles by size-exclusion chromatography. J Extracell vesicles [Internet]. 2014;3(1). Available from: http://www.ncbi.nlm.nih.gov/pubmed/25279113

121. Welton JL, Webber JP, Botos L, Jones M, Clayton A. Ready-made chromatography columns for extracellular vesicle isolation from plasma. J Extracell vesicles [Internet]. 2015;4:27269. Available from: http://www.ncbi.nlm.nih.gov/pubmed/25819214

122. Lozano-Ramos I, Bancu I, Oliveira-Tercero A, Armengol MP, Menezes-Neto A, Del Portillo HA, et al. Size-exclusion chromatography-based enrichment of extracellular vesicles from urine samples. J Extracell vesicles [Internet]. 2015;4:27369. Available from: http://www.pubmedcentral.nih.gov/articlerender.fcgi?artid=4449362&tool= pmcentrez&rendertype=abstract

123. Alvarez ML, Khosroheidari M, Kanchi Ravi R, DiStefano JK. Comparison of protein, microRNA, and mRNA yields using different methods of urinary exosome isolation for the discovery of kidney disease biomarkers. Kidney Int [Internet]. 2012 Nov;82(9):1024–32. Available from: http://dx.doi.org/10.1038/ki.2012.256

124. Cheruvanky A, Zhou H, Pisitkun T, Kopp JB, Knepper MA, Yuen PST, et al. Rapid isolation of urinary exosomal biomarkers using a nanomembrane ultrafiltration concentrator. Am J Physiol Renal Physiol [Internet]. 2007 May;292(5):F1657-61. Available from: http://www.ncbi.nlm.nih.gov/pubmed/17229675

125. Kornilov R, Puhka M, Mannerström B, Hiidenmaa H, Peltoniemi H, Siljander P, et al. Efficient ultrafiltration-based protocol to deplete extracellular vesicles from fetal bovine serum. J Extracell vesicles [Internet]. 2018;7(1):1422674. Available from: https://doi.org/10.1080/20013078.2017.1422674

126. Mørk M, Handberg A, Pedersen S, Jørgensen MM, Bæk R, Nielsen MK, et al. Prospects and limitations of antibody-mediated clearing of lipoproteins from blood plasma prior to nanoparticle tracking analysis of extracellular vesicles. J Extracell vesicles [Internet]. 2017;6(1):1308779. Available from: https://doi.org/10.1080/20013078.2017.1308779

127. Deguchi H, Fernandez JA, Hackeng TM, Banka CL, Griffin JH. Cardiolipin is a normal component of human plasma lipoproteins. Proc Natl Acad Sci U S A [Internet]. 2000 Feb 15;97(4):1743–8. Available from: http://www.ncbi.nlm.nih.gov/pubmed/10677528

128. Linares R, Tan S, Gounou C, Arraud N, Brisson AR. High-speed centrifugation induces aggregation of extracellular vesicles. J Extracell vesicles [Internet]. 2015 Mar;4(3):29509. Available from: http://www.ncbi.nlm.nih.gov/pubmed/15003161

129. Shu S La, Yang Y, Allen CL, Hurley E, Tung KH, Minderman H, et al. Purity and yield of melanoma exosomes are dependent on isolation method. J Extracell vesicles [Internet]. 2020;9(1):1692401. Available from: http://www.ncbi.nlm.nih.gov/pubmed/31807236

130. Royo F, Zuñiga-Garcia P, Sanchez-Mosquera P, Egia A, Perez A, Loizaga A, et al. Different EV enrichment methods suitable for clinical settings yield different subpopulations of urinary extracellular vesicles from human samples. J Extracell Vesicles [Internet]. 2016 Feb 15;5. Available from: http://www.journalofextracellularvesicles.net/index.php/jev/article/view/29497

131. Buschmann D, Kirchner B, Hermann S, Märte M, Wurmser C, Brandes F, et al. Evaluation of serum extracellular vesicle isolation methods for profiling miRNAs by next-generation sequencing. J Extracell vesicles [Internet]. 2018;7(1):1481321. Available from: https://doi.org/10.1080/20013078.2018.1481321

132. Tian Y, Gong M, Hu Y, Liu H, Zhang W, Zhang M, et al. Quality and efficiency assessment of six extracellular vesicle isolation methods by nano-flow cytometry. J Extracell vesicles [Internet]. 2020;9(1):1697028. Available from: http://www.ncbi.nlm.nih.gov/pubmed/31839906

133. Duijvesz D, Versluis CYL, van der Fels CAM, Vredenbregt-van den Berg MS, Leivo J, Peltola MT, et al. Immuno-based detection of extracellular vesicles in urine as diagnostic marker for prostate cancer. Int J cancer [Internet]. 2015 Dec 15;137(12):2869–78. Available from: http://www.ncbi.nlm.nih.gov/pubmed/26139298

134. Ueba T, Haze T, Sugiyama M, Higuchi M, Asayama H, Karitani Y, et al. Level, distribution and correlates of platelet-derived microparticles in healthy individuals with special reference to the metabolic syndrome. Thromb Haemost [Internet]. 2008 Aug;100(2):280–5. Available from: http://www.ncbi.nlm.nih.gov/entrez/query.fcgi?cmd=Retrieve&db=PubMed &dopt=Citation&list_uids=18690348%5Cnfile:///Users/cafen/Dropbox/Pape rs/2008/Thrombosis and haemostasis/Level distribution and correlates of platelet-derived microparticles in healthy indiv

135. Kranendonk MEG, de Kleijn DP V, Kalkhoven E, Kanhai D a, Uiterwaal CSPM, van der Graaf Y, et al. Extracellular vesicle markers in relation to obesity and metabolic complications in patients with manifest cardiovascular disease. Cardiovasc Diabetol [Internet]. 2014;13:37. Available from: http://www.pubmedcentral.nih.gov/articlerender.fcgi?artid=3918107&tool= pmcentrez&rendertype=abstract

136. Jørgensen M, Bæk R, Pedersen S, Søndergaard EKL, Kristensen SR, Varming K. Extracellular Vesicle (EV) Array: microarray capturing of exosomes and other extracellular vesicles for multiplexed phenotyping. J Extracell vesicles [Internet]. 2013;2(1). Available from: http://www.ncbi.nlm.nih.gov/pubmed/24009888

137. Jørgensen MM, Bæk R, Varming K. Potentials and capabilities of the Extracellular Vesicle (EV) Array. J Extracell vesicles [Internet]. 2015;4(2015):26048. Available from: http://www.ncbi.nlm.nih.gov/pubmed/25862471

138. Bæk R, Jørgensen MM. Multiplexed Phenotyping of Small Extracellular Vesicles Using Protein Microarray (EV Array). Methods Mol Biol [Internet]. 2017;1545:117–27. Available from: http://www.ncbi.nlm.nih.gov/pubmed/27943210

139. Koliha N, Wiencek Y, Heider U, Jüngst C, Kladt N, Krauthäuser S, et al. A

novel multiplex bead-based platform highlights the diversity of extracellular vesicles. J Extracell vesicles [Internet]. 2016 Feb 19;5(17):29975. Available from: http://www.journalofextracellularvesicles.net/index.php/jev/article/view/29975/xml_47

140. Wiklander OPB, Bostancioglu RB, Welsh JA, Zickler AM, Murke F, Corso G, et al. Systematic Methodological Evaluation of a Multiplex Bead-Based Flow Cytometry Assay for Detection of Extracellular Vesicle Surface Signatures. Front Immunol [Internet]. 2018;9(June):1326. Available from: http://www.ncbi.nlm.nih.gov/pubmed/29951064

141. Laurent LC, Abdel-Mageed AB, Adelson PD, Arango J, Balaj L, Breakefield X, et al. Meeting report: discussions and preliminary findings on extracellular RNA measurement methods from laboratories in the NIH Extracellular RNA Communication Consortium. J Extracell vesicles [Internet]. 2015;4:26533. Available from: http://www.ncbi.nlm.nih.gov/pubmed/26320937%5Cnhttp://www.pubmedcentral.nih.gov/articlerender.fcgi?artid=PMC4553263

142. Chevillet JR, Kang Q, Ruf IK, Briggs H a., Vojtech LN, Hughes SM, et al. Quantitative and stoichiometric analysis of the microRNA content of exosomes. Proc Natl Acad Sci [Internet]. 2014;111(41):14888–93. Available from: http://www.pnas.org/cgi/doi/10.1073/pnas.1408301111

143. Nielsen T, Kristensen AF, Pedersen S, Christiansen G, Kristensen SR. Investigation of procoagulant activity in extracellular vesicles isolated by differential ultracentrifugation. J Extracell vesicles [Internet]. 2018;7(1):1454777. Available from: https://doi.org/10.1080/20013078.2018.1454777

144. Nielsen T, Kristensen SR, Gregersen H, Teodorescu EM, Christiansen G, Pedersen S. Extracellular vesicle-associated procoagulant phospholipid and tissue factor activity in multiple myeloma. PLoS One [Internet]. 2019;14(1):e0210835. Available from: http://www.ncbi.nlm.nih.gov/pubmed/30640949

145. Rikkert LG, Nieuwland R, Terstappen LWMM, Coumans FAW. Quality of extracellular vesicle images by transmission electron microscopy is operator and protocol dependent. J Extracell vesicles [Internet]. 2019;8(1):1555419. Available from: https://doi.org/10.1080/20013078.2018.1555419

146. Gardiner C, Ferreira YJ, Dragovic RA, Redman CWG, Sargent IL. Extracellular vesicle sizing and enumeration by nanoparticle tracking

analysis. J Extracell vesicles [Internet]. 2013 [cited 2014 Sep 29];2(1):1–11. Available from: http://www.ncbi.nlm.nih.gov/pmc/articles/PMC3760643/

147. Buzás EI, Gardiner C, Lee C, Smith ZJ. Single particle analysis: Methods for detection of platelet extracellular vesicles in suspension (excluding flow cytometry). Platelets [Internet]. 2017 May;28(3):249–55. Available from: http://dx.doi.org/10.1080/09537104.2016.1260704

148. Vestad B, Llorente A, Neurauter A, Phuyal S, Kierulf B, Kierulf P, et al. Size and concentration analyses of extracellular vesicles by nanoparticle tracking analysis: a variation study. J Extracell vesicles [Internet]. 2017;6(1):1344087. Available from: http://www.ncbi.nlm.nih.gov/pubmed/28804597

149. Bachurski D, Schuldner M, Nguyen P-H, Malz A, Reiners KS, Grenzi PC, et al. Extracellular vesicle measurements with nanoparticle tracking analysis - An accuracy and repeatability comparison between NanoSight NS300 and ZetaView. J Extracell vesicles [Internet]. 2019;8(1):1596016. Available from: https://doi.org/10.1080/20013078.2019.1596016

150. Mørk M, Pedersen S, Botha J, Lund SM, Kristensen SR. Preanalytical, analytical, and biological variation of blood plasma submicron particle levels measured with nanoparticle tracking analysis and tunable resistive pulse sensing. Scand J Clin Lab Invest [Internet]. 2016 Sep;76(5):349–60. Available from: http://www.ncbi.nlm.nih.gov/pubmed/27195974

151. Oesterreicher J, Pultar M, Schneider J, Mühleder S, Zipperle J, Grillari J, et al. Fluorescence-Based Nanoparticle Tracking Analysis and Flow Cytometry for Characterization of Endothelial Extracellular Vesicle Release. Int J Mol Sci [Internet]. 2020 Dec 4;21(23):1–16. Available from: http://www.ncbi.nlm.nih.gov/pubmed/33291792

152. Coumans FAW, van der Pol E, Böing AN, Hajji N, Sturk G, van Leeuwen TG, et al. Reproducible extracellular vesicle size and concentration determination with tunable resistive pulse sensing. J Extracell vesicles [Internet]. 2014;3(1):25922. Available from: http://www.ncbi.nlm.nih.gov/pubmed/25498889

153. Vogel R, Coumans FAW, Maltesen RG, Böing AN, Bonnington KE, Broekman ML, et al. A standardized method to determine the concentration of extracellular vesicles using tunable resistive pulse sensing. J Extracell vesicles [Internet]. 2016;5(1):31242. Available from: http://www.ncbi.nlm.nih.gov/pubmed/27680301

154. van den Goor JM, van den Brink A, Nieuwland R, van Oeveren W, Rutten

PM, Tepaske R, et al. Generation of platelet-derived microparticles in patients undergoing cardiac surgery is not affected by complement activation. J Thorac Cardiovasc Surg [Internet]. 2003 Oct [cited 2014 Oct 21];126(4):1101–6. Available from: http://linkinghub.elsevier.com/retrieve/pii/S0022522303010316

155. Hjuler Nielsen M, Irvine H, Vedel S, Raungaard B, Beck-Nielsen H, Handberg A. Elevated atherosclerosis-related gene expression, monocyte activation and microparticle-release are related to increased lipoprotein-associated oxidative stress in familial hypercholesterolemia. Boissonnas A, editor. PLoS One [Internet]. 2015 Apr 13;10(4):e0121516. Available from: http://www.pubmedcentral.nih.gov/articlerender.fcgi?artid=4395270&tool=pmcentrez&rendertype=abstract

156. Nielsen MH, Beck-Nielsen H, Andersen MN, Handberg A. A flow cytometric method for characterization of circulating cell-derived microparticles in plasma. J Extracell vesicles [Internet]. 2014;3:1–12. Available from: http://www.pubmedcentral.nih.gov/articlerender.fcgi?artid=3916676&tool=pmcentrez&rendertype=abstract

157. Shapiro HM. Practical Flow Cytometry. 4th ed. Shapiro HM, editor. Hoboken, NJ, USA: John Wiley & Sons, Inc.; 2003.

158. Cossarizza A, Chang H-D, Radbruch A, Acs A, Adam D, Adam-Klages S, et al. Guidelines for the use of flow cytometry and cell sorting in immunological studies (second edition). Eur J Immunol [Internet]. 2019 Oct;49(10):1457–973. Available from: http://www.ncbi.nlm.nih.gov/pubmed/31633216

159. Givan AL. Instrumentation: Into the Black Box. In: Givan AL, editor. Flow Cytometry: First Principles. 2nd ed. New York: John Wiley & Sons, Inc.; 2001. p. 15–39.

160. Kenyon O. Optical arrangement for a flow cytometer [Internet]. WO, US: World Intellectual Property Organization; WO 2007/000574 A1, 2005. Available from: https://patents.google.com/patent/GB2441251A/en?inventor=oliver+kenyon&oq=oliver+kenyon

161. van der Vlist EJ, Nolte-'t Hoen ENM, Stoorvogel W, Arkesteijn GJ a, Wauben MHM. Fluorescent labeling of nano-sized vesicles released by cells and subsequent quantitative and qualitative analysis by high-resolution flow cytometry. Nat Protoc [Internet]. 2012 Jun 14;7(7):1311–26. Available from: http://www.ncbi.nlm.nih.gov/pubmed/22722367

162.    Morales-Kastresana A, Musich TA, Welsh JA, Telford W, Demberg T, Wood JCS, et al. High-fidelity detection and sorting of nanoscale vesicles in viral disease and cancer. J Extracell vesicles [Internet]. 2019;8(1):1597603. Available from: https://doi.org/10.1080/20013078.2019.1597603

163.    Youker RT. Detectors for Super-Resolution &amp; Single-Molecule Fluorescence Microscopies. In: Photon Counting - Fundamentals and Applications [Internet]. InTech; 2018. Available from: http://www.intechopen.com/books/photon-counting-fundamentals-and-applications/detectors-for-super-resolution-single-molecule-fluorescence-microscopies

164.    Steen HB. Noise, sensitivity, and resolution of flow cytometers. Cytometry [Internet]. 1992;13(8):822–30. Available from: http://www.ncbi.nlm.nih.gov/pubmed/1458999

165.    Chase ES, Hoffman RA. Resolution of dimly fluorescent particles: a practical measure of fluorescence sensitivity. Cytometry [Internet]. 1998 Oct 1;33(2):267–79. Available from: http://www.ncbi.nlm.nih.gov/pubmed/9773890

166.    Gaucher JC, Grunwald D, Frelat G. Fluorescence response and sensitivity determination for ATC 3000 flow cytometer. Cytometry [Internet]. 1988 Nov;9(6):557–65. Available from: http://www.ncbi.nlm.nih.gov/pubmed/3145175

167.    Stoner SA, Duggan E, Condello D, Guerrero A, Turk JR, Narayanan PK, et al. High sensitivity flow cytometry of membrane vesicles. Cytometry A [Internet]. 2016 Feb;89(2):196–206. Available from: http://www.ncbi.nlm.nih.gov/pubmed/26484737

168.    Nolan JP, Stoner SA. A trigger channel threshold artifact in nanoparticle analysis. Cytometry A [Internet]. 2013 Mar;83(3):301–5. Available from: http://www.ncbi.nlm.nih.gov/pubmed/23335161

169.    de Rond L, Coumans FAW, Welsh JA, Nieuwland R, van Leeuwen TG, van der Pol E. Quantification of Light Scattering Detection Efficiency and Background in Flow Cytometry. Cytometry A [Internet]. 2020 Oct 21; Available from: http://www.ncbi.nlm.nih.gov/pubmed/33085220

170.    Spidlen J, Moore W, Parks D, Goldberg M, Blenman K, Cavenaugh JS, et al. Data File Standard for Flow Cytometry, Version FCS 3.2. Cytometry A [Internet]. 2021 Jan;99(1):100–2. Available from: http://www.ncbi.nlm.nih.gov/pubmed/32881398

171.   Esposito K, Ciotola M, Schisano B, Gualdiero R, Sardelli L, Misso L, et al. Endothelial Microparticles Correlate with Endothelial Dysfunction in Obese Women. J Clin Endocrinol Metab [Internet]. 2006 Sep;91(9):3676–9. Available from: http://press.endocrine.org/doi/abs/10.1210/jc.2006-0851

172.   Diamant M. Elevated Numbers of Tissue-Factor Exposing Microparticles Correlate With Components of the Metabolic Syndrome in Uncomplicated Type 2 Diabetes Mellitus. Circulation [Internet]. 2002 Nov 5;106(19):2442–7. Available from: http://circ.ahajournals.org/cgi/doi/10.1161/01.CIR.0000036596.59665.C6

173.   Arteaga RB, Chirinos J a., Soriano AO, Jy W, Horstman L, Jimenez JJ, et al. Endothelial microparticles and platelet and leukocyte activation in patients with the metabolic syndrome. Am J Cardiol [Internet]. 2006 Jul 1;98(1):70–4. Available from: http://www.ncbi.nlm.nih.gov/pubmed/16784924

174.   Agouni A, Lagrue-Lak-Hal AH, Ducluzeau PH, Mostefai HA, Draunet-Busson C, Leftheriotis G, et al. Endothelial Dysfunction Caused by Circulating Microparticles from Patients with Metabolic Syndrome. Am J Pathol [Internet]. 2008 Oct;173(4):1210–9. Available from: http://linkinghub.elsevier.com/retrieve/pii/S000294401061509X

175.   Chen Y, Feng B, Li X, Ni Y, Luo Y. Plasma endothelial microparticles and their correlation with the presence of hypertension and arterial stiffness in patients with type 2 diabetes. J Clin Hypertens (Greenwich) [Internet]. 2012 Jul;14(7):455–60. Available from: http://doi.wiley.com/10.1111/j.1751-7176.2012.00631.x

176.   Chandler WL, Yeung W, Tait JF. A new microparticle size calibration standard for use in measuring smaller microparticles using a new flow cytometer. J Thromb Haemost [Internet]. 2011 Jun;9(6):1216–24. Available from: http://www.ncbi.nlm.nih.gov/pubmed/21481178

177.   van der Pol E, van Gemert MJC, Sturk A, Nieuwland R, van Leeuwen TG. Single vs. swarm detection of microparticles and exosomes by flow cytometry. J Thromb Haemost [Internet]. 2012 May;10(5):919–30. Available from: http://www.ncbi.nlm.nih.gov/pubmed/22394434

178.   Suárez H, Gámez-Valero A, Reyes R, López-Martín S, Rodríguez MJ, Carrascosa JL, et al. A bead-assisted flow cytometry method for the semi-quantitative analysis of Extracellular Vesicles. Sci Rep [Internet]. 2017 Sep 12;7(1):11271. Available from: http://www.ncbi.nlm.nih.gov/pubmed/28900146

179.    Marie, Brussaard, Thyrhaug, Bratbak, Vaulot. Enumeration of marine viruses in culture and natural samples by flow cytometry. Appl Environ Microbiol [Internet]. 1999 Jan;65(1):45–52. Available from: http://www.ncbi.nlm.nih.gov/pubmed/9872758

180.    Brussaard CPD, Marie D, Bratbak G. Flow cytometric detection of viruses. J Virol Methods [Internet]. 2000 Mar;85(1–2):175–82. Available from: http://www.ncbi.nlm.nih.gov/pubmed/10716350

181.    Headland SE, Jones HR, D'Sa AS V, Perretti M, Norling L V. Cutting-edge analysis of extracellular microparticles using ImageStream(X) imaging flow cytometry. Sci Rep [Internet]. 2014 Jun 10;4:5237. Available from: http://www.ncbi.nlm.nih.gov/pubmed/24913598

182.    Erdbrügger U, Rudy CK, Etter ME, Dryden KA, Yeager M, Klibanov AL, et al. Imaging flow cytometry elucidates limitations of microparticle analysis by conventional flow cytometry. Cytometry A [Internet]. 2014 Sep;85(9):756–70. Available from: http://www.ncbi.nlm.nih.gov/pubmed/24903900

183.    Mastoridis S, Bertolino GM, Whitehouse G, Dazzi F, Sanchez-Fueyo A, Martinez-Llordella M. Multiparametric Analysis of Circulating Exosomes and Other Small Extracellular Vesicles by Advanced Imaging Flow Cytometry. Front Immunol [Internet]. 2018;9(July):1583. Available from: http://www.ncbi.nlm.nih.gov/pubmed/30034401

184.    Görgens A, Bremer M, Ferrer-Tur R, Murke F, Tertel T, Horn PA, et al. Optimisation of imaging flow cytometry for the analysis of single extracellular vesicles by using fluorescence-tagged vesicles as biological reference material. J Extracell vesicles [Internet]. 2019;8(1):1587567. Available from: https://doi.org/10.1080/20013078.2019.1587567

185.    Lannigan J, Erdbruegger U. Imaging flow cytometry for the characterization of extracellular vesicles. Methods [Internet]. 2017;112:55–67. Available from: http://dx.doi.org/10.1016/j.ymeth.2016.09.018

186.    Steen HB. Flow cytometer for measurement of the light scattering of viral and other submicroscopic particles. Cytometry A [Internet]. 2004 Feb;57(2):94–9. Available from: http://www.ncbi.nlm.nih.gov/pubmed/14750130

187.    Tang VA, Renner TM, Fritzsche AK, Burger D, Langlois M-A. Single-Particle Discrimination of Retroviruses from Extracellular Vesicles by Nanoscale Flow Cytometry. Sci Rep [Internet]. 2017 Dec 19;7(1):17769. Available from: http://www.ncbi.nlm.nih.gov/pubmed/29259315

188.    Groot Kormelink T, Arkesteijn GJA, Nauwelaers FA, van den Engh G, Nolte-'t Hoen ENM, Wauben MHM. Prerequisites for the analysis and sorting of extracellular vesicle subpopulations by high-resolution flow cytometry. Cytometry A [Internet]. 2016 Feb;89(2):135–47. Available from: http://www.ncbi.nlm.nih.gov/pubmed/25688721

189.    Brittain GC, Chen YQ, Martinez E, Tang VA, Renner TM, Langlois M-A, et al. A Novel Semiconductor-Based Flow Cytometer with Enhanced Light-Scatter Sensitivity for the Analysis of Biological Nanoparticles. Sci Rep [Internet]. 2019;9(1):16039. Available from: http://www.ncbi.nlm.nih.gov/pubmed/31690751

190.    van de Hulst H. Light Scattering by Small Particles. Corrected. Dover: Dover Publications; 1981. 496 p.

191.    Arkesteijn GJA, Lozano-Andrés E, Libregts SFWM, Wauben MHM. Improved Flow Cytometric Light Scatter Detection of Submicron-Sized Particles by Reduction of Optical Background Signals. Cytometry A [Internet]. 2020;97(6):610–9. Available from: http://www.ncbi.nlm.nih.gov/pubmed/32459071

192.    de Rond L, van der Pol E, Bloemen PR, Van Den Broeck T, Monheim L, Nieuwland R, et al. A Systematic Approach to Improve Scatter Sensitivity of a Flow Cytometer for Detection of Extracellular Vesicles. Cytometry A [Internet]. 2020;97(6):582–91. Available from: http://www.ncbi.nlm.nih.gov/pubmed/32017331

193.    Zhu S, Ma L, Wang S, Chen C, Zhang W, Yang L, et al. Light-scattering detection below the level of single fluorescent molecules for high-resolution characterization of functional nanoparticles. ACS Nano [Internet]. 2014 Oct 28;8(10):10998–1006. Available from: http://www.ncbi.nlm.nih.gov/pubmed/25300001

194.    Tian Y, Ma L, Gong M, Su G, Zhu S, Zhang W, et al. Protein Profiling and Sizing of Extracellular Vesicles from Colorectal Cancer Patients via Flow Cytometry. ACS Nano [Internet]. 2018;12(1):671–80. Available from: http://www.ncbi.nlm.nih.gov/pubmed/29300458

195.    Crompot E, Van Damme M, Duvillier H, Pieters K, Vermeesch M, Perez-Morga D, et al. Avoiding false positive antigen detection by flow cytometry on blood cell derived microparticles: the importance of an appropriate negative control. PLoS One [Internet]. 2015;10(5):e0127209. Available from: http://www.ncbi.nlm.nih.gov/pubmed/25978814

196.    Welsh JA, Van Der Pol E, Arkesteijn GJA, Bremer M, Brisson A, Coumans F, et al. MIFlowCyt-EV: a framework for standardized reporting of extracellular vesicle flow cytometry experiments. J Extracell vesicles [Internet]. 2020;9(1):1713526. Available from: http://www.ncbi.nlm.nih.gov/pubmed/32128070

197.    de Rond L, Libregts SFWM, Rikkert LG, Hau CM, van der Pol E, Nieuwland R, et al. Refractive index to evaluate staining specificity of extracellular vesicles by flow cytometry. J Extracell vesicles [Internet]. 2019;8(1):1643671. Available from: https://doi.org/10.1080/20013078.2019.1643671

198.    De Rond L, Van Der Pol E, Hau CM, Varga Z, Sturk A, Van Leeuwen TG, et al. Comparison of generic fluorescent markers for detection of extracellular vesicles by flow cytometry. Clin Chem [Internet]. 2018 Apr;64(4):680–9. Available from: http://www.ncbi.nlm.nih.gov/pubmed/29453194

199.    Li Z, Otvos JD, Lamon-Fava S, Carrasco W V., Lichtenstein AH, McNamara JR, et al. Men and women differ in lipoprotein response to dietary saturated fat and cholesterol restriction. J Nutr [Internet]. 2003 Nov;133(11):3428–33. Available from: http://www.ncbi.nlm.nih.gov/pubmed/14608054

200.    Otvos JD, Jeyarajah EJ, Bennett DW, Krauss RM. Development of a proton nuclear magnetic resonance spectroscopic method for determining plasma lipoprotein concentrations and subspecies distributions from a single, rapid measurement. Clin Chem [Internet]. 1992 Sep;38(9):1632–8. Available from: http://www.ncbi.nlm.nih.gov/pubmed/1326420

201.    Wojczynski MK, Glasser SP, Oberman A, Kabagambe EK, Hopkins PN, Tsai MY, et al. High-fat meal effect on LDL, HDL, and VLDL particle size and number in the Genetics of Lipid-Lowering Drugs and Diet Network (GOLDN): an interventional study. Lipids Health Dis [Internet]. 2011 Oct 18;10(3):181. Available from: http://www.ncbi.nlm.nih.gov/pubmed/10837758

202.    van der Pol E, de Rond L, Coumans FAW, Gool EL, Böing AN, Sturk A, et al. Absolute sizing and label-free identification of extracellular vesicles by flow cytometry. Nanomedicine [Internet]. 2018 Apr;14(3):801–10. Available from: https://doi.org/10.1016/j.nano.2017.12.012

203.    Chernova DN, Konokhova AI, Novikova OA, Yurkin MA, Strokotov DI, Karpenko AA, et al. Chylomicrons against light scattering: The battle for characterization. J Biophotonics [Internet]. 2018;11(10):e201700381. Available from: http://www.ncbi.nlm.nih.gov/pubmed/29603652

204. Sódar BW, Kittel Á, Pálóczi K, Vukman K V, Osteikoetxea X, Szabó-Taylor K, et al. Low-density lipoprotein mimics blood plasma-derived exosomes and microvesicles during isolation and detection. Sci Rep [Internet]. 2016 Apr 18;6(April):24316. Available from: http://www.nature.com/articles/srep24316

205. Aass HCD, Øvstebø R, Trøseid A-MS, Kierulf P, Berg JP, Henriksson CE. Fluorescent particles in the antibody solution result in false TF- and CD14-positive microparticles in flow cytometric analysis. Cytometry A [Internet]. 2011 Dec;79(12):990–9. Available from: http://www.ncbi.nlm.nih.gov/pubmed/21990118

206. Inglis HC, Danesh A, Shah A, Lacroix J, Spinella PC, Norris PJ. Techniques to improve detection and analysis of extracellular vesicles using flow cytometry. Cytometry A [Internet]. 2015 Nov;87(11):1052–63. Available from: http://www.ncbi.nlm.nih.gov/pubmed/25847910

207. Simonsen JB. Pitfalls associated with lipophilic fluorophore staining of extracellular vesicles for uptake studies. J Extracell vesicles [Internet]. 2019;8(1):1582237. Available from: https://doi.org/10.1080/20013078.2019.1582237

208. Pužar Dominkuš P, Stenovec M, Sitar S, Lasič E, Zorec R, Plemenitaš A, et al. PKH26 labeling of extracellular vesicles: Characterization and cellular internalization of contaminating PKH26 nanoparticles. Biochim Biophys acta Biomembr [Internet]. 2018 Jun;1860(6):1350–61. Available from: http://www.ncbi.nlm.nih.gov/pubmed/29551275

209. Takov K, Yellon DM, Davidson SM. Confounding factors in vesicle uptake studies using fluorescent lipophilic membrane dyes. J Extracell vesicles [Internet]. 2017;6(1):1388731. Available from: https://doi.org/10.1080/20013078.2017.1388731

210. Welsh JA, Horak P, Wilkinson JS, Ford VJ, Jones JC, Smith D, et al. FCMPASS Software Aids Extracellular Vesicle Light Scatter Standardization. Cytometry A [Internet]. 2020;97(6):569–81. Available from: http://www.ncbi.nlm.nih.gov/pubmed/31250561

211. Bagwell CB, Adams EG. Fluorescence spectral overlap compensation for any number of flow cytometry parameters. Ann N Y Acad Sci [Internet]. 1993 Mar 20;677(1):167–84. Available from: http://www.ncbi.nlm.nih.gov/pubmed/8494206

212. Roederer M. Spectral compensation for flow cytometry: visualization

artifacts, limitations, and caveats. Cytometry [Internet]. 2001 Nov 1;45(3):194–205. Available from: http://www.ncbi.nlm.nih.gov/pubmed/11746088

213. Roederer M. Distributions of autofluorescence after compensation: Be panglossian, fret not. Cytometry A [Internet]. 2016 Apr;89(4):398–402. Available from: http://doi.wiley.com/10.1002/cyto.a.22820

214. Maecker HT, Trotter J. Flow cytometry controls, instrument setup, and the determination of positivity. Cytometry A [Internet]. 2006 Sep 1;69(9):1037–42. Available from: http://www.ncbi.nlm.nih.gov/pubmed/17211880

215. Poncelet P, Robert S, Bailly N, Garnache-Ottou F, Bouriche T, Devalet B, et al. Tips and tricks for flow cytometry-based analysis and counting of microparticles. Transfus Apher Sci [Internet]. 2015 Oct;53(2):110–26. Available from: http://dx.doi.org/10.1016/j.transci.2015.10.008

216. Schwartz A, Wang L, Early E, Gaigalas A, Zhang Y-Z, Marti GE, et al. Quantitating Fluorescence Intensity from Fluorophore: The Definition of MESF Assignment. J Res Natl Inst Stand Technol [Internet]. 1998;107(1):83–91. Available from: http://dx.doi.org/10.1016/j.jaci.2012.05.050

217. Tchernof A, Despres J-P. Pathophysiology of Human Visceral Obesity: An Update. Physiol Rev [Internet]. 2013 Jan 1;93(1):359–404. Available from: http://physrev.physiology.org/cgi/doi/10.1152/physrev.00033.2011

218. Brownlee M. Biochemistry and molecular cell biology of diabetic complications. Nature [Internet]. 2001 Dec 13;414(6865):813–20. Available from: http://www.ncbi.nlm.nih.gov/pubmed/11742414

219. Brownlee M. The pathobiology of diabetic complications: a unifying mechanism. Diabetes [Internet]. 2005 Jun;54(6):1615–25. Available from: http://www.ncbi.nlm.nih.gov/pubmed/15919781

220. Steneberg P, Sykaras AG, Backlund F, Straseviciene J, Söderström I, Edlund H. Hyperinsulinemia Enhances Hepatic Expression of the Fatty Acid Transporter Cd36 and Provokes Hepatosteatosis and Hepatic Insulin Resistance. J Biol Chem [Internet]. 2015 Jul 31;290(31):19034–43. Available from: http://www.ncbi.nlm.nih.gov/pubmed/26085100

221. Corpeleijn E, Pelsers MMAL, Soenen S, Mensink M, Bouwman FG, Kooi ME, et al. Insulin acutely upregulates protein expression of the fatty acid transporter CD36 in human skeletal muscle in vivo. J Physiol Pharmacol [Internet]. 2008 Mar 6;59(1):77–83. Available from:

http://www.ncbi.nlm.nih.gov/pubmed/22584574

222. Kashyap SR, Ioachimescu AG, Gornik HL, Gopan T, Davidson MB, Makdissi A, et al. Lipid-induced insulin resistance is associated with increased monocyte expression of scavenger receptor CD36 and internalization of oxidized LDL. Obesity (Silver Spring) [Internet]. 2009 Dec 11;17(12):2142–8. Available from: http://www.pubmedcentral.nih.gov/articlerender.fcgi?artid=2836489&tool=pmcentrez&rendertype=abstract

223. Jay AG, Hamilton JA. The enigmatic membrane fatty acid transporter CD36: New insights into fatty acid binding and their effects on uptake of oxidized LDL. Prostaglandins Leukot Essent Fatty Acids [Internet]. 2016 May 20;1–7. Available from: http://linkinghub.elsevier.com/retrieve/pii/S0952327816300291

224. Kennedy DJ, Kashyap SR. Pathogenic role of scavenger receptor CD36 in the metabolic syndrome and diabetes. Metab Syndr Relat Disord [Internet]. 2011 Aug;9(4):239–45. Available from: http://www.ncbi.nlm.nih.gov/pubmed/21428745

225. Canton J, Neculai D, Grinstein S. Scavenger receptors in homeostasis and immunity. Nat Rev Immunol [Internet]. 2013 Sep;13(9):621–34. Available from: http://www.ncbi.nlm.nih.gov/pubmed/23928573

226. Knøsgaard L, Thomsen SB, Støckel M, Vestergaard H, Handberg A. Circulating sCD36 is associated with unhealthy fat distribution and elevated circulating triglycerides in morbidly obese individuals. Nutr Diabetes [Internet]. 2014 Apr 7;4(4):e114. Available from: http://www.pubmedcentral.nih.gov/articlerender.fcgi?artid=4007154&tool=pmcentrez&rendertype=abstract

227. Handberg A, Levin K, Højlund K, Beck-Nielsen H. Identification of the oxidized low-density lipoprotein scavenger receptor CD36 in plasma: a novel marker of insulin resistance. Circulation [Internet]. 2006 Sep 12;114(11):1169–76. Available from: http://circ.ahajournals.org/cgi/doi/10.1161/CIRCULATIONAHA.106.626135

228. Heebøll S, Poulsen MK, Ornstrup MJ, Kjær TN, Pedersen SB, Nielsen S, et al. Circulating sCD36 levels in patients with non-alcoholic fatty liver disease and controls. Int J Obes (Lond) [Internet]. 2017 Feb;41(2):262–7. Available from: http://dx.doi.org/10.1038/ijo.2016.223

229. Alkhatatbeh MJ, Mhaidat NM, Enjeti AK, Lincz LF, Thorne RF. The putative diabetic plasma marker, soluble CD36, is non-cleaved, non-soluble and entirely associated with microparticles. J Thromb Haemost [Internet]. 2011 Apr;9(4):844–51. Available from: http://doi.wiley.com/10.1111/j.1538-7836.2011.04220.x

230. Sanden M, Botha J, Nielsen MRS, Nielsen MH, Schmidt EB, Handberg A. BLTR1 and CD36 Expressing Microvesicles in Atherosclerotic Patients and Healthy Individuals. Front Cardiovasc Med [Internet]. 2018;5(October):156. Available from: https://www.frontiersin.org/article/10.3389/fcvm.2018.00156/full

231. Botha J, Nielsen MH, Christensen MH, Vestergaard H, Handberg A. Bariatric surgery reduces CD36-bearing microvesicles of endothelial and monocyte origin. Nutr Metab (Lond) [Internet]. 2018;15:76. Available from: http://www.ncbi.nlm.nih.gov/pubmed/30386406

232. Nielsen MH, Irvine H, Vedel S, Raungaard B, Beck-Nielsen H, Handberg A. The Impact of Lipoprotein-Associated Oxidative Stress on Cell-Specific Microvesicle Release in Patients with Familial Hypercholesterolemia. Oxid Med Cell Longev [Internet]. 2016;2016:2492858. Available from: http://www.hindawi.com/journals/omcl/2016/2492858/

233. Botha J, Velling Magnussen L, Nielsen MH, Nielsen TB, Højlund K, Andersen MS, et al. Microvesicles Correlated with Components of Metabolic Syndrome in Men with Type 2 Diabetes Mellitus and Lowered Testosterone Levels But Were Unaltered by Testosterone Therapy. J Diabetes Res [Internet]. 2017;2017:4257875. Available from: https://www.hindawi.com/journals/jdr/2017/4257875/

234. Royo F, Schlangen K, Palomo L, Gonzalez E, Conde-Vancells J, Berisa A, et al. Transcriptome of extracellular vesicles released by hepatocytes. PLoS One [Internet]. 2013;8(7):e68693. Available from: http://www.ncbi.nlm.nih.gov/pubmed/23874726

235. Povero D, Panera N, Eguchi A, Johnson CD, Papouchado BG, de Araujo Horcel L, et al. Lipid-induced hepatocyte-derived extracellular vesicles regulate hepatic stellate cell via microRNAs targeting PPAR-gamma. Cell Mol Gastroenterol Hepatol. 2015 Nov;1(6):646-663.e4.

236. Cho Y-E, Im E-J, Moon P-G, Mezey E, Song B-J, Baek M-C. Increased liver-specific proteins in circulating extracellular vesicles as potential biomarkers for drug- and alcohol-induced liver injury. PLoS One [Internet]. 2017;12(2):e0172463. Available from:

http://www.ncbi.nlm.nih.gov/pubmed/28225807

237.    Eguchi A, Lazaro RG, Wang J, Kim J, Povero D, Willliams B, et al. Extracellular vesicles released by hepatocytes from gastric infusion model of alcoholic liver disease contain a MicroRNA barcode that can be detected in blood. Hepatology [Internet]. 2017 Feb;65(2):475–90. Available from: http://www.ncbi.nlm.nih.gov/pubmed/27639178

238.    Lacroix R, Robert S, Poncelet P, Dignat-George F. Overcoming limitations of microparticle measurement by flow cytometry. Semin Thromb Hemost [Internet].        2010        Nov;36(8):807–18.        Available        from: http://www.ncbi.nlm.nih.gov/pubmed/?term=21049381

239.    Lacroix R, Robert S, Poncelet P, Kasthuri RS, Key NS, Dignat-George F. Standardization of platelet-derived microparticle enumeration by flow cytometry with calibrated beads: results of the International Society on Thrombosis and Haemostasis SSC Collaborative workshop. J Thromb Haemost [Internet]. 2010 Nov [cited 2014 Oct 14];8(11):2571–4. Available from: http://www.ncbi.nlm.nih.gov/pubmed/20831623

240.    Botha J, Pugsley HR, Handberg A. Conventional, High-Resolution and Imaging Flow Cytometry: Benchmarking Performance in Characterisation of Extracellular Vesicles. Biomedicines [Internet]. 2021 Jan 27;9(2):124. Available from: http://www.ncbi.nlm.nih.gov/pubmed/33513846

241.    Rasmussen RW, Botha J, Prip F, Sanden M, Nielsen MH, Handberg A. Zoom in on Antibody Aggregates: A Potential Pitfall in the Search of Rare EV Populations. Biomedicines [Internet]. 2021 Feb 18;9(2):206. Available from: https://www.mdpi.com/2227-9059/9/2/206

242.    Osteikoetxea X, Sódar B, Németh A, Szabó-Taylor K, Pálóczi K, Vukman K V., et al. Differential detergent sensitivity of extracellular vesicle subpopulations. Org Biomol Chem [Internet]. 2015 Oct 14;13(38):9775–82. Available from: http://www.ncbi.nlm.nih.gov/pubmed/26264754

243.    Bloom RJ, Elwood JC. Quantitation of lipid profiles from isolated serum lipoproteins using small volumes of human serum. Clin Biochem [Internet]. 1981        Jun;14(3):119–25.        Available        from: http://www.ncbi.nlm.nih.gov/pubmed/7296821

244.    Christinat N, Masoodi M. Comprehensive Lipoprotein Characterization Using Lipidomics Analysis of Human Plasma. J Proteome Res [Internet]. 2017;16(8):2947–53.        Available        from: http://www.ncbi.nlm.nih.gov/pubmed/28650171

245.    Crawford SE, Borensztajn J. Plasma clearance and liver uptake of chylomicron remnants generated by hepatic lipase lipolysis: evidence for a lactoferrin-sensitive and apolipoprotein E-independent pathway. J Lipid Res [Internet]. 1999 May;40(5):797–805. Available from: http://dx.doi.org/10.1016/S0022-2275(20)32114-3

246.    Yang LY, Kuksis A, Myher JJ, Pang H. Surface components of chylomicrons from rats fed glyceryl or alkyl esters of fatty acids: minor components. Lipids [Internet]. 1992 Aug;27(8):613–8. Available from: http://www.ncbi.nlm.nih.gov/pubmed/1406072

247.    Mørk M, Nielsen MH, Bæk R, Jørgensen MM, Pedersen S, Kristensen SR. Postprandial Increase in Blood Plasma Levels of Tissue Factor-Bearing (and Other) Microvesicles Measured by Flow Cytometry: Fact or Artifact? TH open companion J to Thromb Haemost [Internet]. 2018 Apr;2(2):e147–57. Available from: http://www.ncbi.nlm.nih.gov/pubmed/31249938

248.    Botha J, Handberg A, Simonsen JB. Lipid-based strategies used to identify extracellular vesicles in flow cytometry can be confounded by lipoproteins. Submitt to J Extracell Vesicles. 2021;

249.    Schwartz A, Gaigalas AK, Wang L, Marti GE, Vogt RF, Fernandez-Repollet E. Formalization of the MESF unit of fluorescence intensity. Cytometry B Clin Cytom [Internet]. 2004 Jan;57(1):1–6. Available from: http://www.ncbi.nlm.nih.gov/pubmed/14696057

250.    Botha J, Sanden M, Rasmussen RW, Nielsen MH, Pedersen MM, Handberg A. A Systematic Approach to Optimise Analytical Parameters for Optimal Detection of Sub-micron Particles by Flow Cytometry. Prep.

251.    Knöner G, Parkin S, Nieminen TA, Heckenberg NR, Rubinsztein-Dunlop H. Measurement of the index of refraction of single microparticles. Phys Rev Lett [Internet]. 2006 Oct 13;97(15):157402. Available from: http://www.ncbi.nlm.nih.gov/pubmed/17155356

252.    Varga Z, van der Pol E, Pálmai M, Garcia-Diez R, Gollwitzer C, Krumrey M, et al. Hollow organosilica beads as reference particles for optical detection of extracellular vesicles. J Thromb Haemost [Internet]. 2018 Jun 7;16(8):1646–55. Available from: http://www.ncbi.nlm.nih.gov/pubmed/29877049

253.    van der Pol E, Coumans FAW, Sturk A, Nieuwland R, van Leeuwen TG. Refractive index determination of nanoparticles in suspension using nanoparticle tracking analysis. Nano Lett [Internet]. 2014 Nov 12;14(11):6195–201. Available from:

http://www.ncbi.nlm.nih.gov/pubmed/25256919

254.    Gardiner C, Shaw M, Hole P, Smith J, Tannetta D, Redman CW, et al. Measurement of refractive index by nanoparticle tracking analysis reveals heterogeneity in extracellular vesicles. J Extracell vesicles [Internet]. 2014;3(1):25361.                    Available                    from: http://www.ncbi.nlm.nih.gov/pubmed/25425324

255.    Li W, Prabakaran P, Chen W, Zhu Z, Feng Y, Dimitrov D. Antibody Aggregation: Insights from Sequence and Structure. Antibodies. 2016;5(3):19.

256.    Wang W, Nema S, Teagarden D. Protein aggregation-Pathways and influencing factors. International Journal of Pharmaceutics. 2010.

257.    Rikkert LG, van der Pol E, van Leeuwen TG, Nieuwland R, Coumans FAW. Centrifugation affects the purity of liquid biopsy-based tumor biomarkers. Cytometry A [Internet]. 2018 Dec 14;93(12):1207–12. Available from: https://onlinelibrary.wiley.com/doi/abs/10.1002/cyto.a.23641

258.    Fischer H, Polikarpov I, Craievich AF. Average protein density is a molecular-weight-dependent function. Protein Sci [Internet]. 2004 Oct;13(10):2825–8.                    Available                    from: http://www.ncbi.nlm.nih.gov/pubmed/15388866

259.    Milne RW, Marcel YL. Monoclonal antibodies against human low density lipoprotein. Stoichiometric binding studies using Fab fragments. FEBS Lett [Internet].        1982        Sep        6;146(1):97–100.        Available        from: http://www.ncbi.nlm.nih.gov/pubmed/6183147

260.    Dashti M, Kulik W, Hoek F, Veerman EC, Peppelenbosch MP, Rezaee F. A phospholipidomic analysis of all defined human plasma lipoproteins. Sci Rep [Internet].                    2011;1:139.                    Available                    from: http://www.ncbi.nlm.nih.gov/pubmed/22355656

261.    Otzen DE, Blans K, Wang H, Gilbert GE, Rasmussen JT. Lactadherin binds to phosphatidylserine-containing vesicles in a two-step mechanism sensitive to vesicle size and composition. Biochim Biophys Acta [Internet]. 2012 Apr;1818(4):1019–27.                    Available                    from: http://dx.doi.org/10.1016/j.bbamem.2011.08.032

262.    Meers P, Mealy T. Phospholipid determinants for annexin V binding sites and the role of tryptophan 187. Biochemistry [Internet]. 1994 May 17;33(19):5829–37.                    Available                    from:

http://www.ncbi.nlm.nih.gov/pubmed/8180211

263.    Pigault C, Follenius-Wund A, Schmutz M, Freyssinet JM, Brisson A. Formation of two-dimensional arrays of annexin V on phosphatidylserine-containing liposomes. J Mol Biol [Internet]. 1994 Feb 11;236(1):199–208. Available                                            from: https://linkinghub.elsevier.com/retrieve/pii/S0022283684711296

264.    Jay AG, Chen AN, Paz MA, Hung JP, Hamilton JA. CD36 binds oxidized low density lipoprotein (LDL) in a mechanism dependent upon fatty acid binding. J Biol Chem [Internet]. 2015 Feb 20;290(8):4590–603. Available from: http://www.ncbi.nlm.nih.gov/pubmed/25555908

265.    Englyst NA, Taube JM, Aitman TJ, Baglin TP, Byrne CD. A novel role for CD36 in VLDL-enhanced platelet activation. Diabetes [Internet]. 2003 May 1;52(5):1248–55.                  Available                  from: http://www.ncbi.nlm.nih.gov/pubmed/12716760

266.    Ghosh A, Murugesan G, Chen K, Zhang L, Wang Q, Febbraio M, et al. Platelet CD36 surface expression levels affect functional responses to oxidized LDL and are associated with inheritance of specific genetic polymorphisms. Blood [Internet]. 2011 Jun 9;117(23):6355–66. Available from: http://www.ncbi.nlm.nih.gov/pubmed/21478428

267.    Laven P. MiePlot [Internet]. 2021 [cited 2021 Jul 28]. Available from: http://www.philiplaven.com/mieplot.htm

268.    de Rond L, Coumans FAW, Nieuwland R, van Leeuwen TG, van der Pol E. Deriving Extracellular Vesicle Size From Scatter Intensities Measured by Flow Cytometry. Curr Protoc Cytom [Internet]. 2018;86(1):e43. Available from: http://www.ncbi.nlm.nih.gov/pubmed/30168659

269.    Yamanaka M, Saito K, Smith NI, Kawata S, Nagai T, Fujita K. Saturated excitation of fluorescent proteins for subdiffraction-limited imaging of living cells in three dimensions. Interface Focus [Internet]. 2013 Oct 6;3(5):20130007.                  Available                  from: http://www.ncbi.nlm.nih.gov/pubmed/24511385

270.    Yamanaka M, Kawano S, Fujita K, Smith NI, Kawata S. Beyond the diffraction-limit biological imaging by saturated excitation microscopy. J Biomed    Opt    [Internet].    2008;13(5):050507.    Available    from: http://www.ncbi.nlm.nih.gov/pubmed/19021372

271.    Chaze W, Caballina O, Castanet G, Lemoine F. The saturation of the

fluorescence and its consequences for laser-induced fluorescence thermometry in liquid flows. Exp Fluids [Internet]. 2016 Apr 13;57(4):58. Available from: http://link.springer.com/10.1007/s00348-016-2142-8

# APPENDICES

# Appendix A. Paper 1

**Conventional, High-Resolution and Imaging Flow Cytometry: Benchmarking Performance in Characterisation of Extracellular Vesicles.**
<u>**Botha J**</u>, Pugsley HR, Handberg A. (2021). *Biomedicines* 9(2):124.

# Appendix B. Paper 2

**Zoom in on Antibody Aggregates: A Potential Pitfall in the Search of Rare EV Populations.**
Rasmussen RW, **Botha J**, Prip F, Sanden M, Nielsen MH, Handberg A. (2021). *Biomedicines* 9(2):206.

# Appendix C. Paper 3

**Lipid-based strategies used to identify extracellular vesicles in flow cytometry can be confounded by lipoproteins.**
**<u>Botha J</u>**, Handberg A, Simonsen JB. *Submitted to Journal of Extracellular Vesicles*.

# Appendix D. Paper 4

**A systematic approach to optimise analysis protocols for flow cytometry characterisation of sub-micron particles.**
**Botha J**, Sanden M, Rasmussen RW, Nielsen MH, Mellergaard M, Handberg A.
*Manuscript in preparation.*

# Appendix E. Full list of publications

## Articles published in journals (7)

**2021**

**Botha J**, Pugsley HR, Handberg A (2021) Conventional, High-Resolution and Imaging Flow Cytometry: Benchmarking Performance in Characterisation of Extracellular Vesicles. Biomedicines 9(2):124.

Rasmussen RW, **Botha J**, Prip F, Sanden M, Nielsen MH, Handberg A (2021) Zoom in on Antibody Aggregates: A Potential Pitfall in the Search of Rare EV Populations. Biomedicines 9(2):206.

**2018**

Søren Risom Kristensen; **Jaco Botha**; Aase Handberg. Blu-ray beyond music and movies—novel approach to diagnostics measuring specific extracellular vesicles. Journal of Laboratory and Precision Medicine, 3, 1-5. (2018).

Mathilde Sanden; **Jaco Botha**; Michael René Skjelbo Nielsen; Morten Hjuler Nielsen; Erik Berg Schmidt; Aase Handberg. BLTR1 and CD36 Expressing Microvesicles in Atherosclerotic Patients and Healthy Individuals. Frontiers in Cardiovascular Medicine, 5, 1-8. (2018).

**Jaco Botha**; Morten Hjuler Nielsen; Maja Høgh Christensen; Henrik Vestergaard; Aase Handberg. Bariatric surgery reduces CD36-bearing microvesicles of endothelial and monocyte origin. Nutrition & Metabolism, 15(1), 1-9. (2018).

**2017**

**Jaco Botha**; Line Velling Magnussen; Morten Hjuler Nielsen; Tine Bo Nielsen; Kurt Højlund; Marianne Skovsager Andersen; Aase Handberg. Microvesicles Correlated with Components of Metabolic Syndrome in Men with Type 2 Diabetes Mellitus and Lowered Testosterone Levels But Were Unaltered by Testosterone Therapy. Journal of Diabetes Research Volume 2017, Article ID 4257875. (2017).

**2016**

Morten Mørk; Shona Pedersen; **Jaco Botha**; Sigrid Marie Lund; Søren Risom Kristensen. Preanalytical, analytical, and biological variation of blood plasma submicron particle levels measured with nanoparticle tracking analysis and tunable resistive pulse sensing. Scandinavian Journal of Clinical Laboratorial Investigation 76(5), 349-60. (2016).

## Conference abstracts published in journals (12)
**2019**

Anders Askeland; **Jaco Botha**; Rikke Wehner Rasmussen; Aase Handberg. Identification of common EV markers in plasma using high-resolution flow cytometry. Journal of Extracellular Vesicles 8 (suppl. 1), OWP2.01 & PS08.08. (2019).

**Jaco Botha**; Rikke Wehner Rasmussen; Mathilde Sanden; Aase Handberg. Conventional, high-resolution and imaging flow cytometry: potentials, pitfalls and solutions for EV characterization. Journal of Extracellular Vesicles 8 (suppl. 1), OWP2.03 & PS08.10. (2019).

Rikke Wehner Rasmussen; **Jaco Botha**; Mathilde Sanden; Aase Handberg. Lipoprotein particles can be detected by high-resolution flow cytometry and potentially interfere with EV characterization. Journal of Extracellular Vesicles 8 (suppl. 1), PF06.05. (2019).

**2018**

**Jaco Botha**; Mathilde Sanden; Morten Mørk; Søren Risom Kristensen; Aase Handberg. The somewhat forgotten role of isotype control antibodies in selecting and validating phenotype markers and antibody panels for EV characterisation. Journal of Extracellular Vesicles 7 (suppl. 1), PF01.16. (2018).

**Jaco Botha**; Mathilde Sanden; Aase Handberg. Small-particle flow cytometry: A new frontier in detection and characterisation of extracellular vesicles in liquid biopsies. Journal of Extracellular Vesicles 7 (suppl. 1), PS09.14. (2018).

Mathilde Sanden; **Jaco Botha**; Michael R S Nielsen; Morten Hjuler Nielsen; Erik Berg Schmidt; Aase Handberg. Atherosclerotic Patients have Lower Levels of BLTR1 Expressing Microvesicles Compared to Healthy Individuals. Journal of Extracellular Vesicles 7 (suppl. 1), PT08.08. (2018).

Rikke Wehner Rasmussen; Frederik Prip; Mathilde Sanden; Morten Hjuler Nielsen; **Jaco Botha**; Aase Handberg. Antibody aggregates: A potential pitfall in the search of rare EV-populations. Journal of Extracellular Vesicles 7 (suppl. 1), P04.08. (2018).

**2017**

**Jaco Botha**; Mathilde Sanden; Morten Hjuler Nielsen; Aase Handberg. Flow cytometers dedicated to the measurement of small particles: A powerful tool for EV characterization. Journal of Extracellular Vesicles 6 (suppl. 1), PT05.14. (2017).

Mathilde Sanden; **Jaco Botha**; Morten Hjuler Nielsen; Aase Handberg. Novel triggering threshold strategy for discovery of rare microvesicle phenotypes on flow

cytometers dedicated to small particle analysis. Journal of Extracellular Vesicles 6 (suppl. 1), PT05.10. (2017).

Rikke Bæk; Morten H. Nielsen; **Jaco Botha**; Lotte H. Pugholm; Evo K. L. Søndergaard; Kim Varming; Aase Handberg; Malene M. Jørgensen. The phenotypical changes of plasma EVs over time in healthy individuals. Journal of Extracellular Vesicles 6 (suppl. 1), PT03.07. (2017).

**2016**

**Jaco Botha**; Line Velling Magnussen; Morten Hjuler Nielsen; Tine Bo Nielsen; Kurt Højlund; Marianne Skovsager Andersen; Aase Handberg. Levels of circulating microvesicles are associated with plasma lipids and ectopic fat accumulation in type 2 diabetic men with low testosterone and are unchanged after testosterone replacement therapy. Journal of Extracellular Vesicles 5 (suppl. 1), PT3.16. (2016).

**2011**

Pennisi, CP; **Botha, J**; Buhl-Christensen, O et al. Activation of skeletal myogenic differentiation in adipose-derived stem cells by uniaxial cyclic strain. Regenerative Medicine 6(6, suppl. 2), 227 (No. PP-045). (2011). ISSN: 1746-0751.

## Conference abstracts in proceedings (4)

**2017**

**Jaco Botha**; Mathilde Sanden; Morten Hjuler Nielsen; Aase Handberg. Small-particle flow cytometry: A new era in the characterization of extracellular vesicles in liquid biopsies. Nordic Flow Cytometry Meeting. (2017). (Conference Abstract in Proceedings).

**2016**

**Jaco Botha**; Line Velling Magnussen; Morten Hjuler Nielsen; Tine Bo Nielsen; Kurt Højlund; Marianne Skovsager Andersen; Aase Handberg. Circulating microvesicles correlate with body composition, plasma lipids and markers for ectopic fat in testosterone deficient type 2 diabetic men. European Association for the Study of Diabetes Annual Meeting. (2016). (Conference Abstract in Proceedings).

**2012**

Zachar, V; **Botha, J**; Bundgaard-Nielsen, C et al. Effect of uniaxial cyclic strain on myogenesis of adipose-derived stem cells. International Society for Stem Cell Research, ISSCR. (2012). (Conference Abstract in Proceedings).

**2011**

Zachar, V; **Botha, J**; Buhl-Christensen, O et al. Skeletal myogenic differentiation of adipose-derived stem cells is enhanced by cyclic tensile strain. International Federation for Adipose Therapeutics and Science, IFATS. Page 60, No. 59. (2011). (Conference Abstract in Proceedings).

## Meeting Attendance/presentations (16)
**2019**
1st Annual Meeting of the Danish Society for Extracellular Vesicles, Aarhus, 3rd October, 2019. (Co-chair for session on EV function).

61st Annual Meeting of the Danish Society for Flow Cytometry, Copenhagen, 27. May 2019. (Invited oral presentation).
**Topic**: Conventional, high-resolution and imaging flow cytometry: Potentials, pitfalls and solutions for EV characterisation.

International Society for Extracellular Vesicles Annual Meeting 2019, Kyoto, 24.-28. April 2019. (Oral & poster presentation).
**Topic**: Conventional, high-resolution and imaging flow cytometry: Potentials, pitfalls and solutions for EV characterisation.

Imaging Flow Cytometry Meeting at Aarhus University, Aarhus, 14. March 2019. (Invited oral presentation).
**Topic**: Harnessing the Power of Imaging Flow Cytometers for Detection and Characterisation of Small Particles.

**2018**
EVSearch.dk Extracellular Vesicle Symposium 2018, Aalborg, 11. October 2018. (Oral presentation).
**Topic**: High-resolution Flow Cytometry: Potentials and Pitfalls in the Measurement of Small EVs.

International Society for Extracellular Vesicles Annual Meeting 2018, Barcelona, 2.-6. May 2018. (Poster presentation).
**Topic**: The somewhat forgotten role of isotype control antibodies in selecting and validating phenotype markers and antibody panels for EV characterisation.

International Society for Extracellular Vesicles Annual Meeting 2018, Barcelona, 2.-6. May 2018. (Poster presentation).
**Topic**: Small-particle flow cytometry: A new frontier in detection and characterisation of extracellular vesicles in liquid biopsies.

**2017**
Nordic flow cytometry meeting 2017, Copenhagen, 30. August – 1. September 2017. (Oral & poster presentation).
**Topic**: Small-particle flow cytometry: A new era in the characterization of extracellular vesicles in liquid biopsies.

Symposium på Klinisk Biokemisk Afdeling – Sygehus Lillebælt, Vejle, 16. August 2017. (Oral presentation).
**Topic**: Small-particle flow cytometry: A new era in the characterization of extracellular vesicles in liquid biopsies.

Dansk Selskab for Klinisk Biokemi – Årsmøde 2017, Helsingør, 14.-16. June 2017. (Oral presentation).
**Topic**: Har vævsspecifikke mikrovesikler potentiale som markører for patofysiologien bag komplikationer til fedme og DM2?

EVSearch.dk Extracellular Vesicle Symposium 2017, Aalborg, 22. March 2017. (Oral presentation).
**Topic**: The emergence of flow cytometers dedicated to the measurement of small particles: new tools for extracellular vesicle characterization and biomarker discovery.

**2016**
European Association for the Study of Diabetes Annual Meeting, München, 12.-16. September 2016. (Poster presentation).
**Topic**: Circulating microvesicles correlate with body composition, plasma lipids and markers for ectopic fat in testosterone deficient type 2 diabetic men.

International Society for Extracellular Vesicles Annual Meeting 2016, Rotterdam, 3.-7. May 2016. (Poster presentation).
**Topic**: Levels of circulating microvesicles are associated with plasma lipids and ectopic fat accumulation in type 2 diabetic men with low testosterone and are unchanged after testosterone replacement therapy.

European Association for the Study of Diabetes (EASD) Nonalcoholic fatty liver disease (NAFLD) Study group annual meeting, Copenhagen, 4.-5. April 2016. (Meeting attendance).

**2015**
EV workshop and training course, COST Action BM1202, The European Network on Microvesicles and Exosomes in Health and Disease (ME-HaD), Sienna, 26-28 March 2015. (Meeting attendance).

**2011**
World Conference on Regenerative Medicine 2011, Leipzig, 2.-4. November 2011. (Poster presentation).
**Topic**: Activation of skeletal myogenic differentiation in adipose-derived stem cells by uniaxial cyclic strain.